UNIVERSITY OF PADOVA

DEPARTMENT OF INDUSTRIAL ENGINEERING

SECOND-CYCLE DEGEE IN CHEMICAL AND PROCESS ENGINEERING

Graduation thesis in

Chemical and Process Engineering

PREDICTION CRITERIA OF THERMAL RUNAWAY IN THE ACID CATALYZED ESTERIFICATION OF ACETIC ANHYDRIDE

Coordinator: Prof. Giuseppe Maschio

Advisor: Ph.D. Chiara Vianello

Author: ALESSIO BROCCANELLO

ACADEMIC YEAR 2015-2016

Abstract

The main objective of this thesis is the study of the prevention of runaway reactions in chemical reactors. At this purpose, several prediction criteria are applied and compared between each other, considering the sulfuric acid catalyzed esterification of acetic anhydride with methanol as reference system. A kinetic model of the reaction is developed using an *ad hoc MATLAB*® script and validated through the usage of experimental data obtained for mean of a reaction calorimeter ran in isoperibolic conditions. Then, the runaway criteria are applied to both the experimental and the model results and several simulations are performed considering a sudden change of the thermal behavior of the system (from isoperibolic to adiabatic) and a change in the global heat transfer coefficient of the reactor. This work shows that, in the considered conditions, the runaway criteria that are taken into account are able to detect the boundaries between stable and unstable behavior of the system. Besides of that, the developed model proved to have a very good agreement with the experimental data, showing that it is possible to use it to predict the thermal runaway of the system. Moreover, the simulations of several failures help to understand their dramatic effect on the overall thermal behavior and to underline the necessity to introduce effective and reliable preventive actions in real industrial systems.

Index

Introduction

Many of the incidents occurring in an industrial plant are due to the sudden release of a huge amount of energy in a very short period of time and in a confined space. This typically determines a sudden pressure increase, generating a shock wave that is violently propagated in the surroundings, i.e. an explosion. It appears evident that these events must be avoided: this can be done, for example, applying preventive measures that are based on the usage of different criteria that are able to predict the thermal runaway of a system. The main objective of this thesis is to apply and compare different runaway criteria and to develop a model that is able to detect the boundaries between stable and unstable zone of the considered process.

In the first chapter, after a general description of the thermal behavior of a chemical process (including the exposure of the general mass and energy balances), several runaway criteria are presented and discussed from both a qualitative and a mathematical point of view.

In the second chapter, a brief description of reaction calorimetry (i.e. the main technique used to obtain the experimental data required for this work) is followed by a specific description of the experimental apparatus used to retrieve the data and by several considerations on the process that is chosen to apply the runaway criteria. Then, the safety issues concerning the chemicals that are taken into account are exposed.

In chapter three, a kinetic model of the system is developed and validated through the usage of the retrieved experimental data. Then, the considered runaway criteria are applied to both experimental and model data and the results are compared between each other.

In the fourth chapter, several adiabatic simulations of the system are performed in order to simulate a dramatic failure of the cooling system in a real industrial reactor. Finally, a sensitivity analysis of the maximum temperature reachable by the system is performed with respect to the global heat transfer coefficient: this is done to simulate the effect of events such as the fouling of the walls of the heat exchange system.

The fifth and last chapter is dedicated to the conclusions and to the final observations.

Chapter 1

Background

Many industrial activities deal with transport, storage or transformation of chemicals. These substances, because of their intrinsic properties, are often characterized by a high reactivity or a flammable and/or explosive behavior, when specific conditions are met. Therefore, their use can lead to incidents, endangering human beings and environment or, in the best scenario, simply causing an economic damage to the company in which the incident occurs. Many of these events are due to the sudden release of a huge amount of energy in a very short period of time and in a confined space. This typically determines a sudden pressure increase, generating a shock wave that is violently propagated in the surroundings, i.e. an explosion ([1]). It appears evident that these events must be avoided: this can be done analyzing systematically all the potential hazards and performing a risk analysis, trying to minimize the risk of incidents adopting both preventive and protective measures. In this chapter, the focus is on the prevention of runaway (i.e. uncontrolled) reactions, describing the theory of thermal explosion and several mathematical models that can be adopted in order to foresee the occurrence of this kind of events, developing the so called Early Warning Detection Systems (EWDS). Then, a brief description of the main calorimetric techniques used in order to retrieve the information required to apply the above mentioned criteria is presented.

1.1 Runaway reactions

It is well known that an increase of temperature leads to an exponential increase in the kinetic constants of elementary reactions, thus causing, in most cases, an acceleration of the kinetics of the global reaction. Therefore, if the thermal control in a reacting system subject to the production of heat is lost, a runaway reaction may occur. This phenomenon is also called thermal explosion and it also implies the possibility of the occurrence of side decomposition reactions that can lead to the formation of volatile substances and, independently by this, the increase in pressure in the vessel in which the process is carried out.

This type of event is characterized by an incremental increase of heat generation that, at a certain point, determines the overheating of the reacting mass due to the fact that the heat production rate becomes greater than the heat lost or exchanged by an eventual cooling system. In this way, the thermal control of the process is lost and the pressure usually increases because of the vapor pressure of the chemicals or the formation of gaseous by-products. A runaway reaction (or thermal explosion) can occur either because the rate of heat generation is greater than the rate of heat removal or because of chained-branched processes: the former cause leads to a proper thermal runaway, while the latter one characterizes the so called "chain branching-induced explosion". In many events (e.g. in combustions or oxidations), it is quite difficult to distinguish between the two mechanisms.

There is not a unique cause for the occurrence of a runaway reaction. In fact, it can originate because of an incorrect kinetic evaluation, an excessive feed rate of the reagents, the presence of impurities in the reactor, an inadequate mixing of chemicals (leading to the so called *hot spots*) or the failure of one between the cooling and the stirring system. Human error is one of the major causes of this kind of events ([2]).

It is well known that many industrial incidents are caused by runaway reactions ([3]): developing a theory that is able to predict their occurrence is thus fundamental in order to introduce adequate measures that can prevent them.

1.2 Thermal explosion theory

As it was previously said (§ 1.1), runaway reactions are essentially caused by the loss of the thermal control in the system in which the process occurs. Therefore, the understanding of the heat production and removal is essential to describe these phenomena. The theory of thermal explosion concerns the causes of an explosion, the conditions of its occurrence and the prediction of the temperature distribution in the reacting mass during the steady state and of the temperature profile during the transient. It appears evident that the instruments related to this approach have an enormous importance in the safety and risk prevention field ([4]).

The approaches for the description of runaway phenomena that can be found in literature can be essentially classified as geometry or sensitivity based. In the former, the thermal explosion is described according to some geometrical features of the system; on the other hand, the latter are related to the parametric sensitivity of the system and are very suitable for practical applications.

In this work, the focus is posed on the occurrence of an exothermic nth order reaction into a well stirred batch reactor. If the temperature and the physical properties of the species involved in the process are assumed to be uniform inside the reactor itself, the dynamics of the system can be described performing a mass (1.1) and an energy balance (1.2), obtaining the following equations:

$$\frac{\mathrm{d}c}{\mathrm{d}t} = -k(T) \cdot c^n, \tag{1.1}$$

where c (mol/m^3) is the reactant concentration, t (s) is the time, $k(T)$ ((mol/m^3)$^{1-n}$/s) is the reaction rate constant (in which the temperature dependence is highlighted) and n is the reaction order.

$$\rho \cdot V \cdot c_P \cdot \frac{\mathrm{d}T}{\mathrm{d}t} = (-\Delta H_R) \cdot k(T) \cdot c^n \cdot V - U \cdot S \cdot (T - T_a), \tag{1.2}$$

where ρ (kg/m^3) is the density of the reaction mixture, V (m^3) is the volume of the reagents, c_P (J/K/kg) is the specific heat capacity of the reaction mixture, T (K) is the temperature, ΔH_R (J/mol) is the heat of reaction, S (m^2) is the external surface area, U (J/m^2/s/K) is the overall heat transfer coefficient and T_a (K) is the ambient/jacket temperature.

The initial conditions are $c = c^{initial}$ and $T = T^{initial}$ at $t = 0$. The equations (1.1) and (1.2) can be written in dimensionless form using the definitions expressed by equations (1.3), (1.4) and (1.5), representing respectively the dimensionless concentration (i.e. the conversion, X), time (τ) and temperature (θ).

$$X = \frac{c^{initial} - c}{c^{initial}} \tag{1.3}$$

$$\tau = t \cdot k(T) \cdot \left(c^{initial}\right)^{n-1} \tag{1.4}$$

$$\theta = \frac{T - T^{initial}}{T^{initial}} \cdot \gamma, \tag{1.5}$$

where γ (-) is the so called Arrhenius number, defined as the dimensionless activation energy of the reaction, as expressed by equation (1.6):

$$\gamma = \frac{E_{activation}}{R \cdot T^{initial}}, \tag{1.6}$$

in which $E_{activation}$(J/mol) is the activation energy and R (J/K/mol) is the ideal gas constant.

In addition to the previous expressions, the definition of the dimensionless mass and energy balances requires the usage of the so called Semenov number Ψ (1.7), which represents the ratio between the produced and the removed heat, and of the dimensionless heat of reaction called *B* (1.8).

$$\Psi = \frac{(-\Delta H_R)\cdot k(T^{initial})\cdot(c^{initial})^n}{U\cdot S\cdot T^{initial}}\cdot \gamma \tag{1.7}$$

$$B = \frac{(-\Delta H_R)\cdot c^{initial}}{\rho\cdot c_P\cdot T^{initial}}\cdot \gamma \tag{1.8}$$

At this point, the equations (1.1) and (1.2) can be rewritten in the following dimensionless form:

$$\frac{\mathrm{d}X}{\mathrm{d}\,\tau} = \exp\left(\frac{\theta}{1+\frac{\theta}{\gamma}}\right)\cdot(1-X)^n \tag{1.9}$$

$$\frac{\mathrm{d}\,\theta}{\mathrm{d}\,\tau} = B\cdot\exp\left(\frac{\theta}{1+\frac{\theta}{\gamma}}\right)\cdot(1-X)^n - \frac{B}{\Psi}\cdot(\theta - \theta_a)\,, \tag{1.10}$$

where θ_a is the dimensionless ambient/jacket temperature.

It is interesting to notice that, for known reaction kinetics and ambient/jacket temperature, the behavior of the system is completely characterized by *B* and Ψ, being the dimensionless temperature and the conversion the only two dependent variables appearing in the mass and energy balances.

In the following sections, several criteria based on geometry and sensitivity for thermal runaway are briefly presented.

1.*2.1 Geometry based criteria for thermal runaway*

The geometry based criteria for thermal runaway are based on some geometric feature of the profile of a system variable such as dimensionless temperature or heat release rate. The Semenov criterion, which appears to be the first method developed in order to describe runaway reactions, belongs to this category. However, along the years, other criteria have been developed. In this section, apart from the already mentioned Semenov criterion, the Thomas and Bowes criterion, the Adler and Enig method and the van Welsenaere and Froment criterion are also presented.

1.2.1.1 The Semenov criterion

The Semenov criterion was developed in the 1928 ([5]). Semenov theory works well for gas and liquid phase and small particle suspended systems that undergo self-heating in a turbulent regime (as happens in well stirred reactors). It is important to observe that this method is based on the assumption of negligible reactant consumption, which is obviously violated in most real systems. However, its simplicity and explicitness allow one to have a fundamentally correct and synthetic view of the mechanism of thermal explosion phenomena. In addition to this, Semenov theory is a good approximation for a number of real systems, describing quite well the behavior of highly reactive processes, in which the thermal explosions occur at very low values of conversion.

When reactant consumption is neglected (i.e. the conversion *X* tends to zero), the mass balance equation (1.9) can be eliminated, while the energy balance (1.10) reduces to equation (1.11).

$$\frac{\mathrm{d}\,\theta}{\mathrm{d}\,\tau} = B \cdot \exp\left(\frac{\theta}{1+\frac{\theta}{\gamma}}\right) - \frac{B}{\Psi} \cdot (\theta - \theta_a)\,, \tag{1.11}$$

Defining the rate of temperature increase due to the heat released by an eventual reaction as $\theta_+ = \exp\left(\frac{\theta}{1+\theta/\gamma}\right)$ and the rate of temperature decrease due to heat removed by cooling as $\theta_- = \frac{1}{\Psi} \cdot (\theta - \theta_a)$, equation (1.11) can be rearranged in the following way:

$$\frac{1}{B} \cdot \frac{\mathrm{d}\,\theta}{\mathrm{d}\,\tau} = \theta_+ - \theta_- \tag{1.12}$$

It can be demonstrated that the dynamic behavior of the system is fully determined by the Semenov number Ψ. In particular, there are two critical values of Ψ, defining three different operational characteristics of the system:

- If $\Psi > \Psi_c$, the system undergoes thermal runaway;
- If $\Psi'_c < \Psi < \Psi_c$, the reaction can operate at a low temperature steady state but runaway is possible for large perturbations in temperature;
- If $\Psi < \Psi'_c$, the system becomes intrinsically stable in operation temperature.

The critical Semenov numbers Ψ'_c and Ψ_c can be easily found by imposing a tangency condition to the θ_+ vs θ and θ_- vs θ curves, finding, in this way, the critical values of the dimensionless temperature that, being substituted in equation (1.11), allows to obtain the values of Ψ'_c and Ψ_c. Considering only the condition over which the system undergoes thermal

runaway, the following expressions for the critical temperature θ_c (1.13) and for the critical Semenov number Ψ_c (1.14) are obtained:

$$\theta_c = \frac{\gamma}{2} \cdot \left[(\gamma - 2) - \sqrt{\gamma (\gamma - 4) - 4\theta_a} \right] \tag{1.13}$$

$$\Psi_c = (\theta_c - \theta_a) \cdot \exp\left(\frac{-\theta_c}{1+\frac{\theta_c}{\gamma}} \right) \tag{1.14}$$

Although this criterion is simple to understand and explicit, it is surely too conservative when reactant consumption cannot be neglected. For this reason, criteria such as the Thomas and Bowes, the Adler and Enig and the van Welsenaere and Froment ones are also presented.

1.2.1.2 The Thomas and Bowes criterion

The Thomas and Bowes criterion ([6]) is based on physical intuition and proposes to identify thermal runaway as the situation in which a positive second-order derivative appears *before* the dimensionless temperature maximum in the θ-τ plane. In fact, if the θ vs τ curve becomes concave prior to reaching its maximum, the temperature increase results to be accelerated, even if the curve returns to be convex as it approaches the maximum value itself. However, it can be observed that the concave region enlarges as the Semenov number increases. Therefore, Thomas and Bowes identified the critical condition for thermal runaway as the situation in which the concave region first appears but its size is zero, i.e. when the two inflection points are coincident. Formally speaking, this corresponds to the following conditions (1.15):

$$\frac{d^2\theta}{d\tau^2} = 0 \qquad \frac{d^3\theta}{d\tau^3} = 0 \tag{1.15}$$

However, the equation (1.15) defines only the critical inflection point but it does not indicate whether it is before or after the temperature maximum. Thus, with this criterion, it is generally required to use some specific techniques to identify the inflection point that is before the maximum. There exist several numerical strategies in the literature using equation (1.15) to find the critical conditions for runaway, such as the ones proposed by Hlavacek et al. ([7]) or by Morbidelli and Varma ([8]).

1.2.1.3 The Adler and Enig criterion

The criterion proposed by Thomas and Bowes was further examined by Adler and Enig ([9]), who found that is more convenient to work in the θ-*X* plane than in the θ-τ plane, since in this case one need to consider only one balance equation (1.16) that is obtainable dividing equation (1.10) by the (1.9).

$$\frac{1}{B}\cdot\frac{\mathrm{d}\,\theta}{\mathrm{d}X}=1-\frac{1}{\Psi}\cdot\frac{(\theta-\theta_a)}{(1-X)^n}\cdot\exp\left(-\frac{\theta}{1+\frac{\theta}{\gamma}}\right), \tag{1.16}$$

The initial condition is that the dimensionless temperature is equal to zero at *X* equal to zero.

The critical conditions for runaway to occur are then defined, similarly to the ones of the Thomas and Bowes criterion, as the situation where a region with positive second-order derivative first occurs before the maximum in the θ-*X* plane, i.e.:

$$\frac{\mathrm{d}^2\,\theta}{\mathrm{d}X^2}=0 \qquad \frac{\mathrm{d}^3\,\theta}{\mathrm{d}X^3}=0 \tag{1.17}$$

Analogously to the Thomas and Bowes method, also the Adler and Enig one also requires some numerical work to evaluate the critical conditions, because equation (1.17) defines only the critical inflection point but it does not provide indications on its location before or after the temperature maximum. The same numerical strategies enounced in §1.2.1.2 can be adopted to solve this problem.

1.2.1.4 The van Welsenaere and Froment criterion

The criterion derived by van Welsenaere and Froment ([10]) defines criticality using the locus of temperature maxima in the θ-*X* plane. The temperature maximum in the dimensionless temperature-conversion plane can be calculated setting the first derivative of θ with respect to *X* equal to zero in equation (1.16). In this way, the following expression can be obtained:

$$(1-X_m)^n=\frac{(\theta^*-\theta_a)}{\Psi}\cdot\exp\left(-\frac{\theta^*}{1+\frac{\theta^*}{\gamma}}\right), \tag{1.18}$$

where X_m (-) is the conversion value that corresponds to the temperature maximum θ^* (-).

For each set of values of the involved parameters (*n*, Ψ, θ_a and *B*), it can be found a pair of values for X_m and θ^* that are able to satisfy equation (1.18). Therefore, varying the value of the parameter *B* (for example), the locus of the temperature maximum (*maximum curve*) can be constructed in the θ-*X* plane. It can be demonstrated that this maximum curve exhibits a minimum with respect to θ: van Welsenaere and Froment thus defined criticality as the situation where the θ-*X* trajectory goes through the minimum of the maximum curve. This minimum can be obviously found by differentiating equation (1.18) with respect to θ and by imposing the resulting expression equal to zero. This procedure leads to the following expression for the critical dimensionless temperature θ_c:

$$\theta_c = \frac{\gamma}{2} \cdot \left[(\gamma - 2) - \sqrt{\gamma\,(\gamma - 4) - 4\,\theta_a} \right] \tag{1.19}$$

It is very interesting to notice that equation (1.19) and equation (1.13) are exactly the same expression. This equation gives only the critical value of the system temperature: a procedure is thus required in order to identify which set of the system parameters leads to this θ_c value. In general, a numerical technique with a trial and error procedure is required. However, in the case of a first order reaction, van Welsenaere and Froment used an extrapolation procedure to derive an explicit expression for the critical value of a system parameter. This procedure leads to the definition of a modified critical Semenov number (Ψ_c^{VF}), given by equation (1.20):

$$\Psi_c^{VF} = \left(1 + \frac{1}{Q} + \frac{1}{Q^2}\right) \cdot \Psi_c\,, \tag{1.20}$$

where Ψ_c is the classical critical Semenov number and *Q* (-) is a dimensionless parameter defined as:

$$Q = \frac{\sqrt{1 + 4 \cdot \left[\frac{B}{(\theta_c - \theta_a)} - 1\right]} - 1}{2}, \tag{1.21}$$

in which θ_c is computed through equation (1.19) and *B* is calculated considering an arithmetic mean between the upper and the lower bounds of its critical value (calculated using the extrapolation procedure).

It is interesting to notice that, according to equation (1.20), the van Welsenaere and Froment criterion appears to be a second order perturbation correction to the original Semenov criterion (in the case of a first order reaction).

Considering the geometry based criteria for thermal runaway, it appears quite evident that they can be applied only in systems where a temperature profile exists: this is certainly one of the limitations of this kind of methods. Besides of that, they are not able to provide quantitative measures of the extent or intensity of the runaway.

1.*2.2 Sensitivity based criteria for thermal runaway*

The geometry based criteria can be applied only to systems where a temperature profile exists, which is not always the case in applications. Furthermore, they are not able to provide indications on the intensity of the runaway, thus limiting the efficiency of an eventual action taken to prevent the occurrence of a major incident caused by a thermal explosion, in a practical application. For these reasons, a new series of criteria have been developed, based on the concept of *parametric sensitivity*. These methods take advantage of the fact that, close to the boundary between the runaway and non-runaway behavior, the system becomes very sensitive, i.e. its behavior changes dramatically even if the initial values of the system parameters are subject to very small perturbations: identifying this *parametrically sensitive region* thus allows to define the critical conditions for thermal runaway.

In the following sections, the Hub and Jones, the Morbidelli and Varma and the Strozzi and Zaldívar criteria are presented.

1.2.2.1 The Hub and Jones criterion

The Hub and Jones criterion ([11]) states that the critical condition for runaway occurs when the first derivative with respect to time of the temperature difference between the reactor and the jacket is positive and, simultaneously to the previous condition, the second derivative of the reactor temperature (even in this case, with respect to time) becomes equal to zero, i.e.:

$$\frac{\mathrm{d}^2T}{\mathrm{d}t^2} = 0 \qquad \frac{\mathrm{d}(T-T_a)}{\mathrm{d}t} > 0 \tag{1.22}$$

This criterion simply comes from the differentiation of the energy balance. In fact, computing the time derivative of equation (1.2), the following one is obtained:

$$\rho \cdot V \cdot c_P \cdot \frac{\mathrm{d}^2T}{\mathrm{d}t^2} = \frac{\mathrm{d}[(-\Delta H_R)\cdot k(T)\cdot c^n \cdot V]}{\mathrm{d}t} - U \cdot S \cdot \frac{\mathrm{d}(T-T_a)}{\mathrm{d}t} \ , \tag{1.23}$$

in which it can be easily seen that the accumulation of heat in the system becomes ever increasing when both the derivatives that appear in equation (1.22) are positive.

In order to apply this method, only the measured values of the reactor and of the jacket temperature are required to be known. This criterion, differently from the geometry-based ones, does not need a model for the reaction, thus being suitable for the on-line application. However, in practice, the main problem in its usage is the amplification of the noise in the temperature signals due to differentiation. Therefore, in order to avoid false alarms, the application of digital philters or algorithms for data smoothing is required.

1.2.2.2 The Morbidelli and Varma criterion

The Morbidelli and Varma criterion ([4,8,12,13]) is focused on the recognition of the parametrically sensitive region of the system: its aim is to mark, in this way, the boundary for thermal explosion. In order to do this, it is necessary to study the effect of the variation of some parameter on the system behavior: this is done using the tools provided by the sensitivity analysis.

The local sensitivity (s), with respect to a generic parameter Φ_i, of a system whose behavior is described by a single variable x (and its change in time is defined by the equation $dx/dt=f$, with $x(0) = x^{initial}$, where $f(x, \mathbf{\Phi}, t)$ is continuous and differentiable in all its domain and where $\mathbf{\Phi}$ is a vector containing all the parameters of the system) is defined in the following way:

$$s = \frac{\partial x(t,\Phi_i)}{\partial \Phi_i} \tag{1.24}$$

The normalized sensitivity (s_{norm}) of x with respect to the parameter Φ_i is used to normalize the magnitudes of the parameter and of the system variable. It is defined in the following way:

$$s_{norm} = \frac{\Phi_i}{x} \cdot \frac{\partial x(t,\Phi_i)}{\partial \Phi_i} \tag{1.25}$$

In order to study specific characteristics of the system (as required by the Morbidelli and Varma criterion), it is necessary to define the objective function sensitivity (s^{obj}):

$$s^{obj} = \frac{\partial I}{\partial \Phi_i}, \tag{1.26}$$

in which I is the objective function, that is continuous with respect to the Φ_i parameter. Of course, equation (1.26) can be normalized, obtaining the so called normalized objective function sensitivity:

$$s_{norm}^{obj} = \frac{\Phi_i}{I} \cdot \frac{\partial I}{\partial \Phi_i} = \frac{\partial \ln I}{\partial \ln \Phi_i} \tag{1.27}$$

The Morbidelli and Varma criterion utilizes the normalized objective function sensitivity, considering the maximum dimensionless temperature θ^* as objective function. It is based on the fact that, close to the boundary for thermal runaway, the normalized sensitivity of the maximum temperature reaches itself its maximum value. The condition of maximum sensitivity is thus considered the critical condition for thermal runaway in this criterion.

The sign of the sensitivity has a meaning: if positive, it indicates that the temperature maximum increases as the value of the chosen parameter increases (and vice versa), i.e. the thermal explosion occurs when the value of the parameter increases (and vice versa).

It was demonstrated by Morbidelli and Varma ([13]) that, when a system is in the parametrically sensitive region, this criterion is intrinsic, i.e. it provides the same value of the critical Semenov number for thermal runaway independently on the choice of the parameter considered in order to compute the normalized maximum temperature sensitivity. On the other hand, if the critical value is dependent on the choice of the parameter, then the system is said to be *parametrically insensitive*. In this case, one cannot define a general boundary that indicates the transition between non-runaway and runaway behavior, and each situation needs to be analyzed individually according to specific characteristics desired (e.g. maximum temperature lower than a fixed value).

Only when the normalized objective function sensitivity maximum is sharp and essentially independent on the parameter choice, one is really dealing with a potentially explosive system. In fact, the intensity of the maximum provides quantitative information on the extent of the thermal explosion.

1.2.2.3 The Strozzi and Zaldívar criterion

The Strozzi and Zaldivar criterion is based on the chaos theory techniques ([14]). Applying this approach, a mathematical model is not required for the process, thus making this criterion suitable for on-line application in the detection of runaway reactions.

For a chemical reaction occurring in a batch reactor, when $t \to \infty$, the trajectory of the system in the phase space tends to a specific point (for example, that at which the temperature of the reactor is equal to the ambient/jacket temperature and the reactant conversion is complete). In other words, the trajectory of two points that, at the beginning of the reaction, are close to each other in the phase space, have to finish at the same final point when the reaction is complete. However, the orbits of the two points can diverge along the path towards the final one and so, if the system parameters are near the runaway boundary, a small initial position change results in a large change in the phase space trajectories. Evaluating the divergence of the system of ordinary differential equations that describes a chemical process (mass and energy balances), thus allows to individuate the critical condition for thermal runaway. In particular, if, at a certain point of the *T* vs *t* trajectory, a local positive divergence appears, the process operates in runaway conditions. In the Strozzi and Zaldívar approach, the *Lyapunov exponents* are used to define sensitivity, and so to quantify the rate of divergence of the above mentioned trajectories. It is well known that the Lyapunov exponent can monitor the behavior of two neighboring points of a system in a direction of the phase space, as function of time, classifying it depending on the exponent sign:

- If the Laypunov exponent is positive, then the points diverge to each other;
- If the exponent tends to zero, the points remain at the same relative distance;
- If the exponent is negative, the points converge.

The on-line application of this criterion requires the reconstruction of the phase space of the system by non-linear time series analysis using delay coordinate embedding (i.e. the usage of time delays in the temperature measurements). Then, it is required to study the evolution of the divergence during the transient, considering that a positive divergence implies the presence of a runaway behavior.

This method has been validated experimentally by different studies that demonstrated its reliability for batch, semi-batch and continuous reactors operating in both isothermal (i.e. at constant temperature of the reactor) and isoperibolic (i.e. at constant environment/jacket temperature) conditions and with different types of reactions (chain reactions, equilibrium, parallel and competing reactions) ([15,16,17,18]).

1.3 Calorimetric techniques

In order to apply the criteria exposed in §1.2, it is fundamental to obtain several data related to the heat production due to the presence of a reaction or to the heat exchanged by the system with the environment/jacket. Besides of that, most of the methods that were previously presented require the development of a model for the process to which they are applied. All of this information can be retrieved using calorimetry, i.e. the science aimed at the measurement of heat exchanged between a system and the surrounding environment during a chemical reaction or a physical transformation. Although research in this field started in the latter part of the 18th century and calorimetry techniques progressively improved in the 19th century, this science has gained more and more importance in the last years mainly because of its application to the risk analysis field. In fact, it has proved to be very useful in order to evaluate the suitability of a designed process, to avoid to work in conditions that can lead to unexpected side reactions and decomposition of hazardous chemicals, to correctly size protection devices and to perform a variety of engineering calculations.

There are four categories into which monitored parameters relevant to risk analysis can be classified: temperature, pressure, heat or power and time. Temperature and heat are considered to be indicators of the severity of the runaway reaction, even if pressure is the most relevant parameter to control: in fact, it is mainly the sudden increase in pressure to cause damage to equipment, harm to operators and undesired release of chemicals into the environment. In general, it can be stated that the higher the temperature, the rate of heat release and pressure, the higher is the risk of incidents. However, it must not be forgot that, especially in the incident prevention field, the time scale over which the event takes place is fundamental. All of the above mentioned information, as previously stated, can be retrieved applying calorimetric techniques ([19]).

The experimental devices used in calorimetry can be classified on the basis of several criteria, such as the following ones:

- The reaction volume. If it is lower than one milliliter, the calorimeters are called *microcalorimeters* (such as the ones concerning Differential Scanning Calorimetry *DSC* and Differential Thermal Analysis *DTA*). If it is between one millimeter and 0.1 liters, the calorimeters are called *minicalorimeters* (such as the Calvet or Thian calorimeter and the Thermal Screening Unit *TSU*, which is presented in Figure 1.1). If the volume is between 0.3 and 10 liters, the apparatuses are called *reaction calorimeters* ([19, 20]).

- The operating mode. With respect to this criterion, in fact, calorimeters can be classified as isothermal, adiabatic, isoperibolic and oscillating temperature ones.
- The control system, distinguishing between the so called active and passive calorimeters.
- The construction (single or double calorimeters).
- The working principle. There are, for example, differential calorimeters, combustion ones, etc.

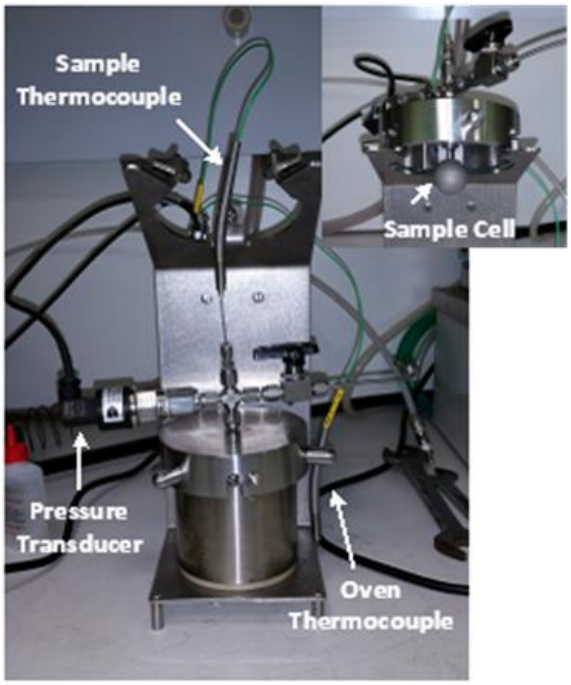

Figure 1.1. *A Thermal Screening Unit (TSU) by HEL. The indication of the main parts of the apparatus is reported in the figure.*

The application of different calorimetric techniques is fundamental in order to retrieve the experimental data required to build an Early Warning Detection System. In this work, an isoperibolic reaction calorimeter is used for this purpose.

Chapter 2

Experimental apparatus and reaction description

In order to compare the thermal runaway criteria presented in §1, it has been decided to consider the sulfuric acid catalyzed esterification of acetic anhydride and methanol. This appears to be a relatively safe reaction for studying thermal runaway in laboratory and, because of the modest reaction enthalpy and low activation energy, this reaction provides a severe test for the runaway criteria. In order to retrieve the experimental data required for the application of the runaway criteria, an isoperibolic reaction calorimeter is used. In this chapter, after a brief description of the main reaction calorimetry techniques, the experimental apparatus used in this work is presented and several considerations on the esterification reaction are briefly exposed. In the last sections, the safety risks concerning the usage of acetic anhydride and methanol are shortly enunciated.

2.1 Reaction calorimetry

As stated in §1, reaction calorimetry concerns the usage of apparatuses that have a volume greater than 0.3 liters but smaller than 10 liters. Reaction calorimetry is based on the resolution of the energy balance for an agitated jacketed reactor, i.e.:

$$\dot{Q}_{acc} = \dot{Q}_{chem} + \dot{Q}_{exc} + \dot{Q}_{loss} + P_{stirrer} + \dot{Q}_{c}, \tag{2.1}$$

where $\dot{Q}_{acc}$ (W) is the accumulated heat flow, $\dot{Q}_{chem}$ (W) is the heat flow generated by the reaction, $\dot{Q}_{exc}$ (W) is the heat flow exchanged by the jacket, $\dot{Q}_{loss}$ (W) is the heat flow dissipated in the environment, $P_{stirrer}$ (W) is the power developed in the mixing process and $\dot{Q}_{c}$ (W) is the compensation heat flow.

These terms can be expressed according to the following equations:

$$\dot{Q}_{acc} = C_P \frac{dT}{dt} \tag{2.2}$$

$$\dot{Q}_{chem} = r \cdot V \cdot (-\Delta H_R) \tag{2.3}$$

$$\dot{Q}_{exc} = U \cdot S \cdot (T_a - T) \quad (2.4)$$

$$P_{stirrer} = 2 \cdot \pi \cdot M_d \cdot N \quad (2.5)$$

in which C_P (J/K) is the heat capacity of the reaction mixture, r (mol/s/m^3) is the reaction velocity, M_d (J) is the stirrer torque and N (s^{-1}) is the agitator speed.

Depending on their operation mode, reaction calorimeters can be classified in isothermal, isoperibolic and adiabatic ones. The corresponding energy balances can be obtained considering one or more of the terms that appear in equation (2.1) equal to zero. In the following sections, the main characteristics of each type of calorimeter are shortly exposed, together with some considerations.

2.1.1 Isothermal calorimeters

The isothermal calorimeters allow to study the behavior of a sample at constant temperature, making possible the determination of the parameters linked to the agitation efficiency and heat exchange. Furthermore, this operation mode allows to determine the global heat exchange coefficient and to obtain in a direct way the reaction velocity.

2.1.2 Isoperibolic calorimeters

Differently from the isothermal calorimeters, in the isoperibolic ones the jacket temperature is maintained constant. This allows to obtain the same information of the isothermal calorimetry without the need of a complex and expensive control system of the reactor temperature. However, the global heat transfer coefficient between the jacket and the reactor (that can be determined through a calibration performed using an heating element) must be high enough, in order to guarantee the pseudo-isothermal conditions of the system. The main disadvantage of this technique is the need of mathematical models in order to eliminate the effects of the reaction temperature variations on the technical data. This limit is usually overcame regulating the resistance between the inside of the reactor and the surroundings in a way that the maximum temperature rise does not become higher than 2 °C.

2.1.3 Adiabatic calorimeters

The adiabatic reaction calorimetry allows to obtain information on the safety of a chemical process: the runaway phenomena, in fact, are very fast and therefore can be considered approximatively adiabatic. Thus, a single experiment in adiabatic conditions can provide many fundamental information useful for the design of chemical reactors and of storage tanks and can become an important tool for the risk assessment in industrial plants. In particular, the adiabatic calorimetry allows to determine several process parameters related to systems in which an exothermic reaction occurs, such as the adiabatic temperature rise ΔT_{ad} (K), the temperature and pressure rise velocity, the global reaction rate and the conversion. The main advantage of this technique is the simplicity of the required experimental apparatus: in order to work in adiabatic conditions, in fact, a system must not exchange a significant amount of heat with the environment (this means that no control system is required for the temperature). However, mathematical models are required in order to decouple temperature and concentration effects in the experimental profiles obtainable using this technique.

The adiabatic temperature rise, i.e. the maximum temperature increment observable in the presence of an exothermic reaction that occurs in an adiabatic system, can be determined using the following equation:

$$\Delta T_{ad} = \frac{m \cdot (-\Delta H_R)}{M c_P}, \tag{2.6}$$

where m (mol) is the initial number of moles of the reagents and M is the mass of the reagents. It appears quite evident that the determination of ΔT_{ad} is affected by the thermic inertia of the eventual sample holder (which can absorb part of the generated heat). This fact is usually taken into account through the so called ϕ-factor (-):

$$\phi = \frac{(\Delta T_{ad})_{theoretical}}{(\Delta T_{ad})_{observed}} = \frac{m_s c_{Ps} + m_h c_{Ph}}{m_s c_{Ps}} = 1 + \frac{m_h c_{Ph}}{m_s c_{Ps}}, \tag{2.7}$$

where m_s and m_h (kg) are respectively the mass of the sample and of the sample order, while c_{Ps} and c_{Ph} (J/K/kg) are the specific heat at constant pressure of the sample and the sample holder itself. Of course, in order to obtain experimental data that are representative of the adiabatic case, the ϕ-factor must be as close as possible to 1.

2.2 Experimental apparatus

In order to retrieve the experimental data required for the study of the thermal runaway in the esterification of acetic anhydride and methanol, the isoperibolic calorimeter represented in Figure 2.1 is used. The experimental apparatus is constituted by the following instruments:

- Jacketed and stirred calorimeter (Buchi);
- Control panel of the engine *CYCLONE 075 BUCHIGLASUSTER*, connected to the personal computer;
- Data acquisition cards National Instruments, connected to the personal computer;
- Thermocriostat (Huber Tango), used to modify the temperature of the heating/cooling fluid (silicon oil);
- Personal computer, using which it is possible to control and acquire the experimental data through a program.

Figure 2.1. *The isoperibolic reaction calorimeter used in this work.*

The stirred reactor is in hastelloy steel and it has a nominal volume of 250 milliliters: it can resist up to 250 °C of temperature and 60 bar of internal pressure. For control purposes, data acquisition and safety reasons, the following devices are installed on the top of the vessel:

- Three platinum resistance thermometers (Pt100): one of them is dedicated to the temperature control in the reaction ambient, while the other two are used to control the temperature in the jacket;

- A pressure transducer used to measure the pressure in the reaction ambient;
- A bursting disk;
- A relief valve;
- A valve for the introduction of the samples.

The set temperature of the jacket ranges from -2 to 20 °C. The experiments are performed by adding acetic anhydride very quickly to a solution of sulfuric acid in methanol, both at the same temperature as the jacket. In order to reach as near as possible the same temperature as the methanol in the calorimeter, the stoppered conical flask filled with a weighted quantity of pure acetic anhydride (99 % purity, on a weight basis) is placed in the bath of the thermostat for a reasonable time.

Before the addition of acetic anhydride, however, a calibration of the instrument is performed. When the calorimeter reaches the steady state (as indicated by an approximatively constant value of the smoothed reactor temperature and small values of its rate of change), the determination of the average value of the temperature of the reactor is started and continues for 10-15 minutes. Then, the values of $U \cdot S$ and c_P are determined considering an average of the experimental measurements performed imposing different temperatures inside the reactor. After the calibration and the return of the calorimeter to a steady state, the flask of acetic anhydride is removed from the thermostatic bath, its outside is wiped dry and the acetic anhydride is quickly poured inside the calorimeter. After the completion of the reaction, a second calibration is made. However, the values of $U \cdot S$ and c_P that are found in the two calibrations are very similar because of the small quantity of acetic anhydride with respect to methanol.

2.3 Considerations on the involved reactions

The acid catalyzed esterification of acetic anhydride and methanol results in the production of methyl acetate and acetic acid, as shown in equation (2.8):

$$\text{Acetic Anhydride} + \text{Methanol} \rightarrow \text{Methyl Acetate} + \text{Acetic Acid} \tag{2.8}$$

As it was previously mentioned, this exothermic reaction is relatively safe for studying thermal runaway in the laboratory and provides a severe test for the runaway criteria.

Besides of this main reaction, a side esterification also appears, leading to the reaction between methanol and acetic acid to give water and methyl acetate, as expressed by equation (2.9):

$$\text{Acetic Acid} + \text{Methanol} \leftrightarrow \text{Methyl Acetate} + \text{Water} \quad (2.9)$$

However, reaction (2.9) presents a negligible heat of reaction, with respect to the one involved in the main reaction. Besides of that, reaction (2.9) is also rather slow in the considered conditions, even if an increase in the reaction rate is observed as temperature and amount of catalyst increase ([21]).

This esterification reaction can be carried out in both homogeneous and heterogeneous way: in the first case, strong liquid mineral acids are used as catalysts (such as H_2SO_4, HCl and HI), while in the second one solid acid catalysts are used (such as Nafion resin on a silica or a zeolite support).

A comparative study between homogeneous and heterogeneous acid catalyzed esterification of acetic acid with methanol was carried out by Liu et al. ([22]), finding out that there is a common reaction mode on the Brønsted acid sites of the two catalysts (H_2SO_4 and Nafion) and that they have a comparable efficiency on a per site basis. Besides of that, it is pointed out that the possible autocatalytic behavior of the acetic acid can be neglected under specific experimental conditions (which are similar to the ones used in this work) and that, as expected, the water produced in the reaction progressively deactivates the catalysts. These reasons allow to neglect the influence of the side reaction on the thermal runaway behavior of the system.

Since some of the criteria for runaway applied in this work require a model, the acid catalyzed esterification of acetic anhydride and methanol has been modelled in both isoperibolic and adiabatic conditions, considering the simultaneous integration of the mass and of the energy balances and assuming a pseudo-first order kinetics for this reaction. The mass balance can be expressed by the following differential equation:

$$\frac{dX}{dt} = k \cdot (1 - X) \,, \quad (2.10)$$

where the conversion X at the time instant t' (s) is defined as the ratio between the reacted moles of acetic anhydride and the initial number of moles of acetic anhydride itself ($n^i_{Ac.\ Anh.}$, expressed in moles), i.e.:

$$X = \frac{n^i_{Ac.\ Anh.} - n_{Ac.\ Anh.}(t')}{n^i_{Ac.\ Anh.}} \,, \quad (2.11)$$

in which $n_{Ac.\ Anh.}(t')$ (mol) is the number of moles of acetic anhydride at the time instant t'.

The isoperibolic energy balance can be written in the following way.

$$m_{Ac.\ Anh.} \cdot c_P \cdot \frac{dT}{dt} = n^i_{Ac.\ Anh.} \cdot (-\Delta H_R) \cdot \frac{dX}{dt} - U \cdot S \cdot (T - T_a), \quad (2.12)$$

in which $m_{Ac.\ Anh.}$ (kg) is the mass of acetic anhydride inside the calorimeter.

In adiabatic conditions, equation (2.3) becomes:

$$m_{Ac.\ Anh.} \cdot c_P \cdot \frac{dT}{dt} = n^i_{Ac.\ Anh.} \cdot (-\Delta H_R) \cdot \frac{dX}{dt} \quad (2.13)$$

By using an appropriate numeric technique in order to integrate simultaneously the mass and the energy balances equations and by using the retrieved experimental data in order to obtain a kinetic model of the esterification reaction and the values of c_P and $U \cdot S$, it is possible to obtain a model for the reaction that allows the reconstruction of the *T* vs *t* curves parametrically with respect to the sulfuric acid concentration and to the jacket temperature (which is approximatively constant, in isoperibolic conditions).

2.4 Safety issues

It is well known that the chemicals involved in this reaction, i.e. acetic anhydride, methanol and sulfuric acid, are dangerous for the human health and for the environment. However, in this case, the sulfuric acid is used as a catalyst: the quantity involved in the reaction is thus small enough to guarantee the absence of safety risks. On the other hand, acetic anhydride and methanol are utilized in relevant quantities: in the following sections, the characteristics of these chemicals are shortly presented, together with several examples of real incidents caused by these substances.

2.4.1 Acetic Anhydride

Acetic Anhydride, at ambient temperature, is a colorless liquid with a characteristic sharp odor. It is used in making plastics, drugs, dyes, explosives, aspirin and perfumes. It is dangerous because it is a highly corrosive chemical: its inhalation can irritate the mouth, the nose and the throat, causing severe damage to the human body. Moreover, this chemical can be adsorbed through the skin, causing irritations, skin allergies and severe damages to the eyes. Apart from toxicity, acetic anhydride is also subject to flammability issues and can generate explosions. The pictograms and the hazard/precautionary statements concerning this chemical are reported in Figure 2.2.

Hazard pictograms :

GHS02 GHS05 GHS07

Signal word : Danger

Hazard statements : H226 - Flammable liquid and vapour
H302+H332 - Harmful if swallowed or if inhaled
H314 - Causes severe skin burns and eye damage
H335 - May cause respiratory irritation

Precautionary statements : P210 - Keep away from heat, hot surfaces, sparks, open flames and other ignition sources. No smoking
P233 - Keep container tightly closed

Figure 2.2. *Pictograms and hazard/precautionary statements reported in the safety data sheet of acetic anhydride.*

Even if this substance can explode with the only need of a comburent, most of the incidents involving acetic anhydride in literature are caused by its tendency to start runaway reactions, in the presence of other chemicals. For example, the following accidents involving acetic anhydride are known:

- On 12/31/1991, in South Charleston (West Virginia, USA), the accidental mixing of acetic anhydride and water caused the explosion of a vessel that, unfortunately, leaded to a fatality;
- On 10/2/1967, in Minamata (Japan), a runaway reaction between acetic anhydride and diketene caused an explosion followed by a fire, making half of the factory collapse and injuring six people.

2.4.2 Methanol

Methanol, at ambient temperature, appears to be a light, volatile, flammable liquid with distinctive odor very similar to that of ethanol (i.e. drinking alcohol). It is a polar liquid used in many applications, e.g. as antifreeze, solvent, fuel, as a denaturant for ethanol or in order to produce biodiesel via a transesterification reaction. If it is inhaled or ingested, methanol is highly toxic: in fact, it is metabolized by the human body first to formaldehyde and then to formic acid or formate salts, which are poisonous for the central nervous system, causing blindness, coma and death. Having a very high vapor pressure, even at ambient temperature, gives to methanol its flammable and explosive characteristics. The pictograms and the hazard/precautionary statements concerning this chemical are reported in Figure 2.3.

CLP pictograms :

GHS02 GHS06 GHS08

Signal word : Danger

Hazard statements (CLP) : H225 - Highly flammable liquid and vapour.
H301 - Toxic if swallowed.
H311 - Toxic in contact with skin.
H331 - Toxic if inhaled.
H370 - Causes damage to organs

Precautionary statements (CLP) : P270 - Do no eat, drink or smoke when using this product
P280 - Wear protective gloves/protective clothing/eye protection/face protection.
P301+P310 - If swallowed, immediately call a doctor.
P302+P352 - IF ON SKIN: Wash with plenty of soap and water
P307+P311 - IF exposed: Call a POISON CENTER or doctor/physician
P405 - Store locked up

Figure 2.3. *Pictograms and hazard/precautionary statements reported in the safety data sheet of methanol.*

It is important to notice that, although its wide use in many applications and its similarity with ethanol tends to give to most people the perception of a safe chemical to handle, methanol is surely a dangerous substance and it is involved in many incidents that can be found in literature. For example, the following accidents involving methanol are known:

- On 10/17/1994, in Lethbridge (Alberta, Canada), a derailment caused the breakage of five tank cars containing methanol, that was dispersed in the environment, requiring the evacuation of a part of the city and damaging the environment due to the loss of the chemical;
- On 01/11/2006, in Daytona Beach (California, USA), an explosion of a methanol tank caused the generation of a fire, the death of two workers and severe burns on another one;
- On 07/26/2012, in Labuan (Malaysia), several explosions concerning a methanol tank caused five fatalities.

Considering these events, it appears evident that methanol is a very dangerous chemical and must be handled with extreme care.

Chapter 3

Application of runaway criteria (isoperibolic case)

In this chapter, the application of several criteria for the prediction of the thermal runaway to the acid catalyzed esterification of acetic anhydride and methanol is presented. In particular, a geometry-based criteria (Thomas and Bowes) and three sensitivity-based ones (Hub and Jones, Morbidelli and Varma, Strozzi and Zaldìvar) are compared between each other, in order to highlight the main differences and the possible limits of these methods, considering their application in the isoperibolic case. As it was stated in §1, the Thomas and Bowes criterion and the Morbidelli and Varma one require a model for the system, in order to be applied. In the following sections, the development of this model is briefly presented, together with the results of the application of the above mentioned runaway criteria and their comparison with the ones presented by Casson et al. ([17]).

3.1 Model of the acid catalyzed esterification

As it was stated in §2.1, a model for the acid catalyzed esterification of acetic anhydride and methanol is constructed by the simultaneous integration of the mass and the isoperibolic energy balances over time, considering a pseudo first order kinetics for the reaction. In order to build this model, an isoperibolic calorimeter is used, performing several measurements (at different concentration of sulfuric acid and jacket temperature) in order to retrieve the experimental curves required for this operation. In each test, 0.8 mol of acetic anhydride and 7.0 mol of methanol are used: the excess of methanol justifies the assumption of a pseudo-first order kinetics for the reaction. The same experimental apparatus is used to obtain, through several calibrations, the mean values of the system's thermal capacity $m_{Ac.\ Anh.} \cdot c_P$ (i.e. 0.88 J/K) and of $U \cdot S$ (i.e. 4.3 W/K).

The experimental curves obtained considering an approximatively constant jacket temperature of 5.3 °C and different concentrations of sulfuric acid are represented in Figure 3.1, while the ones obtained considering a sulfuric acid concentration of 30 mol/m^3 and different jacket temperatures are represented in Figure 3.2.

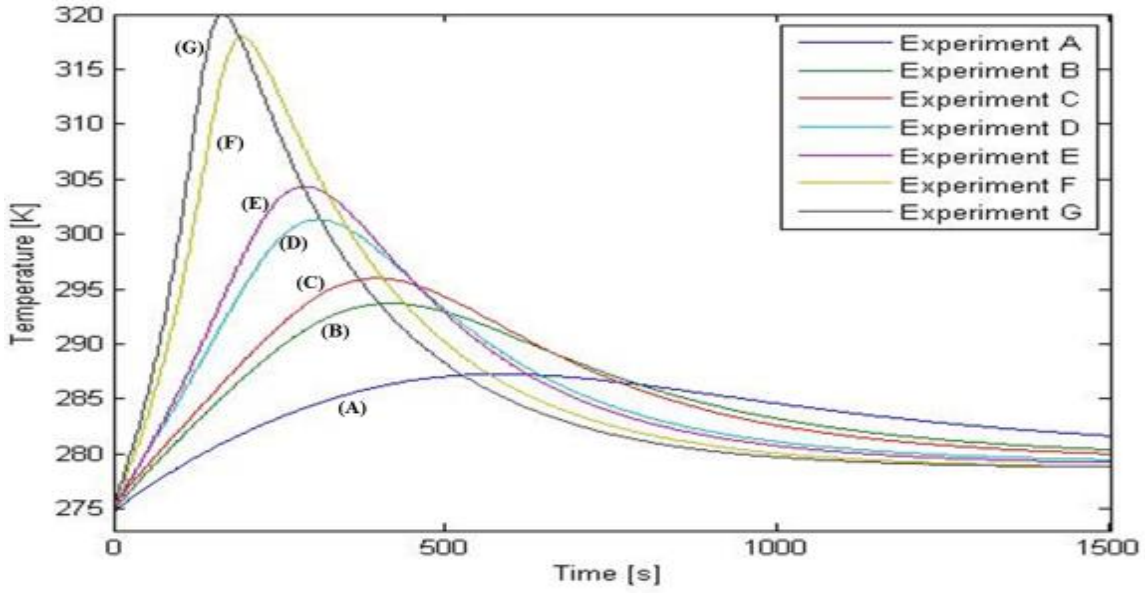

Figure 3.1. Temperature profiles (expressed in K) obtained with respect to the time (expressed in seconds) using a calorimetric reactor in isoperibolic mode, maintaining an approximatively constant jacket temperature of 5.3 °C and using 0.8 mol of acetic anhydride and 7 mol of methanol in order to carry out an acid catalyzed esterification. The different curves are obtained using different concentrations of the catalyst (sulfuric acid), i.e. 16 mol/m^3 for curve (A), 29 mol/m^3 for curve (B), 40 mol/m^3 for curve (C), 45 mol/m^3 for curve (D), 52 mol/m^3 for curve (E), 81 mol/m^3 for curve (F) and 100 mol/m^3 for curve (G).

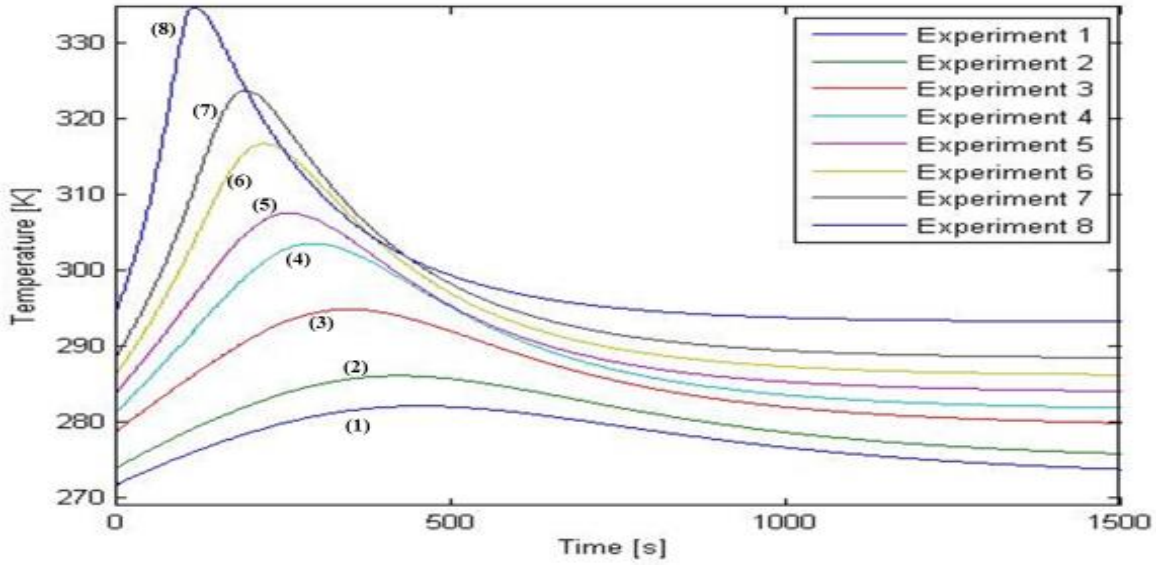

Figure 3.2. Temperature profiles (expressed in K) obtained with respect to the time (expressed in seconds) using a calorimetric reactor in isoperibolic mode, using 0.8 mol of acetic anhydride,7 mol of methanol and a concentration of 30 mol/m^3 of sulfuric acid in order to carry out an acid catalyzed esterification. The different curves are obtained at different jacket temperatures, i.e. -2.25 °C for curve (1), 0.3 °C for curve (2), 5.16 °C for curve (3), 7.62 °C for curve (4), 10.07 °C for curve (5), 12.48 °C for curve (6), 14.94 °C for curve (7) and 19.87 °C for curve (8).

In order to obtain an expression for the kinetic constant of the esterification reaction, thus building a model for the considered process, the mass and the isoperibolic energy balances are integrated using a fourth order Runge-Kutta method and using a *MATLAB*® script (that is reported in the compact disk attached to this thesis and briefly described in the Annex) to

perform a minimization of the squared errors between the model and the experimental data, thus obtaining the values of the parameters appearing in the kinetic constant. The expression of the kinetic constant which was chosen to this purpose is the modified Arrhenius one, in order to give a strong theoretical basis to the model and to take into account the temperature dependence of the pre-exponential term. The effect of the catalyst concentration is taken into account considering a linear dependence of the kinetic constant value from it. These procedures leaded to the following expression:

$$k = 164.68 \cdot T^{1.0554} \cdot [H_2SO_4] \cdot e^{-5932.8/T}, \tag{3.1}$$

where $[H_2SO_4]$ is the sulfuric acid concentration expressed in mol/m^3 and the temperature is expressed in kelvin.

The comparison between the model predictions and the experimental data is represented in the following figures (Figure 3.3, 3.4, 3.5 and 3.6).

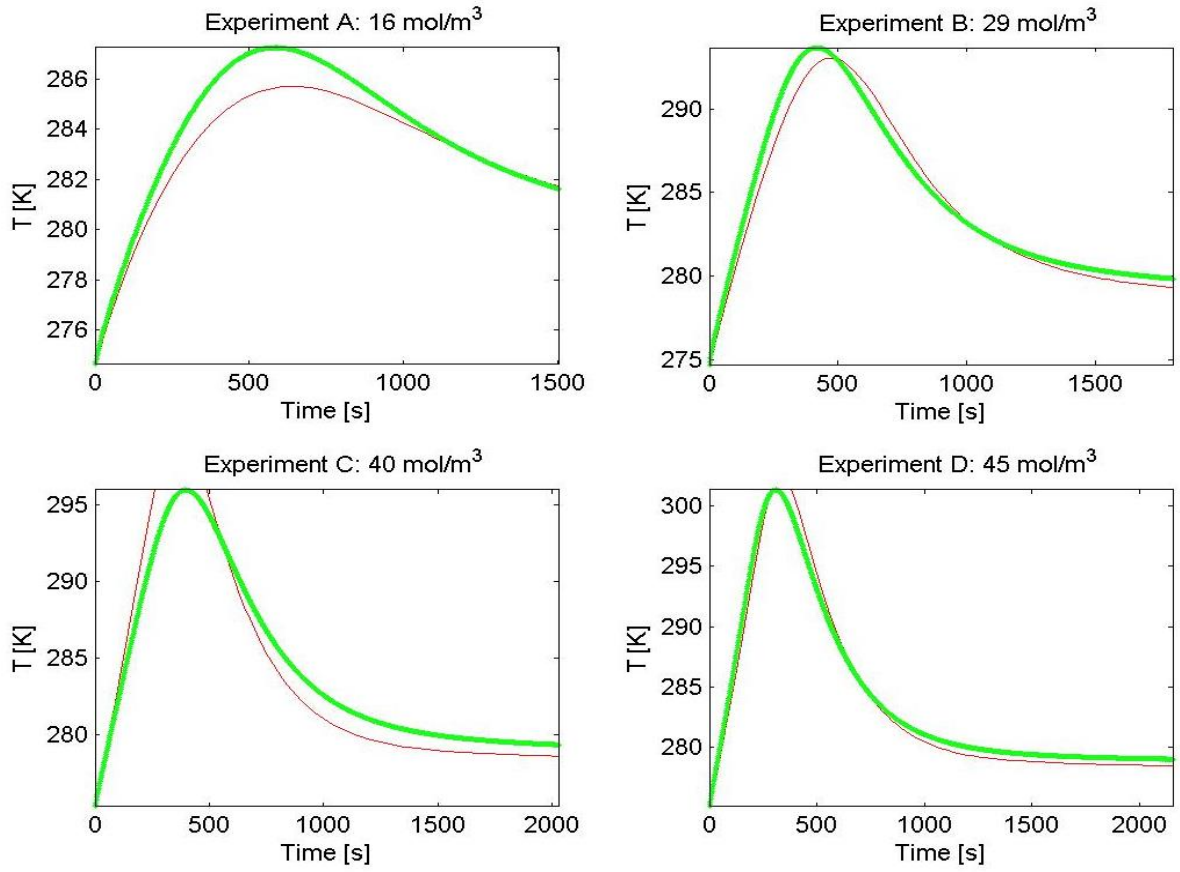

Figure 3.3. Comparison between model predictions and experimental data for the experiments carried out using an approximatively constant jacket temperature of 5.3 °C and different sulfuric acid concentrations, i.e. 16 mol/m^3 for test (A), 29 mol/m^3 for test (B), 40 mol/m^3 for test (C) and 45 mol/m^3 for test (D). The green lines are referred to the experimental data, while the red lines are the model predictions.

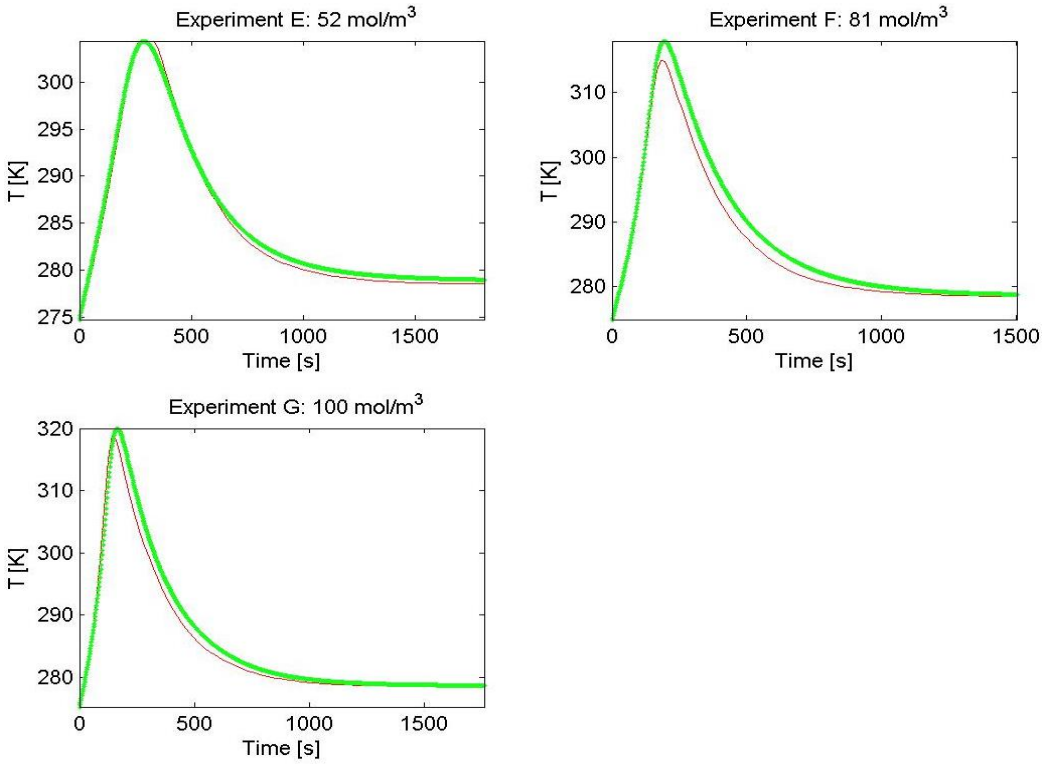

Figure 3.4. Comparison between model predictions and experimental data for the experiments carried out using an approximatively constant jacket temperature of 5.3 °C and different sulfuric acid concentrations, i.e. 52 mol/m^3 for test (E), 81 mol/m^3 for test (F) and 100 mol/m^3 for test (G). The green lines are referred to the experimental data, while the red lines are the model predictions.

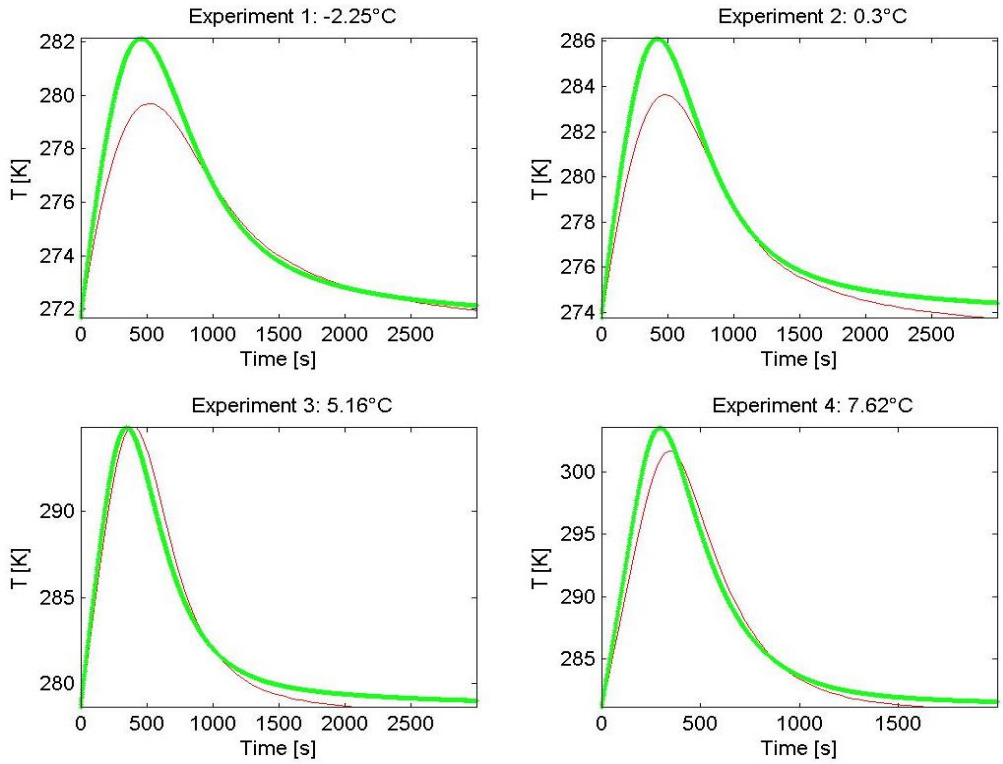

Figure 3.5. Comparison between model predictions and experimental data for the experiments carried out using a sulfuric acid concentration of 30 mol/m^3 and different jacket temperatures, i.e. -2.25 °C for curve (1), 0.3 °C for curve (2), 5.16 °C for curve (3) and 7.62 °C for curve (4). The green lines are referred to the experimental data, while the red lines are the model predictions.

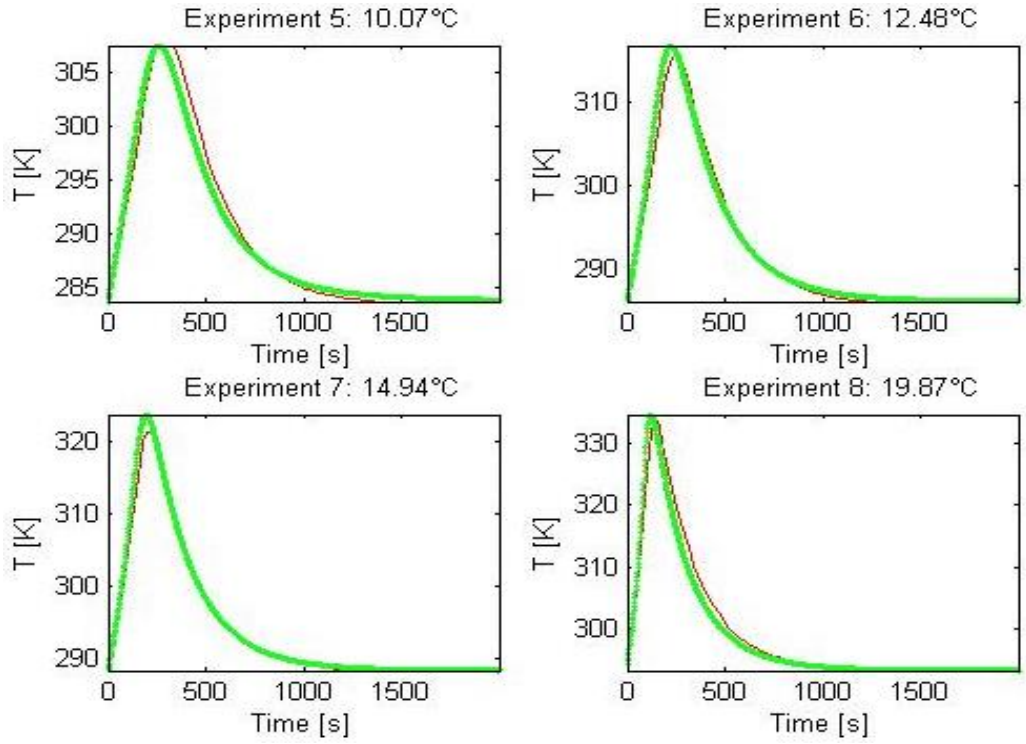

Figure 3.6. Comparison between model predictions and experimental data for the experiments carried out using a sulfuric acid concentration of 30 mol/m^3 and different jacket temperatures, i.e. 10.07 °C for curve (5), 12.48 °C for curve (6), 14.94 °C for curve (7) and 19.87 °C for curve (8). The green lines are referred to the experimental data, while the red lines are the model predictions.

As it can be seen from the previous figures, the developed model seems to predict with a sufficient degree of precision the behavior of the system represented by the experimental data. In the following sections, the runaway criteria mentioned at the beginning of this chapter are applied to both experimental and model data, in order to evaluate quantitatively the accuracy of the model predictions and the differences between the considered criteria.

3.2 Hub and Jones criterion

In order to apply the Hub and Jones criterion, the second derivative of temperature with respect to time is computed for both experimental and model data, in order to find out its maximum value and thus finding out where approximatively is the boundary of the runaway behavior for the considered system. The derivatives are computed numerically as incremental ratios; however, the noise, which is inevitably present in the experimental data, required the application of a filtering technique in order to avoid its amplification in the derivatives calculations. Therefore, a third order Savitzky-Golay filter with a frame length of five experimental points was applied in order to smooth the data without losing information. These calculations are performed using the

MATLAB® scripts that are reported in the compact disk attached to this thesis and briefly described in the Annex.

In the following tables (Table 3.1 and 3.2), the results of the application of this method to the experimental data and to the model are presented.

Table 3.1. Comparison between model predictions and experimental values in the application of the Hub and Jones criterion to the curves referred to tests carried out at a constant jacket temperature of 5.3 °C, using different concentrations of sulfuric acid, 0.7 mol of acetic anhydride and 7 mol of methanol.

Test	H_2SO_4 concentration [mol/m^3]	$10^5 \cdot$Max (d^2T/dt^2) [K/s^2]	
		Exp.	Mod.
A	16	-3.6	-3.87
B	29	-3.57	-5.87
C	40	-0.23	4.75
D	45	13.51	12.96
E	52	28.78	30.44
F	81	230	213.0
G	100	360	458.7

Table 3.2. Comparison between model predictions and experimental values in the application of the Hub and Jones criterion to the curves referred to tests carried out at different jacket temperatures and at a constant sulfuric acid concentration of 30 mol/m^3, using 0.7 mol of acetic anhydride and 7 mol of methanol.

Test	Jacket Temperature [°C]	$10^5 \cdot$Max (d^2T/dt^2) [K/s^2]	
		Exp.	Mod.
1	-2.25	-5.05	-4.88
2	0.3	-4.88	-7.13
3	5.16	-2.52	-4.26
4	7.62	14.39	1.83
5	10.07	18.26	15.44
6	12.48	59.31	39.14
7	14.94	120.0	84.4
8	19.87	480.0	310.0

As can be seen from the previous tables, the second derivative of the temperature with respect to time increases as the jacket temperature and the sulfuric acid concentration increase. The model

seems to predict in a good way the real behavior of the system; however, the error increases close to the boundary between stable and unstable behavior because of the great sensitivity of the system in this zone.

3.3 Thomas and Bowes criterion

In order to apply the Thomas and Bowes criterion, the second derivative of the dimensionless temperature with respect to the dimensionless time is computed for both experimental and model data, in order to find out its maximum value and thus finding out where approximatively is the boundary of the runaway behavior for the considered system. These calculations, even for what concerns the experimental data, require the usage of a model for the reaction: in fact, the knowledge of the kinetic constant value and of the Arrhenius number is fundamental for the reconstruction of the dimensionless temperature vs dimensionless time profiles. Even in this case, a third order Savitzky-Golay filter with a frame length of five points is applied to the experimental curves in order to allow a correct numerical calculation of the second derivatives, as can be seen in the *MATLAB*® scripts reported in the compact disk attached to this thesis and briefly described in the Annex. Considering the dimensionless experimental and model profiles, the following figures can be obtained (Figure 3.7, 3.8, 3.9 and 3.10):

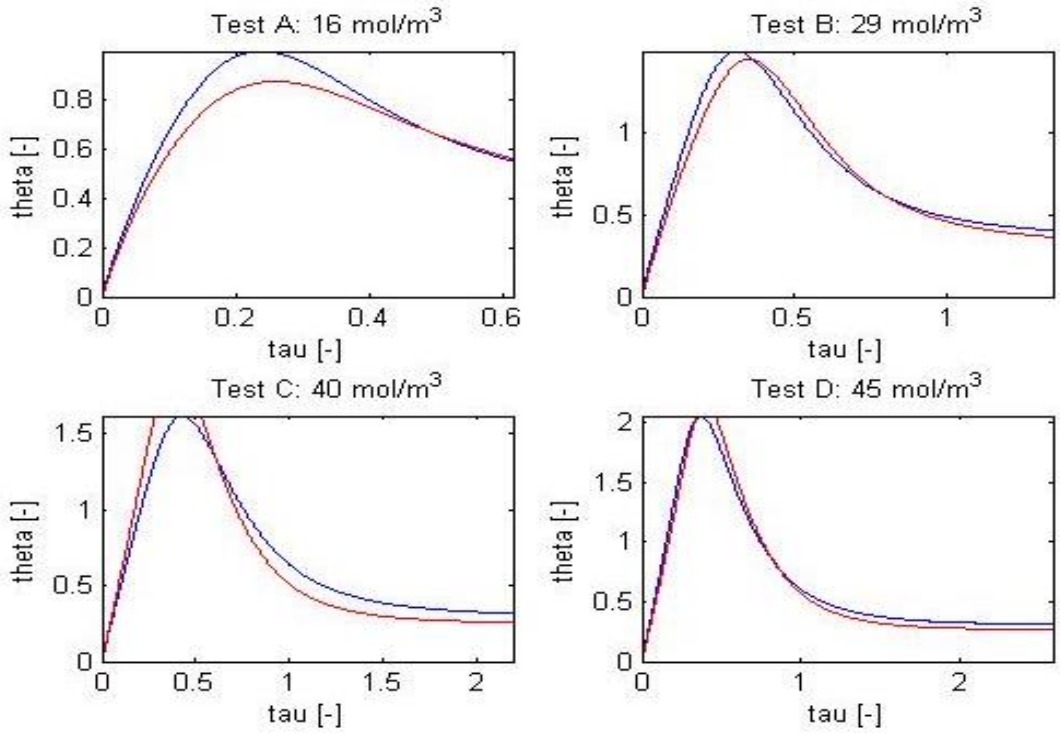

Figure 3.7. Comparison between dimensionless model predictions and dimensionless experimental data for the experiments carried out using an approximatively constant jacket temperature of 5.3 °C and different sulfuric acid concentrations, i.e. 16 mol/m^3 for test (A), 29 mol/m^3 for test (B), 40 mol/m^3 for test (C) and 45 mol/m^3 for test (D). The blue lines are referred to the experimental data, while the red lines are the model predictions.

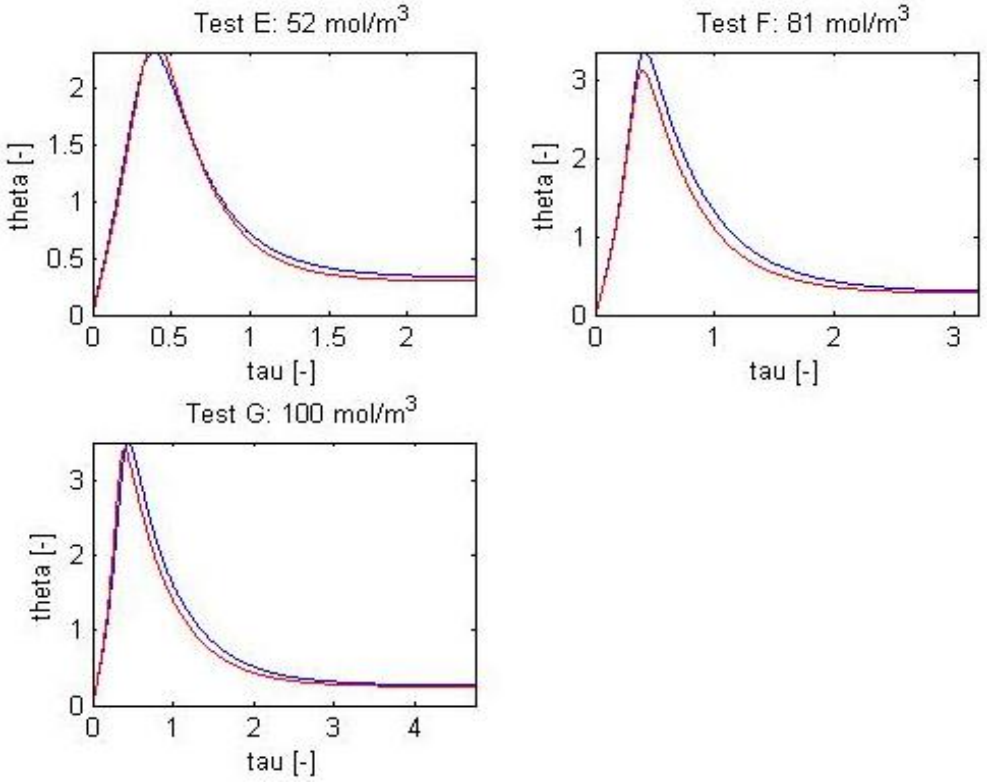

Figure 3.8. Comparison between dimensionless model predictions and dimensionless experimental data for the experiments carried out using an approximatively constant jacket temperature of 5.3 °C and different sulfuric acid concentrations, i.e. 52 mol/m^3 for test (E), 81 mol/m^3 for test (F) and 100 mol/m^3 for test (G). The blue lines are referred to the experimental data, while the red lines are the model predictions.

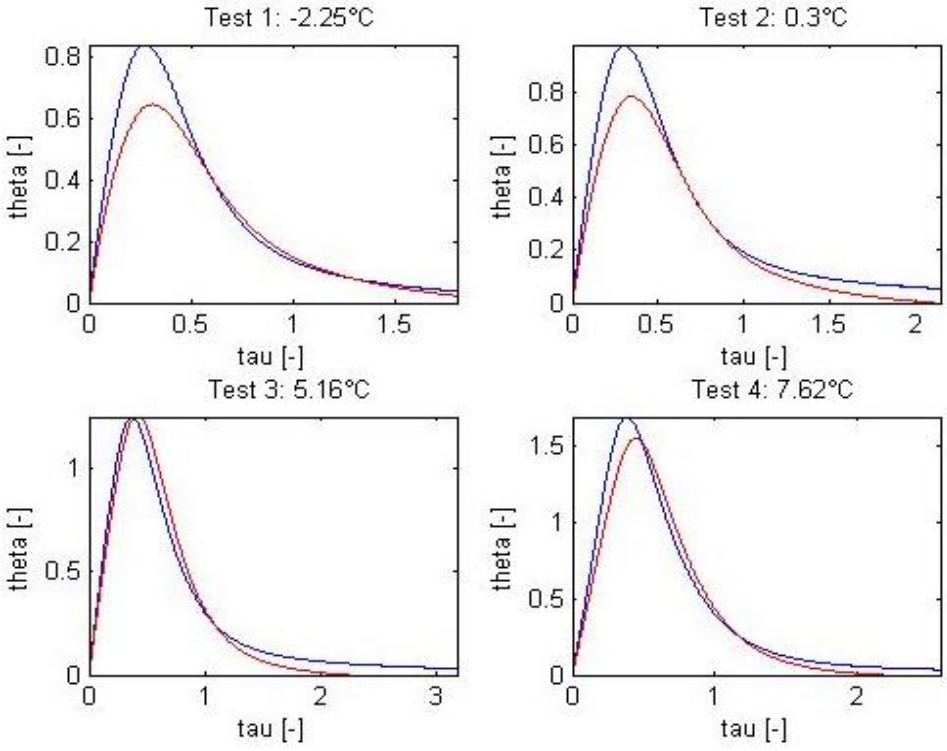

Figure 3.9. Comparison between dimensionless model predictions and dimensionless experimental data for the experiments carried out using a sulfuric acid concentration of 30 mol/m^3 and different jacket temperatures, i.e. -2.25 °C for curve (1), 0.3 °C for curve (2), 5.16 °C for curve (3) and 7.62 °C for curve (4). The blue lines are referred to the experimental data, while the red lines are the model predictions.

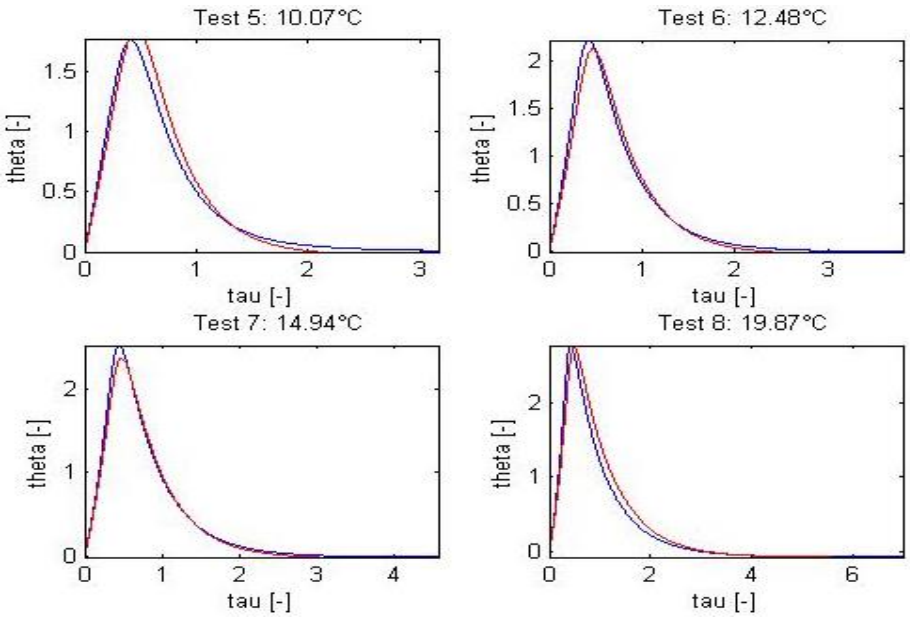

Figure 3.10. Comparison between dimensionless model predictions and dimensionless experimental data for the experiments carried out using a sulfuric acid concentration of 30 mol/m^3 and different jacket temperatures, i.e. 10.07 °C for curve (5), 12.48 °C for curve (6), 14.94 °C for curve (7) and 19.87 °C for curve (8). The blue lines are referred to the experimental data, while the red lines are the model predictions.

As it can be seen from the previous figures, the developed model seems to predict with a sufficient degree of precision the behavior of the system represented by the experimental data. However, in the absence of runaway phenomena, there are higher discrepancies between experimental data and model predictions. In the following tables (Table 3.3 and 3.4), the results of the application of the Thomas and Bowes method to the experimental data and to the model are presented.

Table 3.3. Comparison between model predictions and experimental values in the application of the Thomas and Bowes criterion to the curves referred to tests carried out at a constant jacket temperature of 5.3 °C, using different concentrations of sulfuric acid, 0.7 mol of acetic anhydride and 7 mol of methanol.

Test	H_2SO_4 concentration [mol/m^3]	Max ($d^2\theta/d\tau^2$) [-]	
		Exp.	Mod.
A	16	-17.3	-17.7
B	29	-5.04	-8.63
C	40	-0.15	3.25
D	45	7.36	7.03
E	52	12.26	13.21
F	81	39.73	36.43
G	100	38.97	49.25

Table 3.4. Comparison between dimensionless model predictions and dimensionless experimental values in the application of the Thomas and Bowes criterion to the curves referred to tests carried out at different jacket temperatures and at a constant sulfuric acid concentration of 30 mol/m^3, using 0.7 mol of acetic anhydride and 7 mol of methanol.

Test	Jacket Temperature [°C]	Max ($d^2\theta/d\tau^2$) [-]	
		Exp.	Mod.
1	-2.25	-11.29	-10.91
2	0.3	-7.58	-10.97
3	5.16	-1.71	-2.90
4	7.62	6.49	0.78
5	10.07	4.88	4.27
6	12.48	11.65	7.80
7	14.94	16.31	11.57
8	19.87	26.75	17.03

As can be seen from the previous tables, the second derivative of the dimensionless temperature with respect to the dimensionless time increases as the jacket temperature and the sulfuric acid concentration increase. The model seems to predict in a good way the real behavior of the system; however, the error increases close to the boundary between stable and unstable behavior because of the great sensitivity of the system in this zone. This is exactly what happens applying the Hub and Jones criterion, because the transformation of temperature and time into their dimensionless form is linear.

3.4 Morbidelli and Varma criterion

The application of the Morbidelli and Varma criterion requires the evaluation of the so called sensitivity of the process, i.e. a quantitative measure of the dependence of a variable (e.g. the temperature of the reaction environment) from one or more characteristic parameters (such as jacket temperature or catalyst concentration, for example). In particular, this criterion is based on the consideration that the runaway occurs when the normalized sensitivity of the maximum temperature reaches its maximum itself. It was demonstrated by Morbidelli and Varma ([13]) that, when a system is in the parametrically sensitive region, this criterion is intrinsic, i.e. it provides the same value of the critical Semenov number for thermal runaway independently on the choice of the parameter considered in order to compute the normalized maximum temperature

sensitivity. For this reason, in this section, the normalized sensitivity is analyzed with respect to the jacket temperature and to the sulfuric acid concentration. In order to apply this criterion to the experimental data, the maximum temperature is collected for each experimental run and is expressed in function of the considered characteristic parameter of the process through the usage of a four parameters sigmoid fitting function. In this way, the local and the normalized sensitivities are computed analytically. The Morbidelli and Varma criterion is also applied to the model data, computing in a numeric way the sensitivities after the application of a third order Savitzsky-Golay filter to smooth the small oscillations given by the model itself. These calculations are performed using several *MATLAB*® that are reported in the compact disk attached to this thesis and briefly described in the Annex.

3.4.*1 Sensitivity with respect to the jacket temperature*

In this case, the local sensitivity of the system is defined in the following way:

$$s = \frac{\partial T_{max}}{\partial T_a}, \tag{3.2}$$

where T_{max} (K) is the locus of the temperature maxima for the experimental runs carried out varying the jacket temperature T_a (K). The normalized sensitivity is thus defined according to the following equation:

$$s_{norm} = \frac{T_a}{T_{max}} \cdot \frac{\partial T_{max}}{\partial T_a} \tag{3.3}$$

As it was previously stated, a four parameters sigmoid is used to fit the experimental data, minimizing the errors between the fitting function and the experimental points and thus finding the optimal values of the sigmoid parameters. This procedure leads to the following function:

$$T_{max} = 270.4892 + \frac{86.5375}{1+e^{\left[-\frac{(T_a-284.8807)}{7.4721}\right]}} \tag{3.4}$$

In the following figure (Figure 3.11), the comparison between fitting function and experimental data is shown.

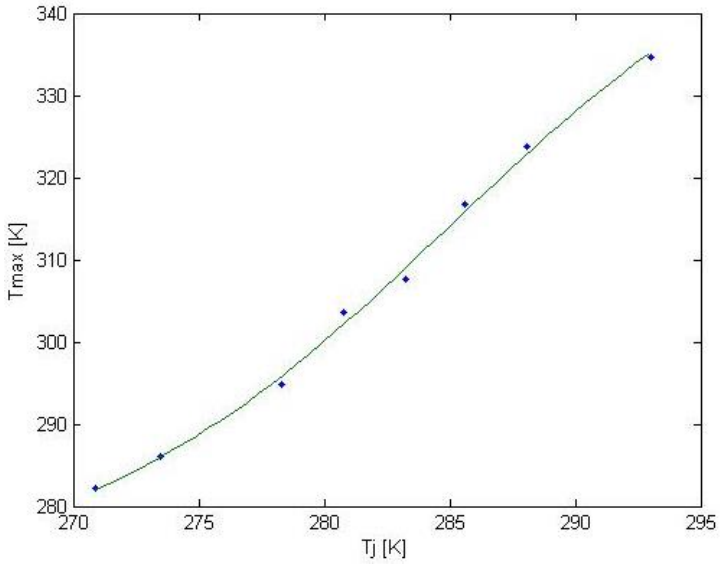

Figure 3.11. Comparison between sigmoidal fitting function (green curve) and maximum temperatures experimental points (blue) for the experiments carried out using a sulfuric acid concentration of 30 mol/m^3 and different jacket temperatures. The temperatures are expressed in kelvin.

The fitting function is used to calculate analytically the local and the normalized sensitivity of the system, obtaining the curves represented in Figure 3.12.

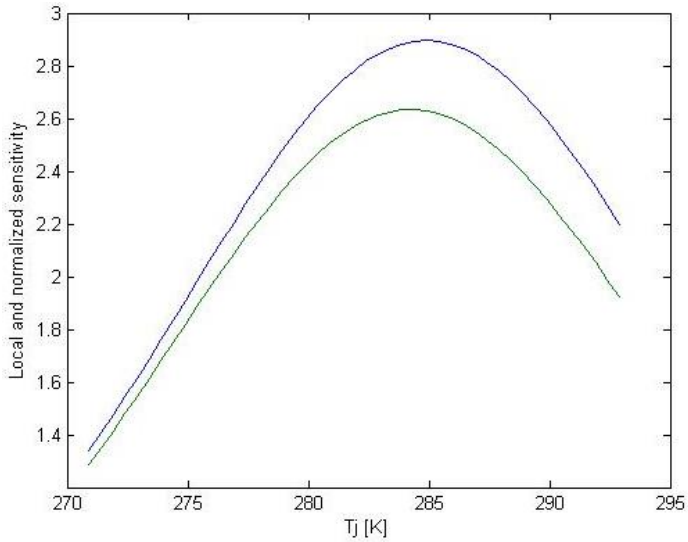

Figure 3.12. Sensitivity of the experimental locus of the maximum temperature with respect to the jacket temperature. The local sensitivity is represented by the blue curve, while the normalized sensitivity is represented by the green one. The temperatures are expressed in kelvin.

As can be seen from the previous figure, the sensitivity is always positive: this means that the maximum temperature increases as the jacket temperature increases. According to the Morbidelli and Varma criterion, the thermal runaway occurs when the normalized sensitivity is at its maximum. Therefore, in this case, the method states that the boundary between stable and unstable behavior of the system is around a jacket temperature of 284.4 K.

The Morbidelli and Varma criterion is also applied to the model data. In the following figure, the comparison between the experimental data and the model prediction is shown.

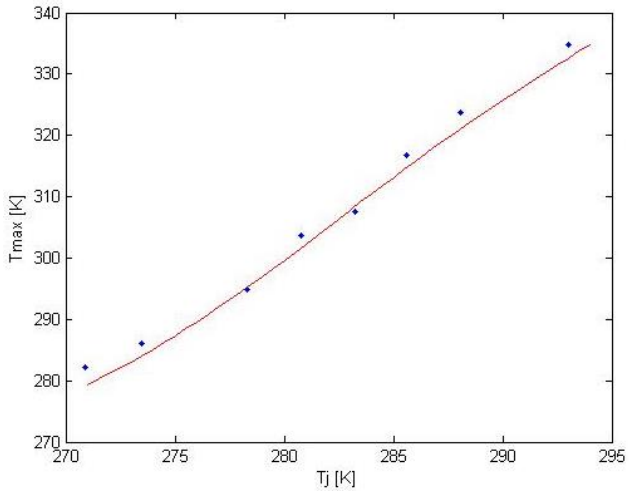

Figure 3.13. Comparison between model predictions (red curve) and maximum temperatures experimental points (blue) for the experiments carried out using a sulfuric acid concentration of 30 mol/m^3 and different jacket temperatures. The temperatures are expressed in kelvin.

In this case, the sensitivities are calculated numerically, applying a Savitzky-Golay filter and approximating the derivative as the incremental ratio. This procedure leads to the following figure:

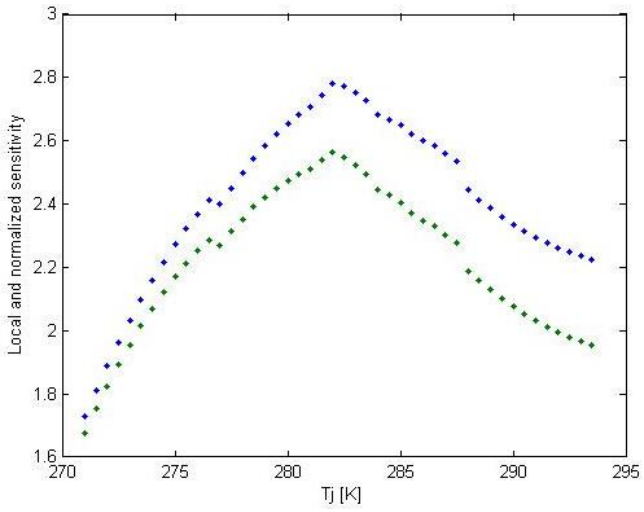

Figure 3.14. Sensitivity of the modelled locus of the maximum temperature with respect to the jacket temperature. The local sensitivity is represented by the blue points, while the normalized sensitivity is represented by the green ones. The temperatures are expressed in kelvin.

Considering the previous figure, it is possible to observe that the Morbidelli and Varma criterion states that the boundary between stable and unstable behavior, concerning the model of the system, is around a jacket temperature of 282 K. Therefore, the model is able to predict in a good way the real behavior of the system.

3.4.2 Sensitivity with respect to the sulfuric acid concentration

In this case, the local sensitivity of the system is defined in the following way:

$$s = \frac{\partial T_{max}}{\partial [H_2SO_4]}, \tag{3.5}$$

where T_{max} (K) is the locus of the temperature maxima for the experimental runs carried out varying the sulfuric acid concentration $[H_2SO_4]$ (mol/m^3). The normalized sensitivity is thus defined according to the following equation:

$$s_{norm} = \frac{[H_2SO_4]}{T_{max}} \cdot \frac{\partial T_{max}}{\partial [H_2SO_4]} \tag{3.6}$$

As it was previously stated, a four parameters sigmoid is used to fit the experimental data, minimizing the errors between the fitting function and the experimental points and thus finding the optimal values of the sigmoid parameters. This procedure leads to the following function:

$$T_{max} = 283.8642 + \frac{38.6050}{1+e^{\left[-\frac{([H_2SO_4]-50.1)}{16.5695}\right]}} \tag{3.7}$$

In the following figure (Figure 3.15), the comparison between fitting function and experimental data is shown.

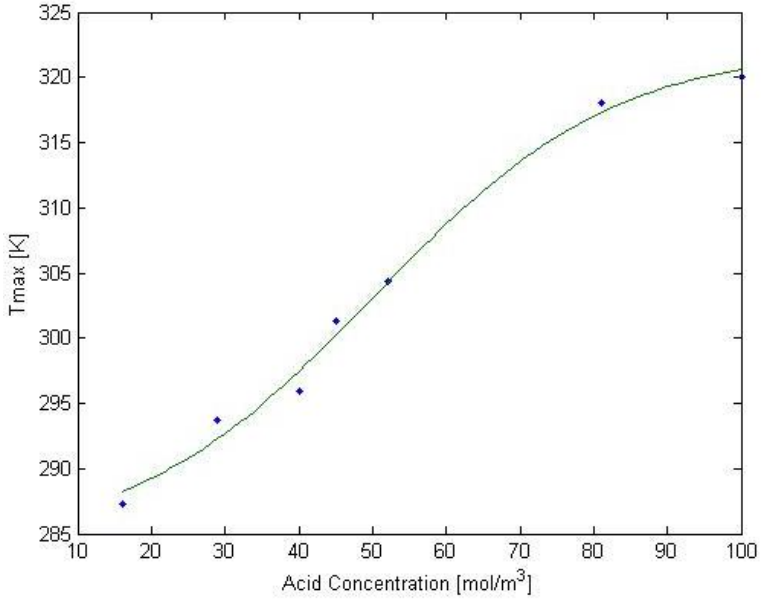

Figure 3.15. Comparison between sigmoidal fitting function (green curve) and maximum temperatures experimental points (blue) for the experiments carried out using a jacket temperature of 5.3°C and different sulfuric acid concentrations. The temperature is expressed in kelvin, while the concentration in mol/m^3.

The fitting function is used to calculate analytically the local and the normalized sensitivity of the system, obtaining the curves represented in Figure 3.16.

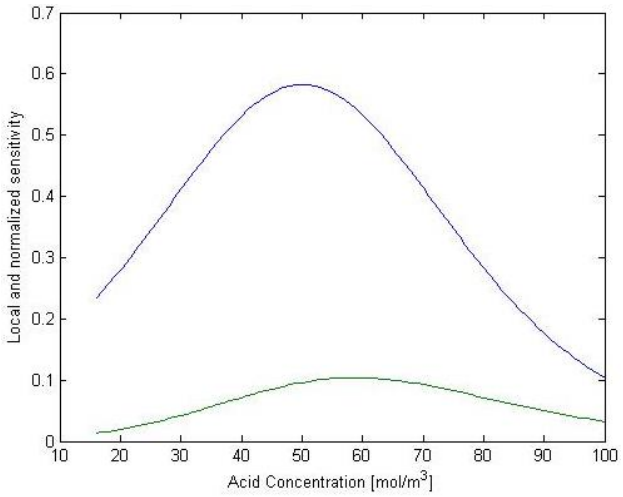

Figure 3.16. Sensitivity of the experimental locus of the maximum temperature with respect to the sulfuric acid concentration. The local sensitivity is represented by the blue curve, while the normalized sensitivity is represented by the green one. The temperature is expressed in kelvin, while the concentration in mol/m^3.

As can be seen from the previous figure, the sensitivity is always positive: this means that the maximum temperature increases as the sulfuric acid concentration increases. According to the Morbidelli and Varma criterion, the thermal runaway occurs when the normalized sensitivity is at its maximum. Therefore, in this case, the method states that the boundary between stable and unstable behavior of the system occurs for a catalyst concentration of approximatively 59 mol/m^3.

The Morbidelli and Varma criterion is also applied to the model data. In the following figure, the comparison between experimental data and the model prediction is shown.

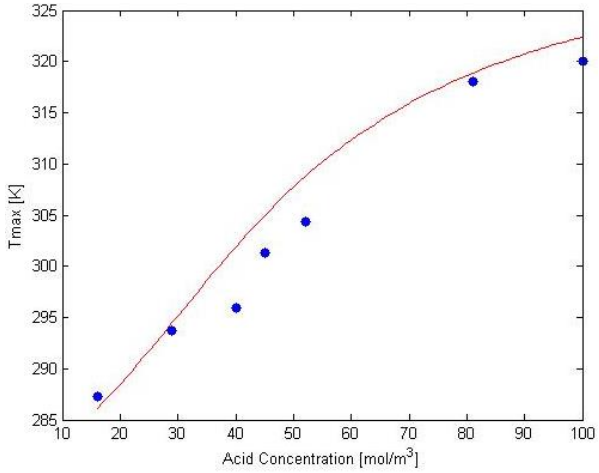

Figure 3.17. Comparison between model predictions (red curve) and maximum temperatures experimental points (blue) for the experiments carried out using a jacket temperature of 5.3°C and different sulfuric acid concentrations. The temperature is expressed in kelvin, while the concentration in mol/m^3.

In this case, the sensitivities are calculated numerically, applying a third order Savitzky-Golay filter and approximating the derivative as the incremental ratio. This procedure leads to the following figure:

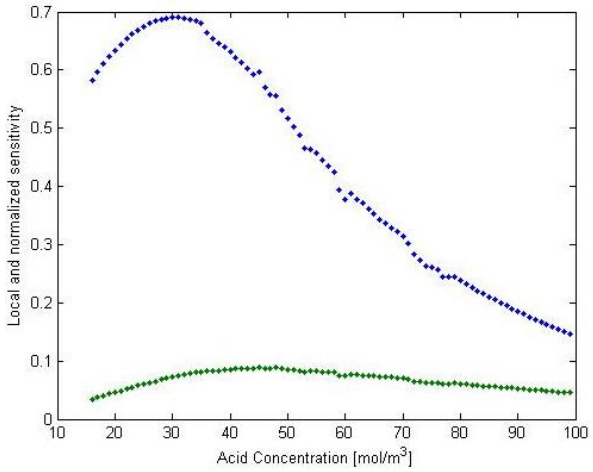

Figure 3.18. Sensitivity of the modeled locus of the maximum temperature with respect to the sulfuric acid concentration. The local sensitivity is represented by the blue points, while the normalized sensitivity is represented by the green ones. The temperature is expressed in kelvin, while the concentration in mol/m^3.

Considering the previous figure, it is possible to observe that the Morbidelli and Varma criterion states that the boundary between stable and unstable behavior, concerning the model of the system, is around a sulfuric acid concentration of 45 mol/m^3. Therefore, the model is not able to predict in a good way the real behavior of the system. This could be related to the model itself, to experimental errors or to the Morbidelli and Varma criterion: this method, in fact, does not work well for reactions characterized by a low Arrhenius number.

3.5 Strozzi and Zaldívar criterion

In order to apply the Strozzi and Zaldívar criterion to both experimental data and developed model (as can be seen in the *MATLAB*® scripts which are reported in the compact disk attached to this thesis and briefly described in the Annex), a phase space reconstruction technique is used. This allows to evaluate the local behavior of the infinitesimal volume variations (dV) of the system in the phase space, which provides an indication of the system divergence (and thus it is an index of the stability of the system itself). In fact, if dV is greater than zero, this means that the system is in runaway conditions. In order to increase the signal to noise ratio, a third order Savitzky-Golay filter is applied to both experimental and model data.

In the following tables (Table 3.5 and 3.6), the results of the application of this method to the experimental data and to the model are presented.

Table 3.5. Comparison between model predictions and experimental values in the application of the Strozzi and Zaldívar criterion to the curves referred to tests carried out at a constant jacket temperature of 5.3 °C, using different concentrations of sulfuric acid, 0.7 mol of acetic anhydride and 7 mol of methanol.

Test	H_2SO_4 concentration [mol/m^3]	$10^4 \cdot$Max (dV)	
		Exp.	Mod.
A	16	-2.6	-2.3
B	29	-2.6	-4.1
C	40	-0.8	5.4
D	45	16.6	17.0
E	52	40.4	49.3
F	81	885	798
G	100	1822	2582

Table 3.6. Comparison between model predictions and experimental values in the application of the Strozzi and Zaldívar criterion to the curves referred to tests carried out at different jacket temperatures and at a constant sulfuric acid concentration of 30 mol/m^3, using 0.7 mol of acetic anhydride and 7 mol of methanol.

Test	Jacket Temperature [°C]	$10^4 \cdot$Max (dV)	
		Exp.	Mod.
1	-2.25	-2.4	-1.6
2	0.3	-3.3	-2.4
3	5.16	-3.0	-2.8
4	7.62	15.3	2.9
5	10.07	21.9	18.7
6	12.48	119	70
7	14.94	334	215
8	19.87	2887	1456

As can be seen from the previous tables, the maximum values of dV tend to increase as the jacket temperature and the sulfuric acid concentration increase. The model seems to predict in a good way the real behavior of the system; however, the error increases close to the boundary between stable and unstable behavior because of the great sensitivity of the system in this zone.

3.6 Comparison with the results obtained by Casson et al.

In order to have a further indication of the effectiveness of the model developed for the system, the above exposed results are compared with the ones obtained in the scientific publication "Comparison of criteria for prediction of runaway reactions in the sulfuric acid catalyzed esterification of acetic anhydride and methanol" by Casson et al. ([17]). The latter, in fact, compared different runaway criteria using the same experimental apparatus utilized in this thesis work; however, a different model was developed for the esterification reaction. In the following sections, the results of the two works are reported, only considering the runaway criteria and the experimental conditions that are common to the two works.

3.6.*1 Comparison of results for the Hub and Jones criterion*

In the following table (Table 3.7), the comparison between the results obtained in this work applying the Hub and Jones criterion to the experimental runs at different sulfuric acid concentration and the ones reported in the work by Casson et al. is exposed.

Table 3.7. Comparison between the results obtained applying the Hub and Jones criterion in this thesis work and in the scientific publication by Casson et al. ([17]). The tests are carried out at a constant jacket temperature of 5.3 °C, using different concentrations of sulfuric acid, 0.7 mol of acetic anhydride and 7 mol of methanol. Both model and experimental results are reported.

H_2SO_4 Concentration [mol/m^3]	$10^5 \cdot$Max (d^2T/dt^2) [K/s^2]		$10^5 \cdot$Max (d^2T/dt^2) Casson et al. [K/s^2]	
	Exp.	Mod.	Exp.	Mod.
29	-3.57	-5.87	-6	-5
45	13.51	12.97	8	20
52	28.78	30.44	20	48
81	230	213	300	290
100	360	459	400	640

In the following table (Table 3.8), the comparison between the results obtained in this work applying the Hub and Jones criterion to the experimental runs at different jacket temperature and the ones reported in the work by Casson et al. is exposed.

Table 3.8. Comparison between the results obtained applying the Hub and Jones criterion in this thesis work and in the scientific publication by Casson et al. ([17]). The tests are carried out at different jacket temperature, using a sulfuric acid concentration of 30 mol/m^3, 0.7 mol of acetic anhydride and 7 mol of methanol. Both model and experimental results are reported.

Jacket temperature [°C]	$10^5 \cdot$Max (d^2T/dt^2) [K/s^2]		$10^5 \cdot$Max (d^2T/dt^2) Casson et al. [K/s^2]	
	Exp.	Mod.	Exp.	Mod.
5.16	-2.52	-4.26	-2	-5
10.07	18.26	15.44	6	10
12.48	59.31	39.14	30	44
14.94	120.0	84.40	93	100
19.87	480.0	310.0	300	260

Observing the previous tables, it can be seen that the model developed in this work is able to predict in a good way the experimental behavior of the system, concerning the application of the Hub and Jones criterion. Furthermore, it can be observed that the discrepancies between model data and experimental ones obtained considering different concentrations of sulfuric acid are lower in this work. Besides of that, it is important to say that the kinetic model of the reaction described in §3.1 has a physical meaning; in contrast to this, the one developed in the scientific publication of Casson et al. is merely empirical.

3.6.2 Comparison of results for the Thomas and Bowes criterion

In the following table (Table 3.9), the comparison between the results obtained in this work applying the Thomas and Bowes criterion to the experimental runs at different sulfuric acid concentration and the ones reported in the work by Casson et al. is exposed.

Table 3.9. Comparison between the results obtained applying the Thomas and Bowes criterion in this thesis work and in the scientific publication by Casson et al. ([17]). The tests are carried out at a constant jacket temperature of 5.3 °C, using different concentrations of sulfuric acid, 0.7 mol of acetic anhydride and 7 mol of methanol. Both model and experimental results are reported.

H_2SO_4 Concentration [mol/m^3]	Max ($d^2\theta/d\tau^2$) [-]		Max ($d^2\theta/d\tau^2$) Casson et al. [-]	
	Exp.	Mod.	Exp.	Mod.
16	-17.3	-17.7	-27	-27
29	-5.04	-8.63	-1	-7
45	7.36	7.03	5	11
52	12.26	13.21	8	20
81	39.73	36.43	30	50
100	38.97	49.25	32	73

In the following table (Table 3.10), the comparison between the results obtained in this work applying the Thomas and Bowes criterion to the experimental runs at different jacket temperature and the ones reported in the work by Casson et al. is exposed.

Table 3.10. Comparison between the results obtained applying the Thomas and Bowes criterion in this thesis work and in the scientific publication by Casson et al. ([17]). The tests are carried out at different jacket temperature, using a sulfuric acid concentration of 30 mol/m^3, 0.7 mol of acetic anhydride and 7 mol of methanol. Both model and experimental results are reported.

Jacket temperature [°C]	Max ($d^2\theta/d\tau^2$) [-]		Max ($d^2\theta/d\tau^2$) Casson et al. [-]	
	Exp.	Mod.	Exp.	Mod.
5.16	-1.71	-2.90	-1	-6
10.07	4.88	4.27	1	6
12.48	11.65	7.80	11	20
14.94	16.31	11.57	19	28
19.87	26.75	17.03	32	31

Observing the previous tables, it can be seen that the model developed in this work is able to predict in a good way the experimental behavior of the system, concerning the application of the Thomas and Bowes criterion. Furthermore, it can be observed that the discrepancies between

model data and experimental ones are lower in this work. Even in this case, it is important to notice that the kinetic model of the reaction used in this thesis has a physical meaning, while the one developed in the scientific publication of Casson et al. is merely empirical.

3.6.*3 Comparison of results for the Strozzi and Zaldívar criterion*

In the following tables (Table 3.11 and Table 3.12), the comparison between the results obtained in this work applying the Strozzi and Zaldívar criterion and the ones reported in the scientific publication by Casson et al. is exposed. The first one is referred to the data obtained considering different sulfuric acid concentrations, while the second one is related to the consideration of different jacket temperatures.

Table 3.11. Comparison between the results obtained applying the Strozzi and Zaldívar criterion in this thesis work and in the scientific publication by Casson et al. ([17]). The tests are carried out at a constant jacket temperature of 5.3 °C, using different concentrations of sulfuric acid, 0.7 mol of acetic anhydride and 7 mol of methanol. Both model and experimental results are reported.

H_2SO_4 Concentration [mol/m^3]	10^4 ·Max (dV)		10^4 ·Max (dV) Casson et al.	
	Exp.	Mod.	Exp.	Mod.
29	-2.6	-4.1	-4	-5
45	16.6	17.0	20	40
52	40.4	49.3	40	100
81	885	798	840	1300
100	1822	2582	1700	2800

Table 3.12. Comparison between the results obtained applying the Strozzi and Zaldívar criterion in this thesis work and in the scientific publication by Casson et al. ([17]). The tests are carried out at different jacket temperature, using a sulfuric acid concentration of 30 mol/m^3, 0.7 mol of acetic anhydride and 7 mol of methanol. Both model and experimental results are reported.

Jacket temperature [°C]	10^4 ·Max (dV)		10^4 ·Max (dV) Casson et al.	
	Exp.	Mod.	Exp.	Mod.
5.16	-3.0	-2.8	-2	-5
10.07	21.9	18.7	5	110
12.48	119	70	73	120
14.94	334	215	230	370
19.87	2887	1456	1500	1200

Observing the previous tables, it can be seen that the model developed in this work is able to predict in a good way the experimental behavior of the system, concerning the application of the Strozzi and Zaldívar criterion. Furthermore, it can be observed that the discrepancies between model data and experimental ones are lower in this work. Even in this case, it is important to notice that the kinetic model of the reaction used in this thesis has a physical meaning (using a modified Arrhenius expression for the kinetic constant), while the one developed by Casson et al. [17] is merely empirical.

3.7 Comments and observations

The results obtained in this work allow to compare the different criteria that can be used in order to predict the thermal runaway of a system in which an exothermic reaction is taking place. Concerning the considered system, it has been shown that basically every runaway criteria applied in this thesis is able to detect the boundary between stable and unstable behavior and that the construction of a model of the system is the major problem in the correct application of many of these methods, often leading to huge errors (especially close to the boundary between the stable and the unstable zones). Besides of that, the need of a model implies a knowledge of the process and a calculation speed that is usually not available in real industrial systems. Therefore, runaway criteria that does not require models (such as the Hub and Jones and the Strozzi and Zaldívar criteria) are the most suitable for the application in real industrial systems subject to a possible runaway.

Chapter 4

Simulation of deviations from the desired behavior of the system

Using the model of the acid catalyzed esterification reaction developed in §3.1, it is also possible to perform adiabatic simulations of the reactive system behavior. This is very important because the adiabatic conditions are the most dangerous ones: when a system cannot exchange heat with its surroundings and an exothermic reaction is occurring, the self-heating rate and the temperature rise reach their maximum values. The usage of the previously developed model thus allows to simulate a sudden failure of the cooling system, e.g. the shift of the system behavior from isoperibolic to adiabatic (worst conditions) or a change in the global heat transfer coefficient of the system itself. In this chapter, after the presentation of the results obtained performing adiabatic simulations, the case of the shift from isoperibolic to adiabatic behavior (at different time instants of the tests) is analyzed. In the last section, the application of the Morbidelli and Varma criterion is exploited in order to study the effect of a change in the global heat transfer coefficient on the system behavior.

4.1 Adiabatic simulations

As previously stated, the model developed in §3.1 allows to perform adiabatic simulations of the sulfuric acid catalyzed esterification of acetic anhydride with methanol. With these data, it is also possible to apply the runaway criteria exposed in §1; however, it appears quite obvious that an adiabatic system in which occurs an exothermic reaction will surely become unstable. In Figure 4.1, the temperature profiles obtained by simulating the adiabatic behavior for the tests performed considering different concentrations of sulfuric acid are exposed. Observing it, it appears quite evident that the system becomes more and more unstable as the concentration of sulfuric acid increases. This qualitative observation is numerically confirmed by the application of the Hub and Jones criterion. It is interesting to notice that the final temperature is the same for every test: this is due to the facts that the simulations consider a complete conversion of the reagents and that the amount of catalyst only affects the rate of the temperature rise but not the final value of the temperature itself.

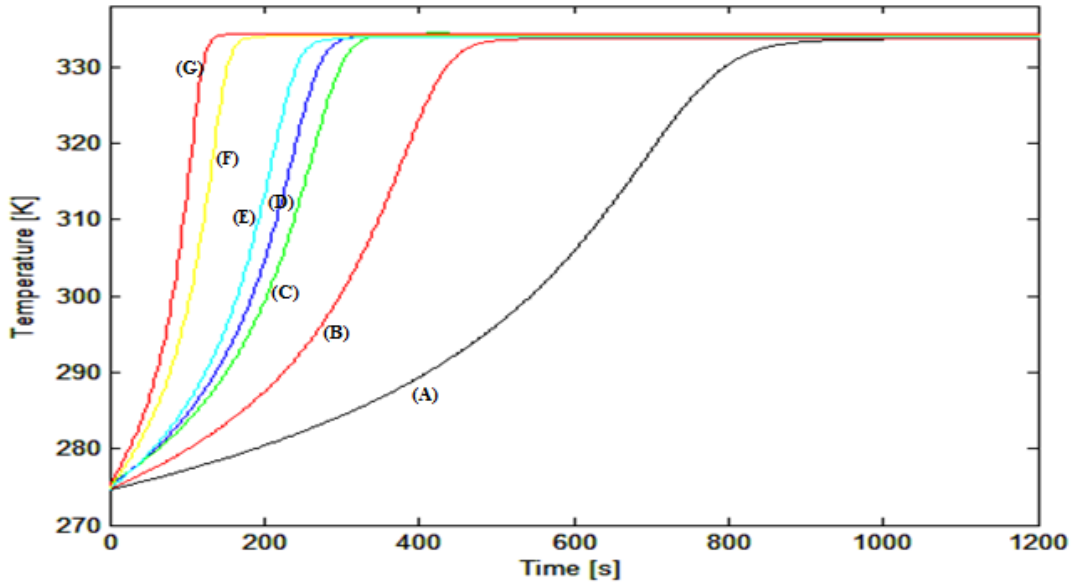

Figure 4.1. Temperature profiles (expressed in K) obtained with respect to the time (expressed in seconds) performing adiabatic simulations and considering 0.8 mol of acetic anhydride and 7 mol of methanol in order to simulate an acid catalyzed esterification. The different curves are obtained considering different concentrations of the catalyst (sulfuric acid), i.e. 16 mol/m^3 for curve (A), 29 mol/m^3 for curve (B), 40 mol/m^3 for curve (C), 45 mol/m^3 for curve (D), 52 mol/m^3 for curve (E), 81 mol/m^3 for curve (F) and 100 mol/m^3 for curve (G).

In Figure 4.2, the temperature profiles obtained by simulating the adiabatic behavior for the tests performed considering different initial temperatures of the system are exposed:

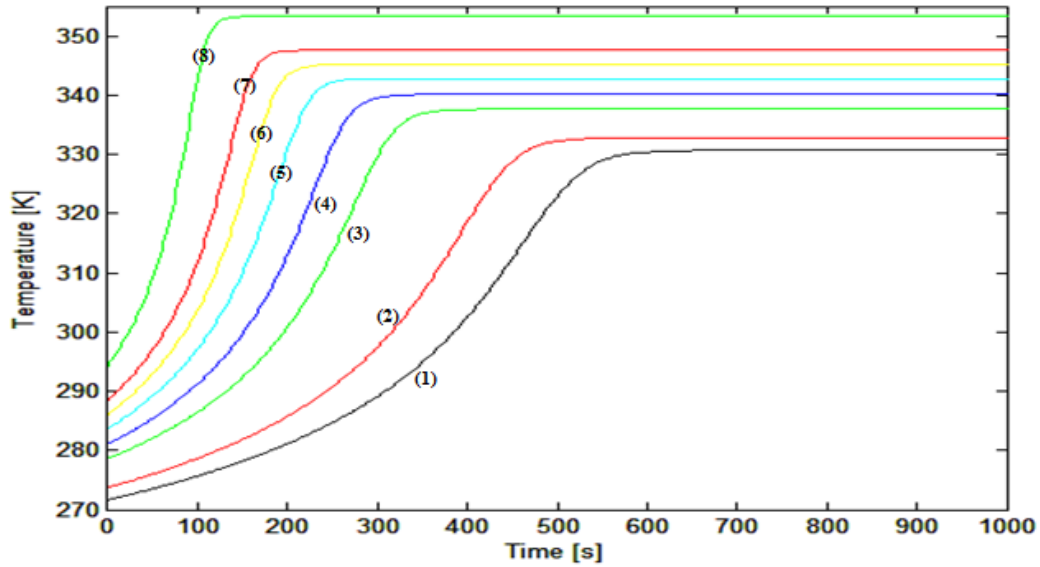

Figure 4.2. Temperature profiles (expressed in K) obtained with respect to the time (expressed in seconds) performing adiabatic simulations and considering a constant sulfuric acid concentration of 30 mol/m^3, 0.8 mol of acetic anhydride and 7 mol of methanol in order to simulate an acid catalyzed esterification. The different curves are obtained considering different initial temperatures i.e. -2.25 °C for curve (1), 0.3 °C for curve (2), 5.16 °C for curve (3), 7.62 °C for curve (4), 10.07 °C for curve (5), 12.48 °C for curve (6), 14.94 °C for curve (7) and 19.87 °C for curve (8).

Observing the previous figure, it appears quite evident that the system becomes more and more unstable as the initial temperature increases. This qualitative observation is numerically confirmed by the application of the Hub and Jones criterion. It is interesting to notice that the final temperature is different for each simulation, but the difference between the final and the initial temperature is the same for everyone (adiabatic temperature rise).

The same tests are performed considering the dimensionless time and temperature, thus applying the Thomas and Bowes criterion in order to verify the presence of a runaway behavior. In Figure 4.3, the dimensionless temperature profiles obtained by simulating the adiabatic behavior for the tests performed considering different concentrations of sulfuric acid are exposed:

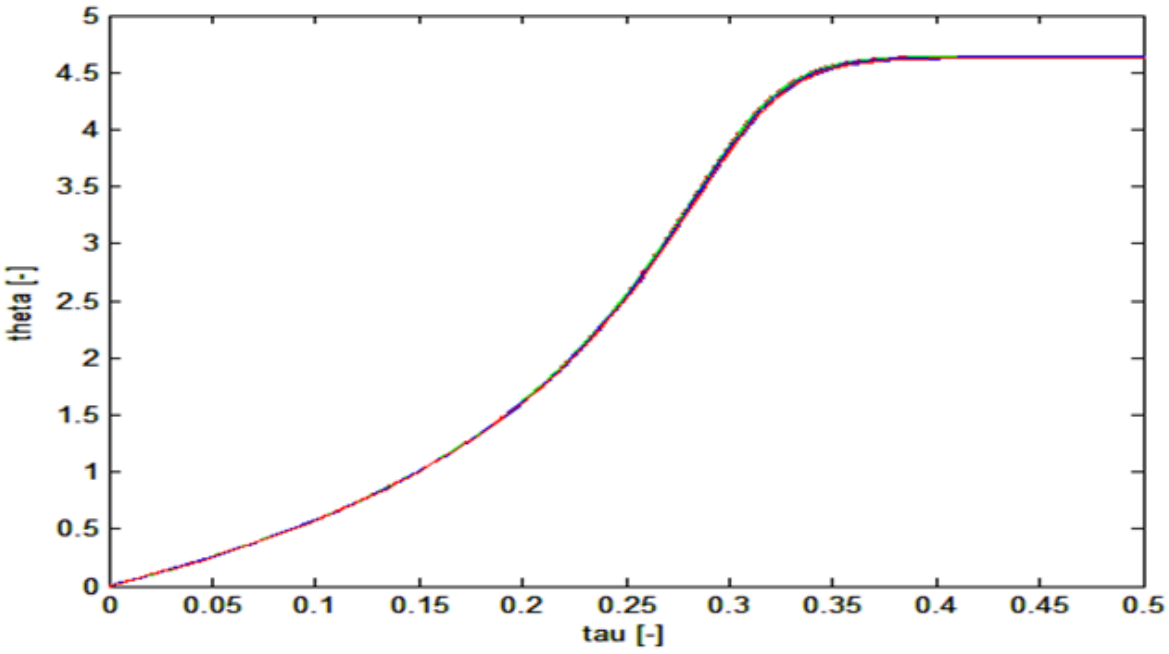

Figure 4.3. Dimensionless temperature profiles obtained with respect to the dimensionless time performing adiabatic simulations and considering 0.8 mol of acetic anhydride and 7 mol of methanol in order to simulate an acid catalyzed esterification. The different curves are obtained considering different concentrations of the catalyst (sulfuric acid), but they appear to be approximatively coincident.

Observing the previous figure, it appears that the curves related to different catalyst concentration are approximatively coincident, if plotted in dimensionless form. This is probably due to the fact that the dimensionless time is computed using the initial value of the kinetic constant, whose expression depends linearly on the sulfuric acid concentration. Of course, the coincidence of the curves does not allow the Thomas and Bowes criterion to detect any difference between them (even if the criterion is able to see that, in each case, the behavior of the system is unstable).

In Figure 4.4, the dimensionless temperature profiles obtained by simulating the adiabatic behavior for the tests performed considering different initial temperatures are exposed:

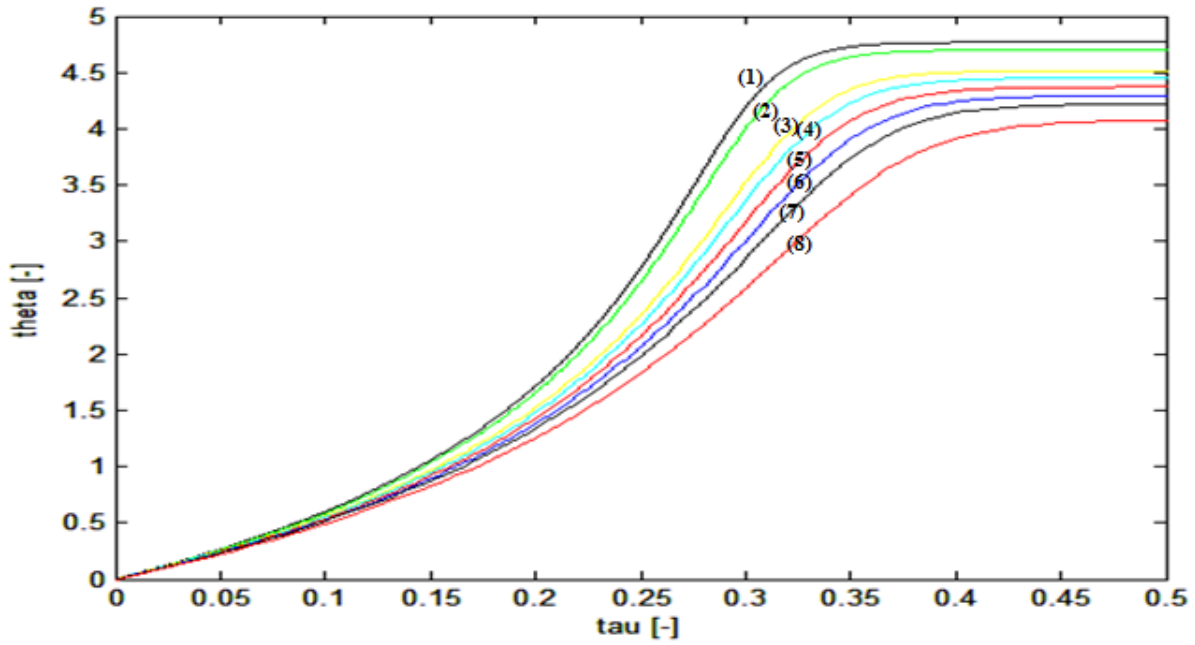

Figure 4.4. Dimensionless temperature profiles obtained with respect to the dimensionless time performing adiabatic simulations and considering a sulfuric acid concentration of 30 mol/m^3, 0.8 mol of acetic anhydride and 7 mol of methanol in order to simulate an acid catalyzed esterification. . The different curves are obtained at different initial temperatures, i.e. -2.25 °C for curve (1), 0.3 °C for curve (2), 5.16 °C for curve (3), 7.62 °C for curve (4), 10.07 °C for curve (5), 12.48 °C for curve (6), 14.94 °C for curve (7) and 19.87 °C for curve (8).

Observing the previous figure, it seems that the intensity of the runaway decreases as the initial temperature increases. This is in contrast with the considerations exposed after the presentation of Figure 4.2 and it is due to the definition of the dimensionless temperature (in which the initial temperature appears at the denominator). Because of this, the Thomas and Bowes criterion cannot be used to evaluate the intensity of the runaway in an adiabatic system: it can only be used to discriminate between stable and unstable behavior.

4.2 Cooling system failure simulation

Using the model developed in §3.1, it is also possible to simulate many failures that can occur in an industrial reactor. For instance, a sudden shift from isoperibolic to adiabatic behavior can be simulated, considering, in this way, the worst possible failure conditions. The time at which this shift occurs is very important: in order to study this effect, several simulations are carried out, considering the tests that, in isoperibolic-only conditions, leaded to a stable behavior.

The temperature profiles obtained through the simulation of a shift from isoperibolic to adiabatic behavior occurring after 100 seconds from the beginning of the tests are represented in Figures 4.5 and 4.6. The first one represents the curves obtained considering different acid concentrations, while the second one concerns the ones obtained at different jacket temperature (in the isoperibolic section, of course). In Figures 4.7 and 4.8, the temperature and conversion profiles are compared for each test.

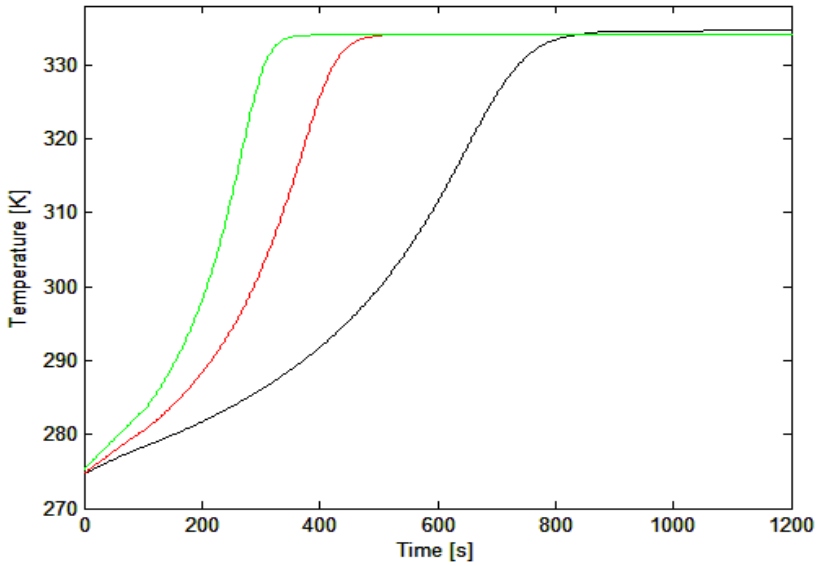

Figure 4.5. Temperature profiles (expressed in K) obtained with respect to the time (expressed in seconds) considering a shift from isoperibolic (jacket temperature equal to 5.3°C) to adiabatic behavior occurring at 100 s and considering 0.8 mol of acetic anhydride and 7 mol of methanol in order to simulate an acid catalyzed esterification. The different curves are obtained considering different concentrations of the catalyst (sulfuric acid), i.e. 16 mol/m^3 for the black curve, 29 mol/m^3 for the red curve and 40 mol/m^3 for the green curve.

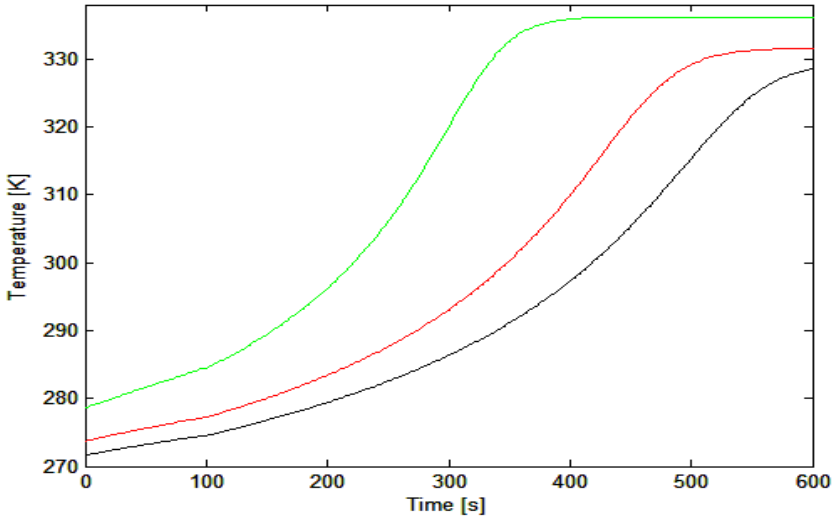

Figure 4.6. Temperature profiles (expressed in K) obtained with respect to the time (expressed in seconds) considering a shift from isoperibolic) to adiabatic behavior occurring at 100 s and considering 0.8 mol of acetic anhydride, 7 mol of methanol and a sulfuric acid concentration of 30 mol/m^3 in order to simulate an acid catalyzed esterification. The different curves are obtained considering different jacket temperatures (for the isoperibolic section, of course), i.e. -2.25°C for the black curve, 0.3°C for the red curve and 5.16°C for the green curve.

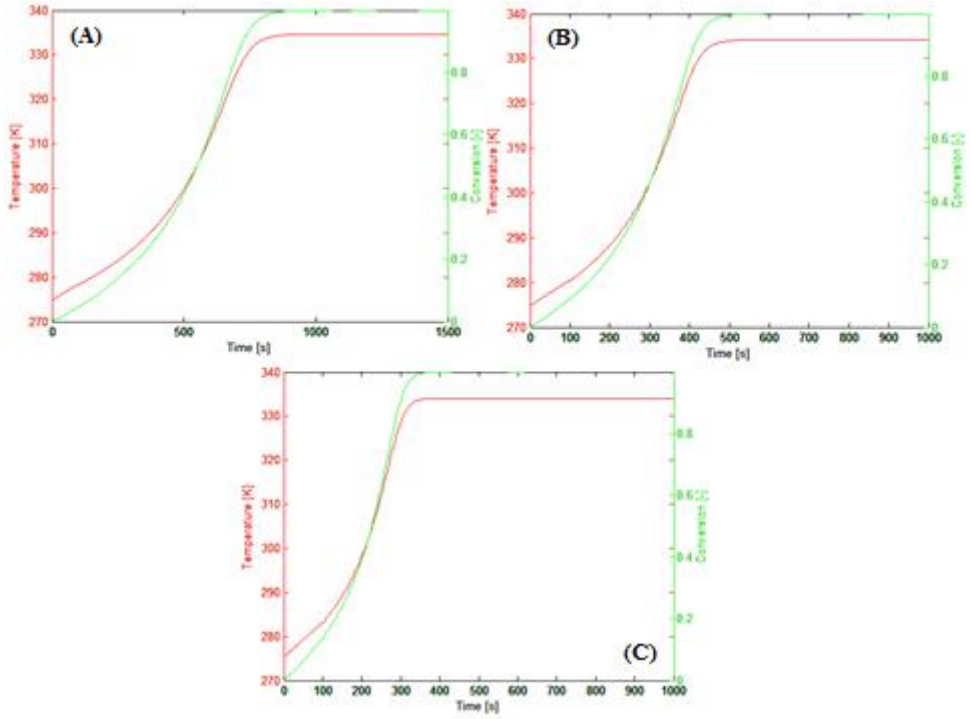

Figure 4.7. Temperature (expressed in K, red lines) and conversion (green lines) profiles obtained with respect to the time (expressed in seconds) considering a shift from isoperibolic (jacket temperature equal to 5.3°C) to adiabatic behavior occurring at 100 s and considering 0.8 mol of acetic anhydride and 7 mol of methanol in order to simulate an acid catalyzed esterification. The different curves are obtained considering different concentrations of the catalyst (sulfuric acid), i.e. 16 mol/m^3 for the (A) curves, 29 mol/m^3 for the (B) curves and 40 mol/m^3 for the (C) curves.

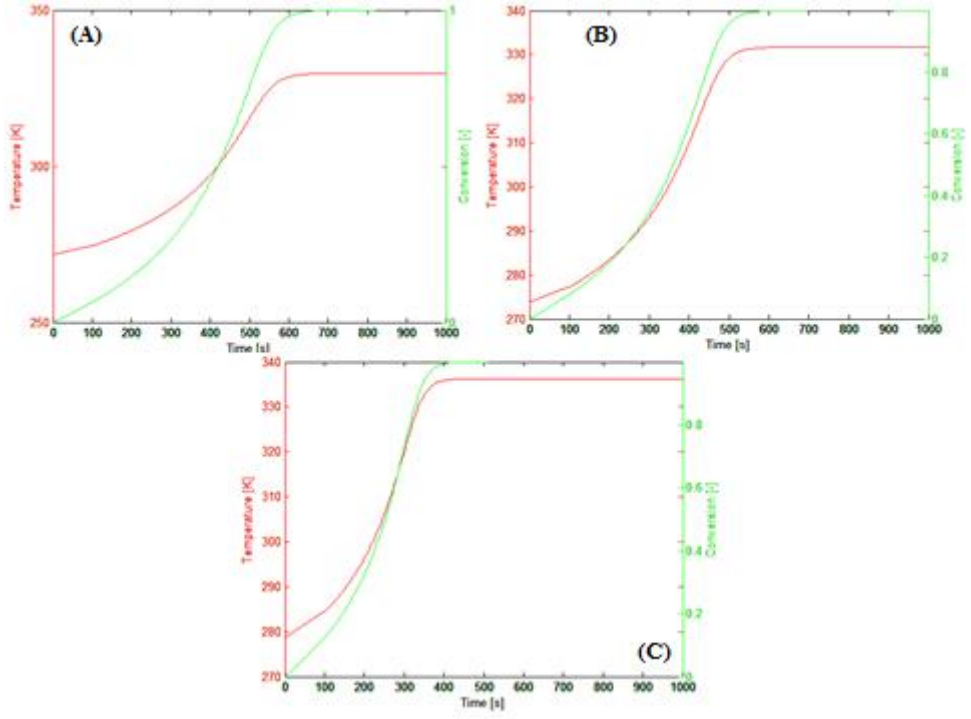

Figure 4.8. Temperature (expressed in K, red lines) and conversion (green lines) profiles obtained with respect to the time (expressed in seconds) considering a shift from isoperibolic) to adiabatic behavior occurring at 100 s and considering 0.8 mol of acetic anhydride, 7 mol of methanol and a sulfuric acid concentration of 30 mol/m^3 in order to simulate an acid catalyzed esterification. The different curves are obtained considering different jacket temperatures (for the isoperibolic section, of course), i.e. -2.25°C for the (A) curves, 0.3°C for the (B) curves and 5.16°C for the (C) curves.

The temperature profiles obtained through the simulation of a shift from isoperibolic to adiabatic behavior occurring after 200 seconds from the beginning of the tests are represented in Figures 4.9 and 4.10. The first one represents the curves obtained considering different acid concentrations, while the second one concerns the ones obtained at different jacket temperature (in the isoperibolic section, of course). In Figures 4.11 and 4.12, the temperature and conversion profiles are compared for each test.

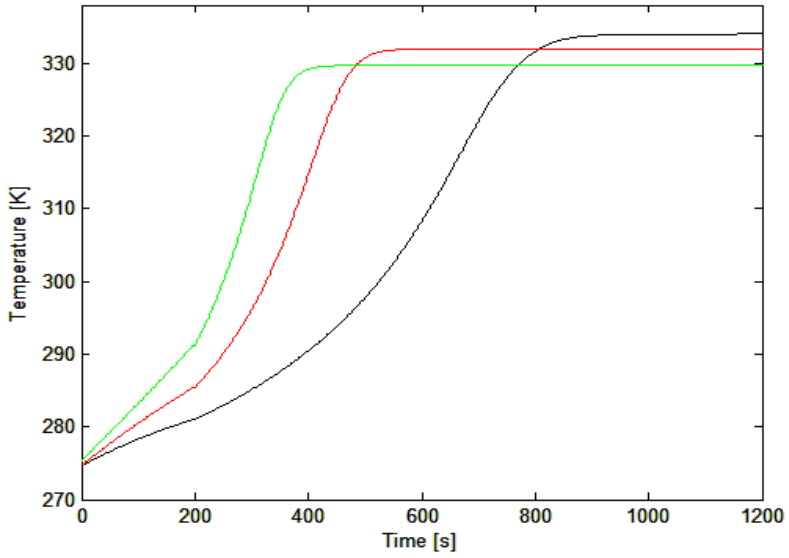

Figure 4.9. Temperature profiles (expressed in K) obtained with respect to the time (expressed in seconds) considering a shift from isoperibolic (jacket temperature equal to 5.3°C) to adiabatic behavior occurring at 200 s and considering 0.8 mol of acetic anhydride and 7 mol of methanol in order to simulate an acid catalyzed esterification. The different curves are obtained considering different concentrations of the catalyst (sulfuric acid), i.e. 16 mol/m^3 for the black curve, 29 mol/m^3 for the red curve and 40 mol/m^3 for the green curve.

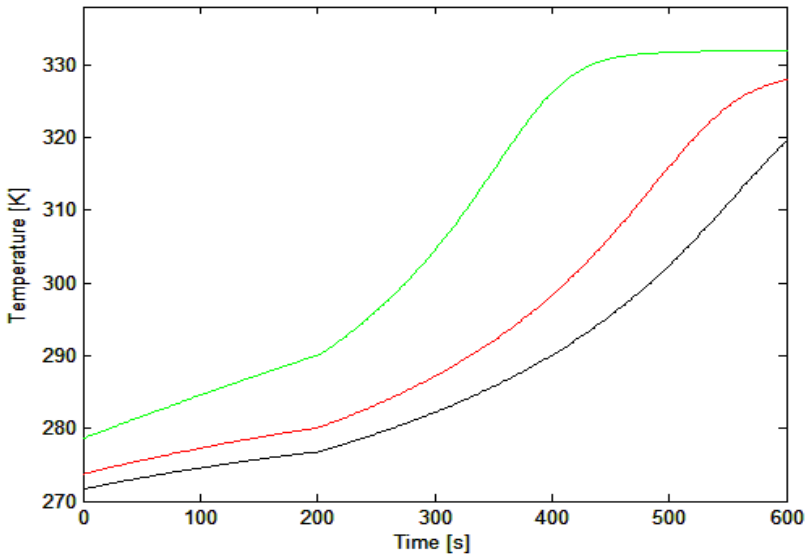

Figure 4.10. Temperature profiles (expressed in K) obtained with respect to the time (expressed in seconds) considering a shift from isoperibolic) to adiabatic behavior occurring at 200 s and considering 0.8 mol of acetic anhydride, 7 mol of methanol and a sulfuric acid concentration of 30 mol/m^3 in order to simulate an acid catalyzed esterification. The different curves are obtained considering different jacket temperatures (for the isoperibolic section, of course), i.e. -2.25°C for the black curve, 0.3°C for the red curve and 5.16°C for the green curve.

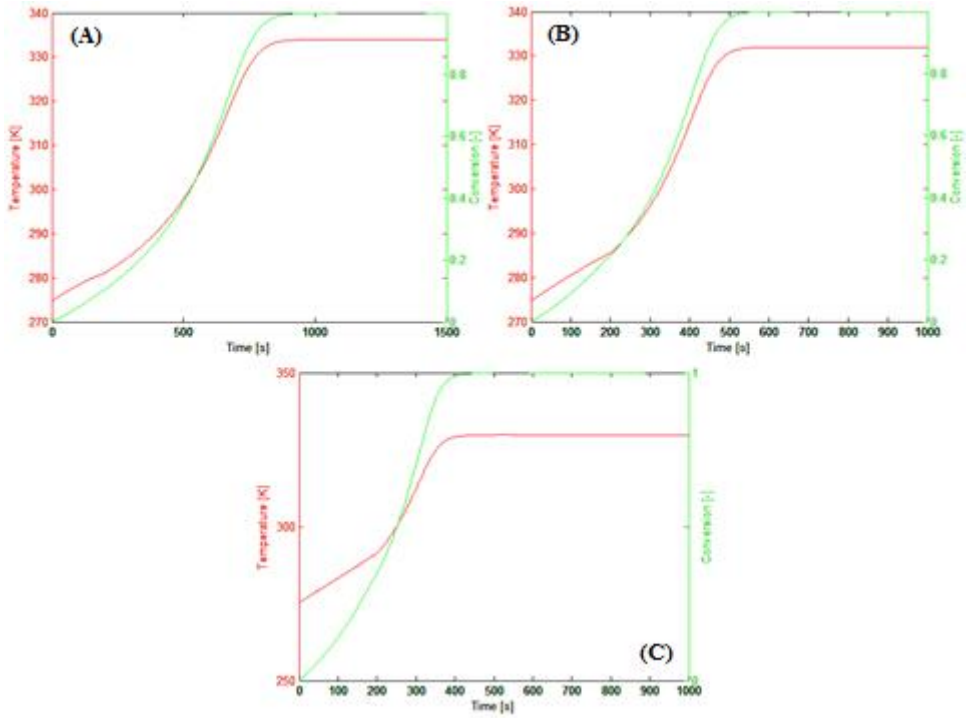

Figure 4.11. Temperature (expressed in K, red lines) and conversion (green lines) profiles obtained with respect to the time (expressed in seconds) considering a shift from isoperibolic (jacket temperature equal to 5.3°C) to adiabatic behavior occurring at 200 s and considering 0.8 mol of acetic anhydride and 7 mol of methanol in order to simulate an acid catalyzed esterification. The different curves are obtained considering different concentrations of the catalyst (sulfuric acid), i.e. 16 mol/m^3 for the (A) curves, 29 mol/m^3 for the (B) curves and 40 mol/m^3 for the (C) curves.

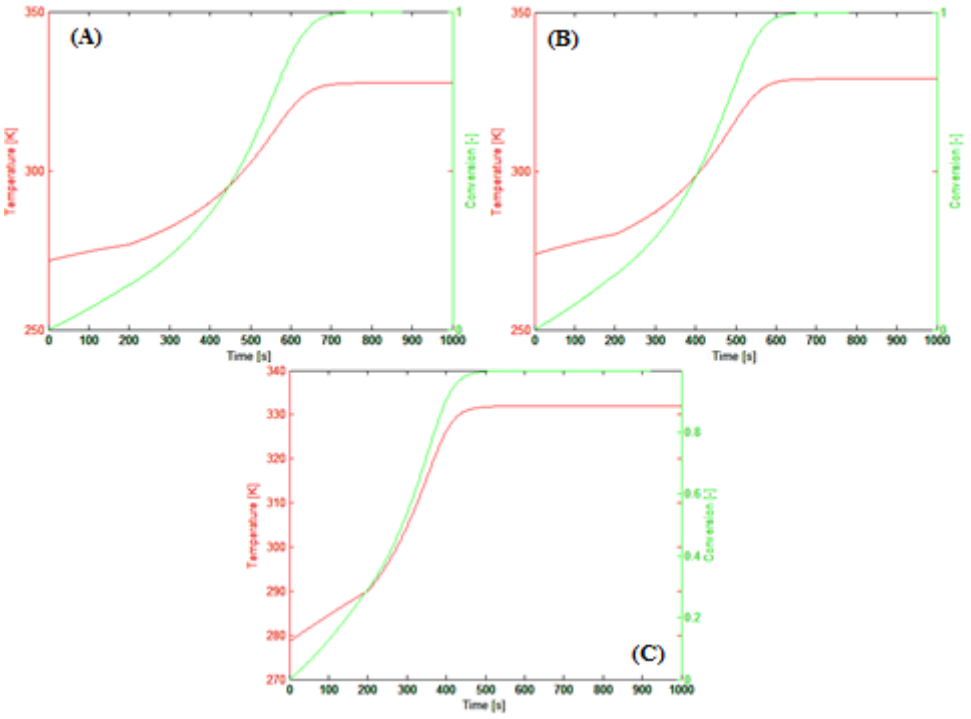

Figure 4.12. Temperature (expressed in K, red lines) and conversion (green lines) profiles obtained with respect to the time (expressed in seconds) considering a shift from isoperibolic) to adiabatic behavior occurring at 200 s and considering 0.8 mol of acetic anhydride, 7 mol of methanol and a sulfuric acid concentration of 30 mol/m^3 in order to simulate an acid catalyzed esterification. The different curves are obtained considering different jacket temperatures (for the isoperibolic section, of course), i.e. -2.25°C for the (A) curves, 0.3°C for the (B) curves and 5.16°C for the (C) curves.

The temperature profiles obtained through the simulation of a shift from isoperibolic to adiabatic behavior occurring after 300 seconds from the beginning of the tests are represented in Figures 4.13 and 4.14. The first one represents the curves obtained considering different acid concentrations, while the second one concerns the ones obtained at different jacket temperature (in the isoperibolic section, of course). In Figures 4.15 and 4.16, the temperature and conversion profiles are compared for each test.

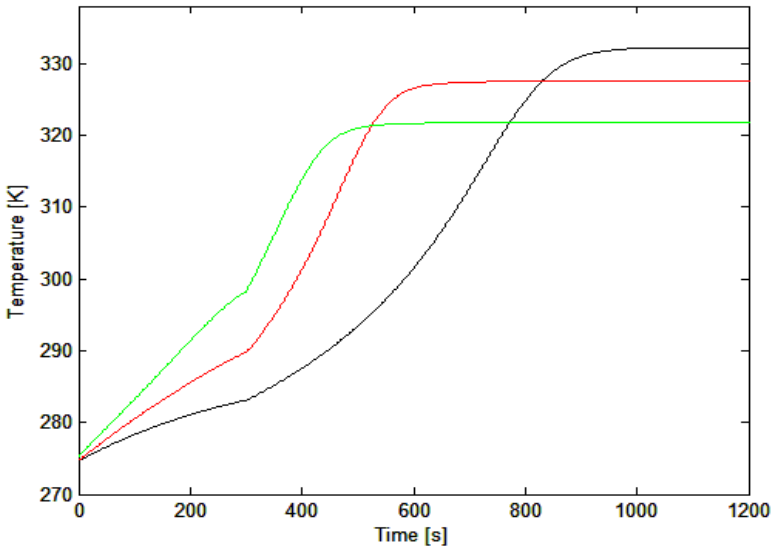

Figure 4.13. Temperature profiles (expressed in K) obtained with respect to the time (expressed in seconds) considering a shift from isoperibolic (jacket temperature equal to 5.3°C) to adiabatic behavior occurring at 300 s and considering 0.8 mol of acetic anhydride and 7 mol of methanol in order to simulate an acid catalyzed esterification. The different curves are obtained considering different concentrations of the catalyst (sulfuric acid), i.e. 16 mol/m^3 for the black curve, 29 mol/m^3 for the red curve and 40 mol/m^3 for the green curve.

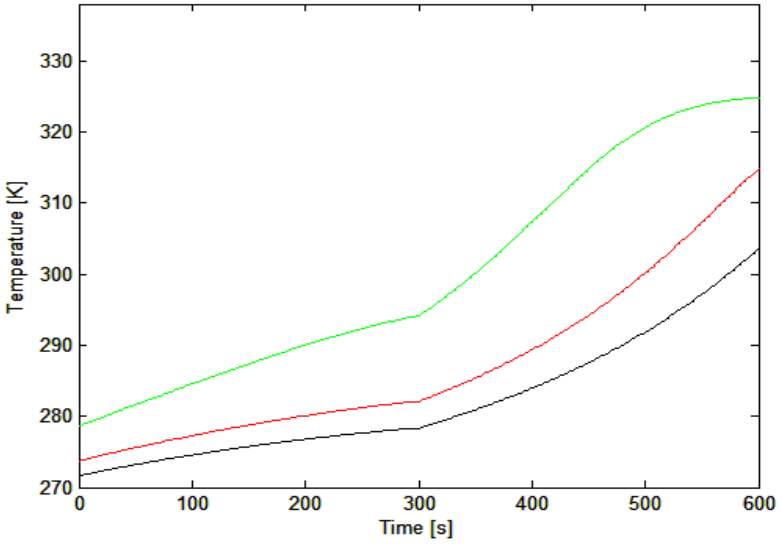

Figure 4.14. Temperature profiles (expressed in K) obtained with respect to the time (expressed in seconds) considering a shift from isoperibolic) to adiabatic behavior occurring at 300 s and considering 0.8 mol of acetic anhydride, 7 mol of methanol and a sulfuric acid concentration of 30 mol/m^3 in order to simulate an acid catalyzed esterification. The different curves are obtained considering different jacket temperatures (for the isoperibolic section, of course), i.e. -2.25°C for the black curve, 0.3°C for the red curve and 5.16°C for the green curve.

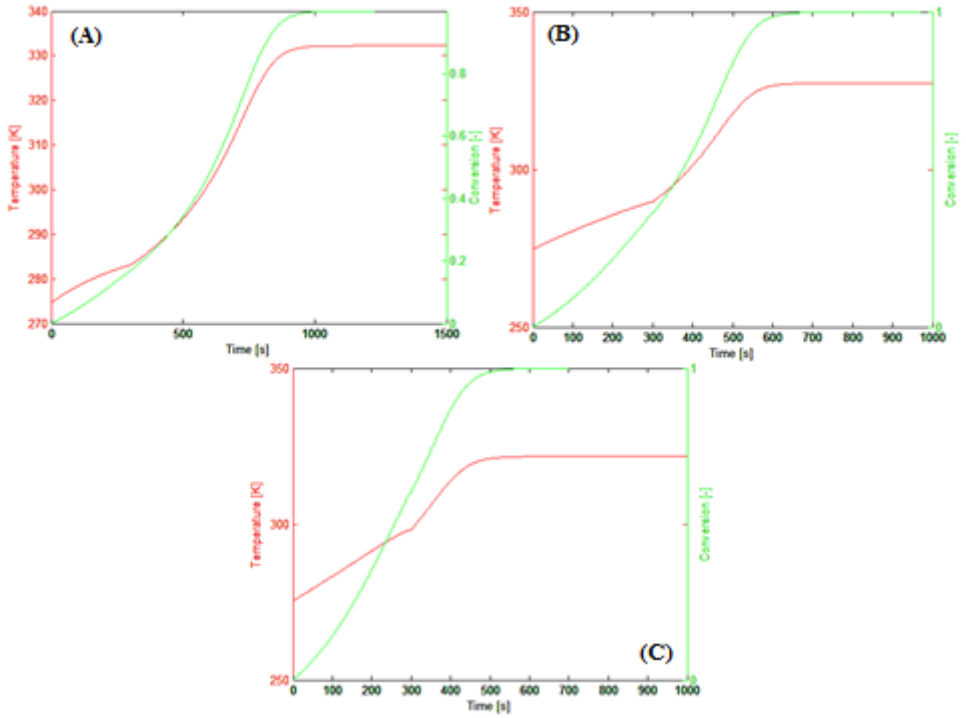

Figure 4.15. Temperature (expressed in K, red lines) and conversion (green lines) profiles obtained with respect to the time (expressed in seconds) considering a shift from isoperibolic (jacket temperature equal to 5.3°C) to adiabatic behavior occurring at 300 s and considering 0.8 mol of acetic anhydride and 7 mol of methanol in order to simulate an acid catalyzed esterification. The different curves are obtained considering different concentrations of the catalyst (sulfuric acid), i.e. 16 mol/m^3 for the (A) curves, 29 mol/m^3 for the (B) curves and 40 mol/m^3 for the (C) curves.

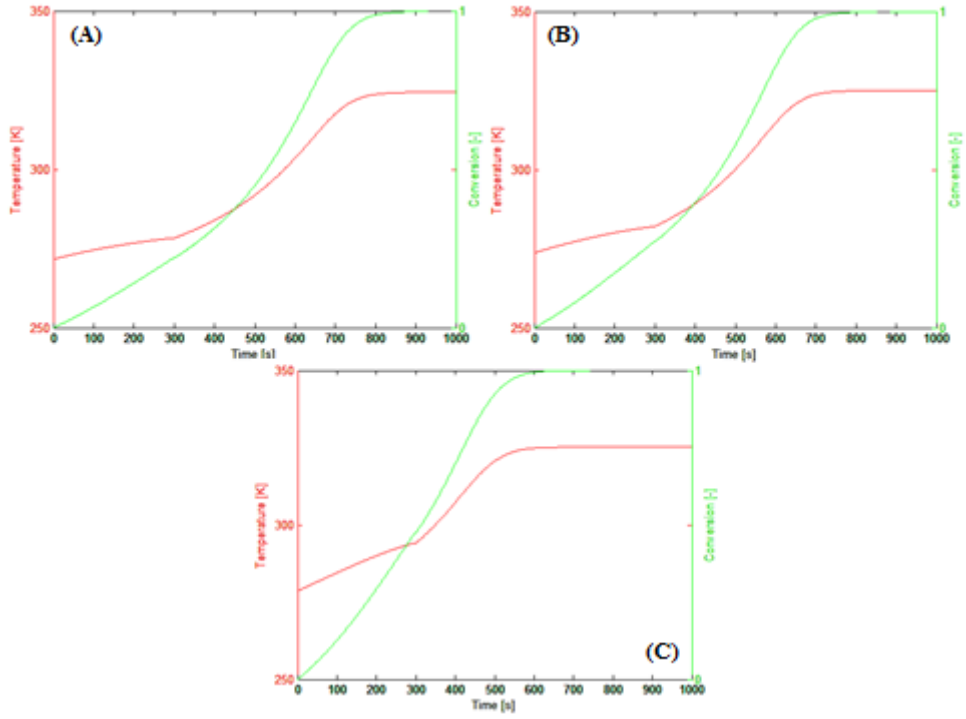

Figure 4.16. Temperature (expressed in K, red lines) and conversion (green lines) profiles obtained with respect to the time (expressed in seconds) considering a shift from isoperibolic) to adiabatic behavior occurring at 300 s and considering 0.8 mol of acetic anhydride, 7 mol of methanol and a sulfuric acid concentration of 30 mol/m^3 in order to simulate an acid catalyzed esterification. The different curves are obtained considering different jacket temperatures (for the isoperibolic section, of course), i.e. -2.25°C for the (A) curves, 0.3°C for the (B) curves and 5.16°C for the (C) curves.

The temperature profiles obtained through the simulation of a shift from isoperibolic to adiabatic behavior occurring after 400 seconds from the beginning of the tests are represented in Figures 4.17 and 4.18. The first one represents the curves obtained considering different acid concentrations, while the second one concerns the ones obtained at different jacket temperature (in the isoperibolic section, of course). In Figures 4.19 and 4.20, the temperature and conversion profiles are compared for each test.

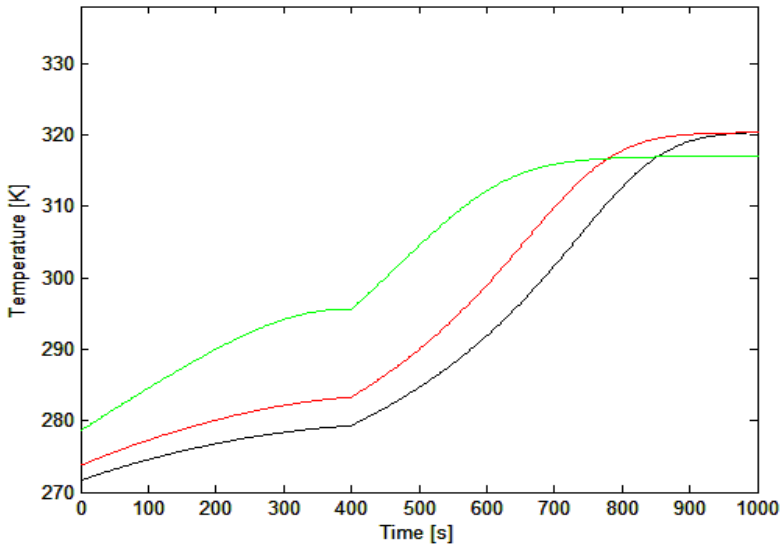

Figure 4.17. Temperature profiles (expressed in K) obtained with respect to the time (expressed in seconds) considering a shift from isoperibolic (jacket temperature equal to 5.3°C) to adiabatic behavior occurring at 400 s and considering 0.8 mol of acetic anhydride and 7 mol of methanol in order to simulate an acid catalyzed esterification. The different curves are obtained considering different concentrations of the catalyst (sulfuric acid), i.e. 16 mol/m^3 for the black curve, 29 mol/m^3 for the red curve and 40 mol/m^3 for the green curve.

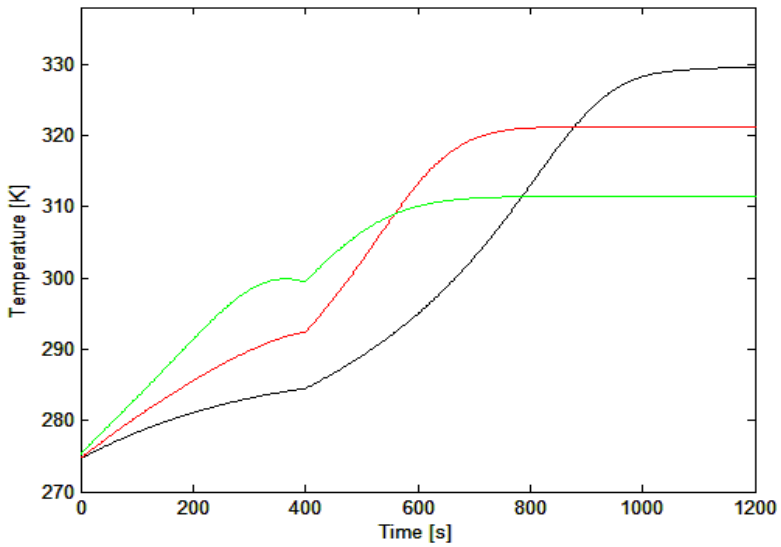

Figure 4.18. Temperature profiles (expressed in K) obtained with respect to the time (expressed in seconds) considering a shift from isoperibolic) to adiabatic behavior occurring at 400 s and considering 0.8 mol of acetic anhydride, 7 mol of methanol and a sulfuric acid concentration of 30 mol/m^3 in order to simulate an acid catalyzed esterification. The different curves are obtained considering different jacket temperatures (for the isoperibolic section, of course), i.e. -2.25°C for the black curve, 0.3°C for the red curve and 5.16°C for the green curve.

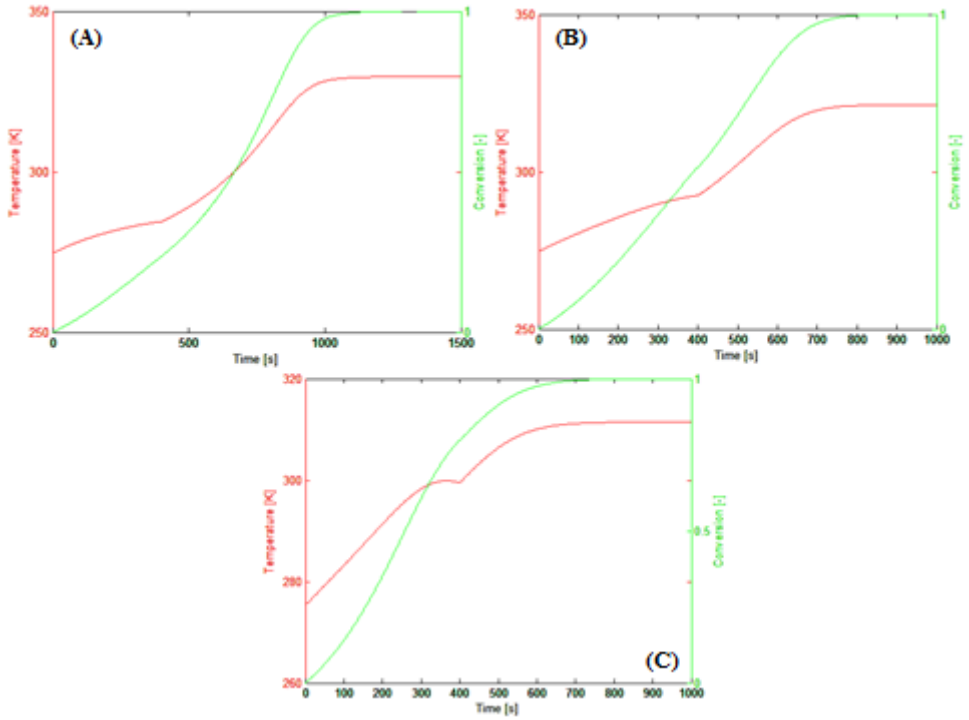

Figure 4.19. Temperature (expressed in K, red lines) and conversion (green lines) profiles obtained with respect to the time (expressed in seconds) considering a shift from isoperibolic (jacket temperature equal to 5.3°C) to adiabatic behavior occurring at 400 s and considering 0.8 mol of acetic anhydride and 7 mol of methanol in order to simulate an acid catalyzed esterification. The different curves are obtained considering different concentrations of the catalyst (sulfuric acid), i.e. 16 mol/m^3 for the (A) curves, 29 mol/m^3 for the (B) curves and 40 mol/m^3 for the (C) curves.

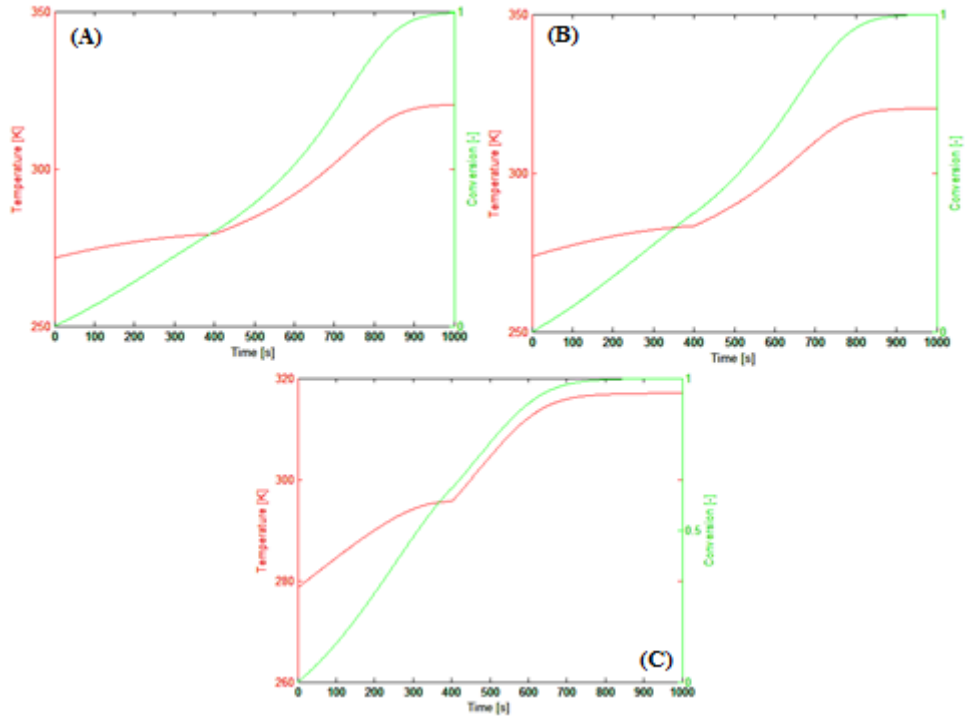

Figure 4.20. Temperature (expressed in K, red lines) and conversion (green lines) profiles obtained with respect to the time (expressed in seconds) considering a shift from isoperibolic) to adiabatic behavior occurring at 400 s and considering 0.8 mol of acetic anhydride, 7 mol of methanol and a sulfuric acid concentration of 30 mol/m^3 in order to simulate an acid catalyzed esterification. The different curves are obtained considering different jacket temperatures (for the isoperibolic section, of course), i.e. -2.25°C for the (A) curves, 0.3°C for the (B) curves and 5.16°C for the (C) curves.

The temperature profiles obtained through the simulation of a shift from isoperibolic to adiabatic behavior occurring after 500 seconds from the beginning of the tests are represented in Figures 4.21 and 4.22. The first one represents the curves obtained considering different acid concentrations, while the second one concerns the ones obtained at different jacket temperature (in the isoperibolic section, of course). In Figures 4.23 and 4.24, the temperature and conversion profiles are compared for each test.

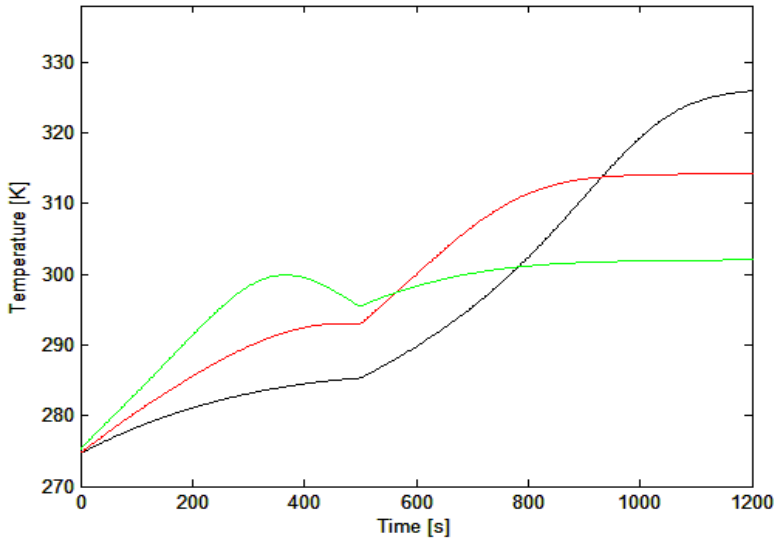

Figure 4.21. Temperature profiles (expressed in K) obtained with respect to the time (expressed in seconds) considering a shift from isoperibolic (jacket temperature equal to 5.3°C) to adiabatic behavior occurring at 500 s and considering 0.8 mol of acetic anhydride and 7 mol of methanol in order to simulate an acid catalyzed esterification. The different curves are obtained considering different concentrations of the catalyst (sulfuric acid), i.e. 16 mol/m^3 for the black curve, 29 mol/m^3 for the red curve and 40 mol/m^3 for the green curve.

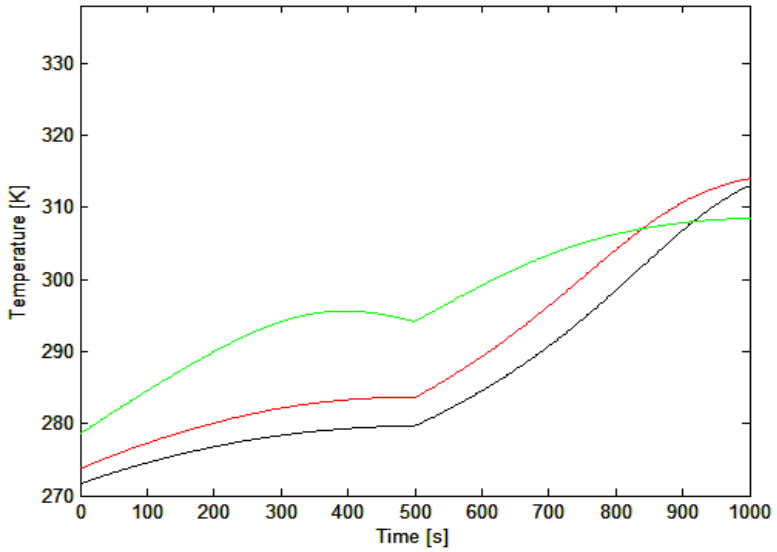

Figure 4.22. Temperature profiles (expressed in K) obtained with respect to the time (expressed in seconds) considering a shift from isoperibolic) to adiabatic behavior occurring at 500 s and considering 0.8 mol of acetic anhydride, 7 mol of methanol and a sulfuric acid concentration of 30 mol/m^3 in order to simulate an acid catalyzed esterification. The different curves are obtained considering different jacket temperatures (for the isoperibolic section, of course), i.e. -2.25°C for the black curve, 0.3°C for the red curve and 5.16°C for the green curve.

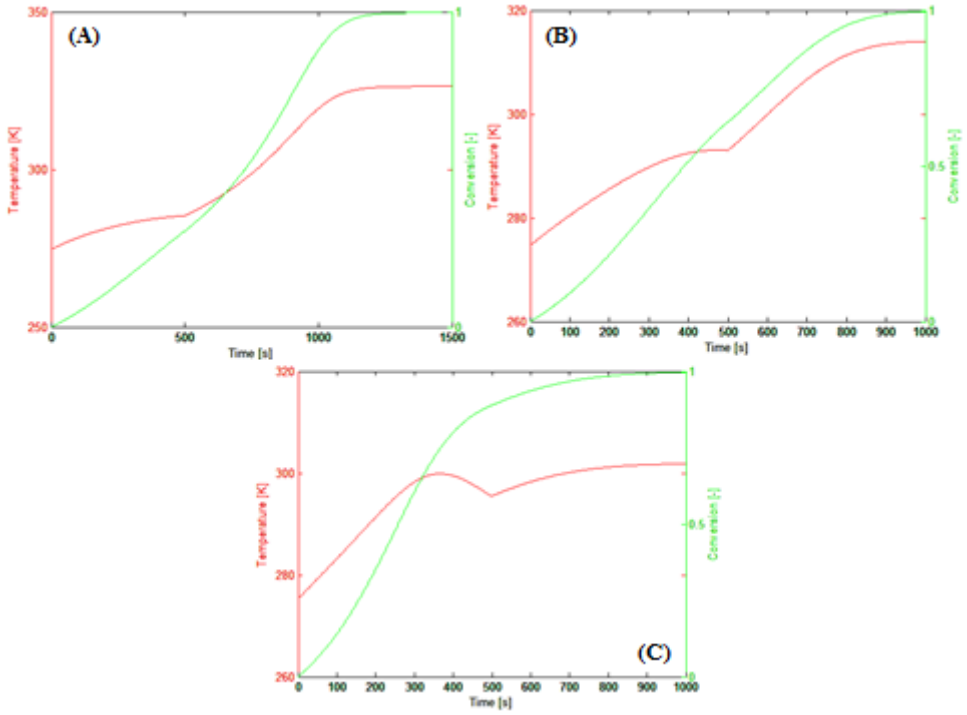

Figure 4.23. Temperature (expressed in K, red lines) and conversion (green lines) profiles obtained with respect to the time (expressed in seconds) considering a shift from isoperibolic (jacket temperature equal to 5.3°C) to adiabatic behavior occurring at 500 s and considering 0.8 mol of acetic anhydride and 7 mol of methanol in order to simulate an acid catalyzed esterification. The different curves are obtained considering different concentrations of the catalyst (sulfuric acid), i.e. 16 mol/m^3 for the (A) curves, 29 mol/m^3 for the (B) curves and 40 mol/m^3 for the (C) curves.

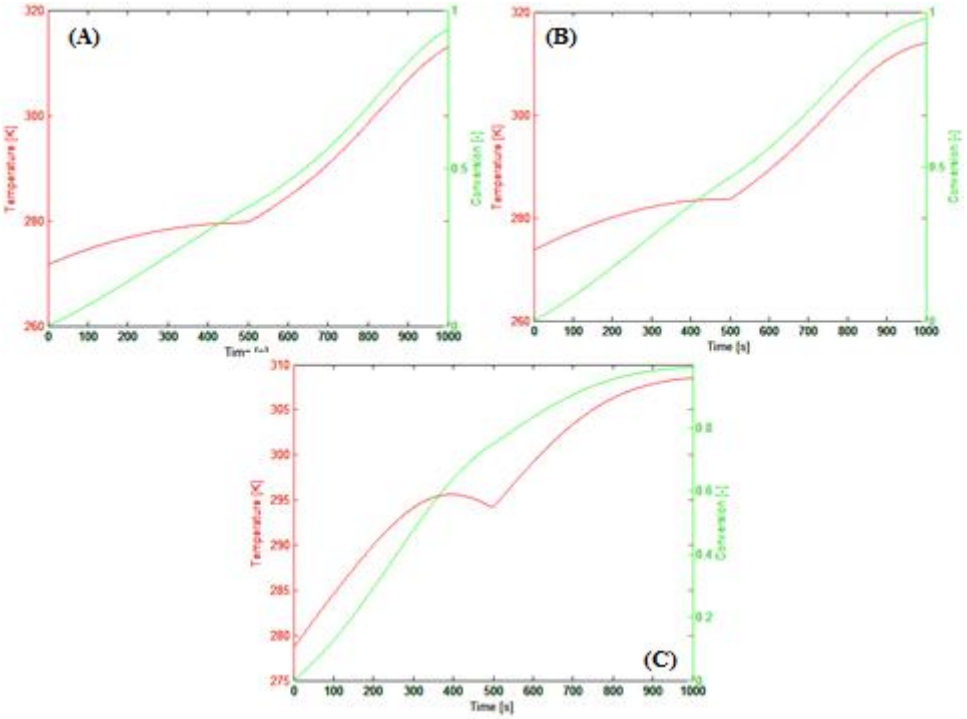

Figure 4.24. Temperature (expressed in K, red lines) and conversion (green lines) profiles obtained with respect to the time (expressed in seconds) considering a shift from isoperibolic) to adiabatic behavior occurring at 500 s and considering 0.8 mol of acetic anhydride, 7 mol of methanol and a sulfuric acid concentration of 30 mol/m^3 in order to simulate an acid catalyzed esterification. The different curves are obtained considering different jacket temperatures (for the isoperibolic section, of course), i.e. -2.25°C for the (A) curves, 0.3°C for the (B) curves and 5.16°C for the (C) curves.

The temperature profiles obtained through the simulation of a shift from isoperibolic to adiabatic behavior occurring after 600 seconds from the beginning of the tests are represented in Figures 4.25 and 4.26. The first one represents the curves obtained considering different acid concentrations, while the second one concerns the ones obtained at different jacket temperature (in the isoperibolic section, of course). In Figures 4.27 and 4.28, the temperature and conversion profiles are compared for each test.

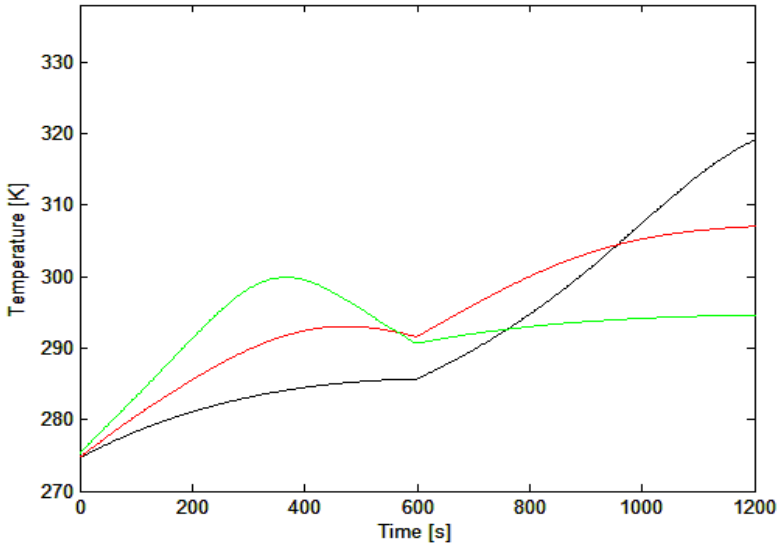

Figure 4.25. Temperature profiles (expressed in K) obtained with respect to the time (expressed in seconds) considering a shift from isoperibolic (jacket temperature equal to 5.3°C) to adiabatic behavior occurring at 600 s and considering 0.8 mol of acetic anhydride and 7 mol of methanol in order to simulate an acid catalyzed esterification. The different curves are obtained considering different concentrations of the catalyst (sulfuric acid), i.e. 16 mol/m^3 for the black curve, 29 mol/m^3 for the red curve and 40 mol/m^3 for the green curve.

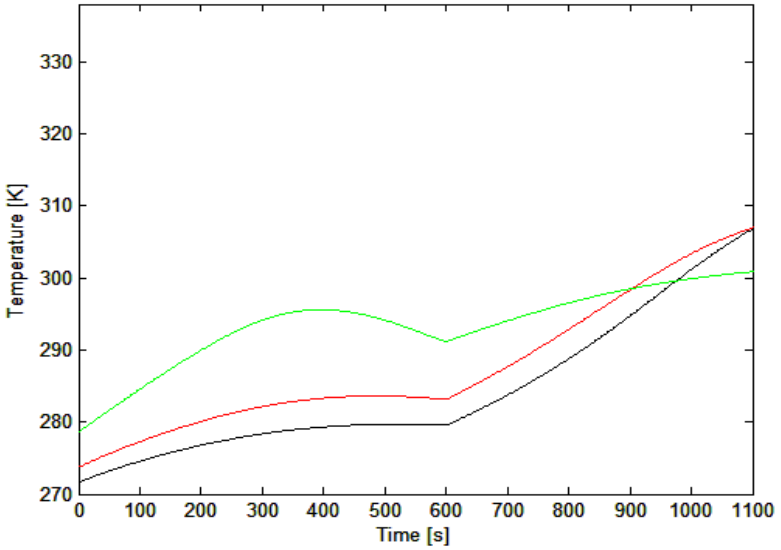

Figure 4.26. Temperature profiles (expressed in K) obtained with respect to the time (expressed in seconds) considering a shift from isoperibolic) to adiabatic behavior occurring at 600 s and considering 0.8 mol of acetic anhydride, 7 mol of methanol and a sulfuric acid concentration of 30 mol/m^3 in order to simulate an acid catalyzed esterification. The different curves are obtained considering different jacket temperatures (for the isoperibolic section, of course), i.e. -2.25°C for the black curve, 0.3°C for the red curve and 5.16°C for the green curve.

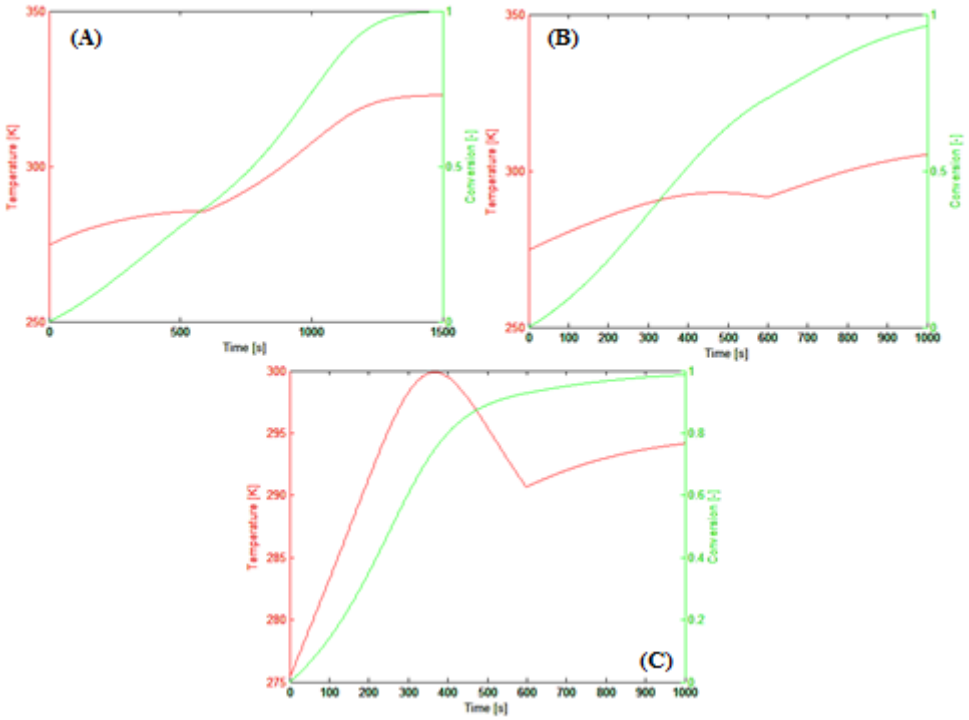

Figure 4.27. Temperature (expressed in K, red lines) and conversion (green lines) profiles obtained with respect to the time (expressed in seconds) considering a shift from isoperibolic (jacket temperature equal to 5.3°C) to adiabatic behavior occurring at 600 s and considering 0.8 mol of acetic anhydride and 7 mol of methanol in order to simulate an acid catalyzed esterification. The different curves are obtained considering different concentrations of the catalyst (sulfuric acid), i.e. 16 mol/m^3 for the (A) curves, 29 mol/m^3 for the (B) curves and 40 mol/m^3 for the (C) curves.

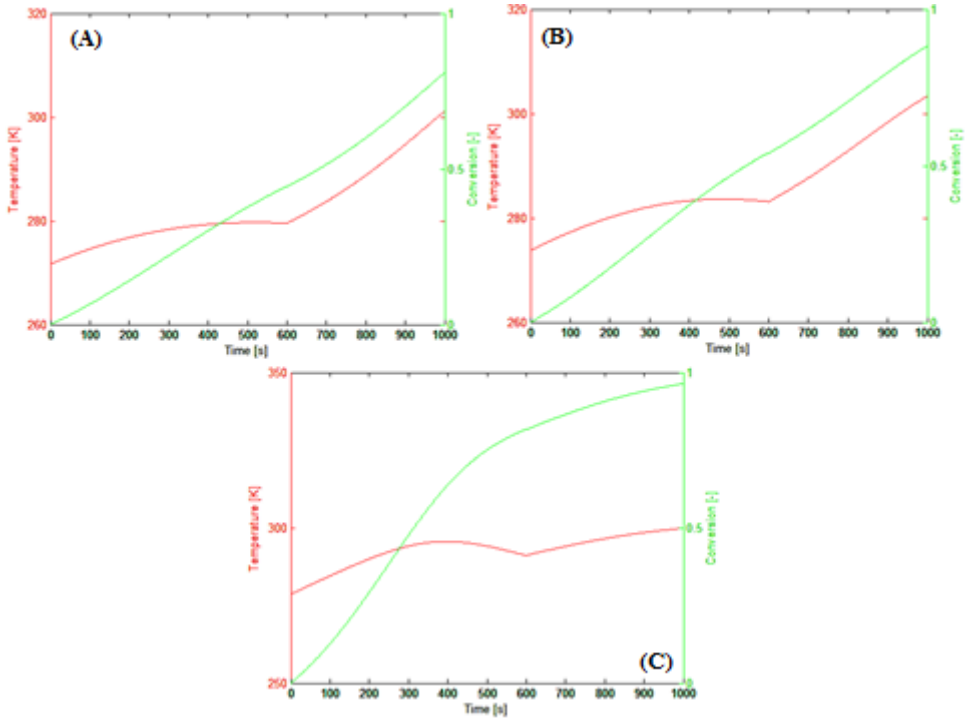

Figure 4.28. Temperature (expressed in K, red lines) and conversion (green lines) profiles obtained with respect to the time (expressed in seconds) considering a shift from isoperibolic) to adiabatic behavior occurring at 600 s and considering 0.8 mol of acetic anhydride, 7 mol of methanol and a sulfuric acid concentration of 30 mol/m^3 in order to simulate an acid catalyzed esterification. The different curves are obtained considering different jacket temperatures (for the isoperibolic section, of course), i.e. -2.25°C for the (A) curves, 0.3°C for the (B) curves and 5.16°C for the (C) curves.

As can be seen from the previous figures and confirmed by the application of the Hub and Jones criterion, the system behavior becomes unstable when there is the shift from isoperibolic to adiabatic conditions. This happens independently on the considered catalyst concentrations or jacket temperatures of the isoperibolic sections. However, it appears evident that the difference between the maximum and the minimum temperature is strongly different for each curve. In the following tables (Table 4.1 and 4.2), these temperature differences are reported for the adiabatic case, the isoperibolic behavior and the shifts at different times from isoperibolic to adiabatic conditions.

Table 4.1. Difference between the maximum and the minimum temperature (expressed in K) for simulations performed considering 0.8 mol of acetic anhydride and 7 mol of methanol in order to carry out a sulfuric acid catalyzed esterification. The simulations are obtained considering three different sulfuric acid concentrations (16, 29 and 40 mol/m^3) and several thermal behaviors of the system: adiabatic, isoperibolic and the shift from isoperibolic to adiabatic behavior occurring at different times (100 s, 200 s, 300 s, 400 s, 500 s and 600 s). In the isoperibolic sections, the jacket temperature is 5.3 °C.

Case \ Concentration [mol/m^3]	16	29	40
Adiabatic case	59 K	59 K	59 K
Shift at 100 s	59 K	59 K	59 K
Shift at 200 s	59 K	57 K	55 K
Shift at 300 s	58 K	53 K	47 K
Shift at 400 s	55 K	47 K	36 K
Shift at 500 s	52 K	40 K	27 K
Shift at 600 s	48 K	33 K	25 K
Isoperibolic case	11 K	19 K	25 K

Table 4.2. Difference between the maximum and the minimum temperature (expressed in K) for simulations performed considering 0.8 mol of acetic anhydride and 7 mol of methanol in order to carry out an acid catalyzed esterification. The simulations are obtained considering three different jacket temperatures (-2.25 °C, 0.3 °C and 5.16 °C) and several thermal behaviors of the system: adiabatic, isoperibolic and the shift from isoperibolic to adiabatic behavior occurring at different times (100 s, 200 s, 300 s, 400 s, 500 s and 600 s). In each simulation, the considered sulfuric acid concentration is 30 mol/m^3.

Case \ Jacket temperature [°C]	-2.25	0.3	5.16
Adiabatic case	59 K	59 K	59 K
Shift at 100 s	58 K	58 K	58 K
Shift at 200 s	56 K	55 K	53 K
Shift at 300 s	53 K	51 K	47 K
Shift at 400 s	49 K	47 K	39 K
Shift at 500 s	45 K	42 K	30 K
Shift at 600 s	41 K	37 K	23 K
Isoperibolic case	8 K	10 K	17 K

Observing Tables 4.1 and 4.2, it can be noticed that the difference between the maximum and the minimum values of the temperature decreases when the time at which the shift in the thermal

conditions occurs is increased. Besides of that, in the curves of the behavior shift, it can be observed that the temperature difference decreases as both the sulfuric acid concentration and the jacket temperature increase. These phenomena can be explained considering that the reaction is faster (i.e. it goes to total conversion in a lower time, in this case) as the catalyst concentration and the jacket temperature are increased. This means that, for high values of these variables, most of the reaction takes place *before* the shift from isoperibolic to adiabatic conditions, thus reducing the temperature rise in the adiabatic section.

4.3 Effect of a global heat transfer coefficient change

In a real industrial system, many equipment failures may occur, leading to changes in the process behavior/conditions that can degenerate into severe incidents. However, together with these events, the process characteristics can also be modified by continuous and inevitable events. For example, the fouling of the walls of the jacket of a cooled reactor can lead to a change in the global heat transfer coefficient of the system, reducing dramatically the heat removed and thus leading to a runaway phenomenon, as can be qualitatively seen performing several isoperibolic simulations of the considered system (Figure 4.29).

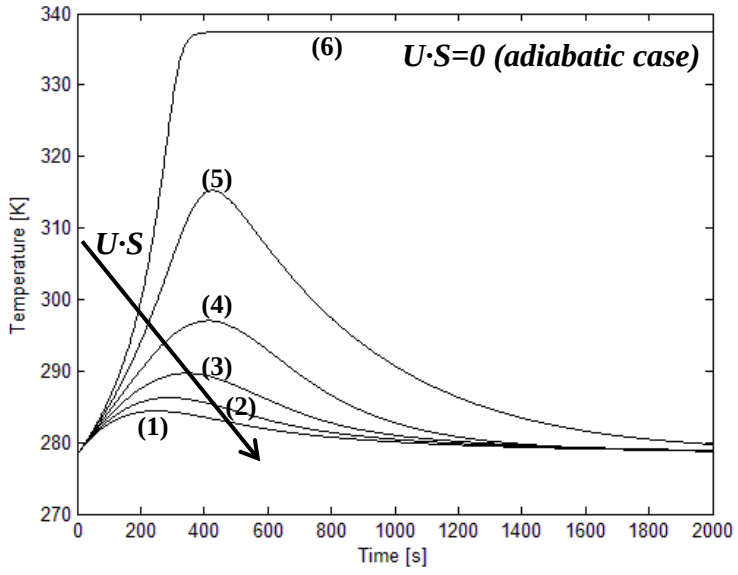

Curve	$U \cdot S$ [kW/K]
1	0.01
2	0.008
3	0.006
4	0.004
5	0.002
6	0

Figure 4.29. Temperature (K) profiles obtained with respect to time (expressed in seconds) considering several isoperibolic simulations of the sulfuric acid catalyzed esterification of acetic anhydride with methanol performed at different values of the product between the global heat transfer coefficient and the exchange surface ($U \cdot S$). The considered sulfuric acid concentration is 30 mol/m^3, while the considered jacket temperature is 5°C. The direction of increment of $U \cdot S$ is highlighted in the figure and the legend is reported.

Observing this figure, it is possible to see (in a qualitative way) that a reduction in the product between the global heat transfer coefficient and the exchange surface ($U \cdot S$) can lead to the system runaway and to sever incidents. In order to study the dependence of the system analyzed in this work from the value of $U \cdot S$, the modeled system sensitivity is computed and the Morbidelli and Varma criterion is applied to several isoperibolic simulations (performed considering different values of $U \cdot S$, sulfuric acid concentration and jacket temperature) in order to find the critical value of $U \cdot S$. The local sensitivity of the system is thus defined in the following way:

$$s = \frac{\partial T_{max}}{\partial (U \cdot S)}, \tag{4.1}$$

where T_{max} (K) is the locus of the temperature maxima for the experimental runs carried out varying $U \cdot S$ (kW/K). The normalized sensitivity is then defined according to the following equation:

$$s_{norm} = \frac{U \cdot S}{T_{max}} \cdot \frac{\partial T_{max}}{\partial (U \cdot S)} \tag{4.2}$$

The Morbidelli and Varma criterion is applied to the model data, computing in a numeric way the sensitivities after the application of a third order Savitzsky-Golay filter to smooth the small oscillations given by the model itself.

Calculating the normalized sensitivity with respect to $U \cdot S$, considering different sulfuric acid concentrations and a constant jacket temperature of 5°C, the following figure can be obtained (Figure 4.30).

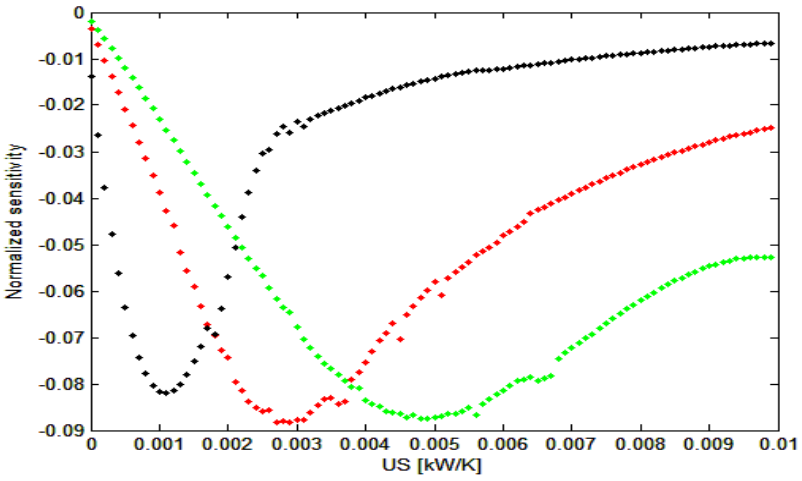

Figure 4.30. Normalized sensitivities of the modeled loci of the maximum temperature with respect to $U \cdot S$ (kW/K) for data obtained considering a constant jacket temperature (5°C) but different sulfuric acid concentrations, i.e. 10 mol/m^3 for the black curve, 30 mol/m^3 for the red one and 50 mol/m^3 for the green one.

As can be seen from the previous figure, the normalized sensitivity with respect to $U \cdot S$ is always negative. This means that the maximum temperature that the system can reach decreases as $U \cdot S$ increases. Moreover, it can be observed that the minimum of the normalized sensitivity (which indicates the runaway boundary, according to the Morbidelli and Varma criterion) shifts towards higher values when the sulfuric acid concentration increases, indicating that the unstable zone enlarges as the catalyst concentration increases.

Calculating the normalized sensitivity with respect to $U \cdot S$, considering different jacket temperatures and a constant sulfuric acid concentration of 30 mol/m^3, the following figure can be obtained (Figure 4.31).

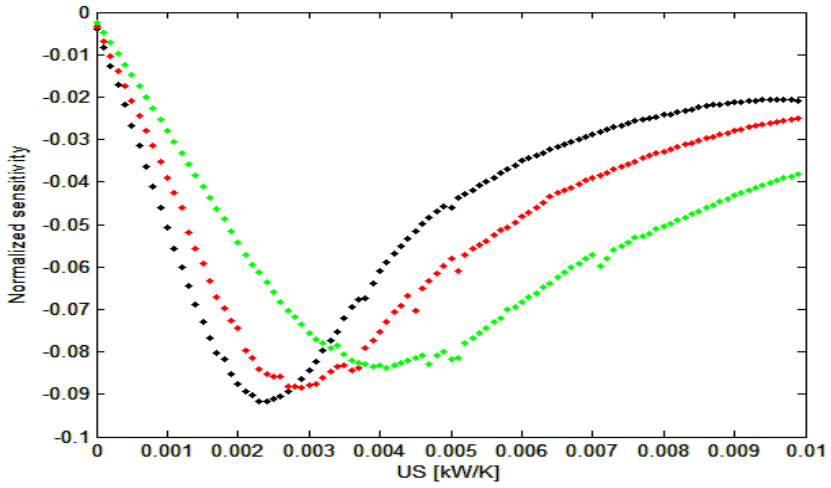

Figure 4.31. Normalized sensitivities of the modeled loci of the maximum temperature with respect to $U \cdot S$ (kW/K) for data obtained considering a constant sulfuric acid concentration (30 mol/m^3) but different jacket temperatures, i.e. 2°C for the black curve, 5°C for the red one and 10°C for the green one.

As can be seen from the previous figure and as stated before, the normalized sensitivity with respect to $U \cdot S$ is always negative: this means that the maximum temperature that the system can reach decreases as $U \cdot S$ increases. Moreover, it can be observed that the minimum of the normalized sensitivity (which indicates the runaway boundary, according to the Morbidelli and Varma criterion) shifts towards higher values when the jacket temperature increases, indicating that the unstable zone enlarges as the value of this parameter increases.

Chapter 5
Conclusions and Observations

Many of the incidental events occurring in an industrial plant are due to the sudden release of a huge amount of energy in a very short period of time and in a confined space. This typically determines a sudden pressure increase, generating a shock wave that is violently propagated in the surroundings, i.e. an explosion. It appears evident that these events must be avoided: this can be done, for example, applying preventive measures that are based on the usage of different criteria that are able to predict the thermal runaway of a system. The main objective of this thesis was to apply and compare different runaway criteria (i.e. Hub and Jones, Thomas and Bowes, Morbidelli and Varma, Strozzi and Zaldívar criterion) and to develop a model that is able to detect the boundaries between stable and unstable zone of the considered process. The exothermic reaction that was chosen to this purpose is the sulfuric acid catalyzed esterification of acetic anhydride with methanol. This choice was performed for two reasons:

- This reaction is relatively safe to be studied in laboratory;
- The esterification of acetic anhydride with methanol has a low activation energy, so it represents a severe test for the runaway criteria.

Some of the previously mentioned criteria required the usage of a model of the reaction. Therefore, a *MATLAB*® script was used to develop it and it was validated through several experimental runs carried out using a reaction calorimeter ran in isoperibolic mode. The runaway criteria were applied to both experimental and model data, in order to compare the obtained results. The model appeared to be in good accord with the experimental data, showing that the boundary between stable and unstable zone, in the considered conditions, appears to be around a sulfuric acid concentration of 40 mol/m^3 (for a jacket temperature of 5.3 °C) and a jacket temperature of 6 or 7°C (for a catalyst concentration of 30 mol/m^3). Moreover, the comparison of the results obtained in this work with the ones exposed in the scientific publication "Comparison of criteria for prediction of runaway reactions in the sulfuric acid catalyzed esterification of acetic anhydride and methanol" by Casson et al., showed that the model utilized in this thesis is able to provide a better agreement with the experimental data. Besides of that, it is important to notice that this model of the reaction has a physical meaning, using a modified Arrhenius expression for the kinetic constant. For this reason, it was possible to perform several simulations in adiabatic conditions (different from the isoperibolic

ones), furtherly validating the model and simulating several failures that may occur in a real industrial reactor. For example, in Figure 5.1, the effect of a change in the system behavior (from isoperibolic to adiabatic) in the temperature profiles, occurring at different times, is exposed.

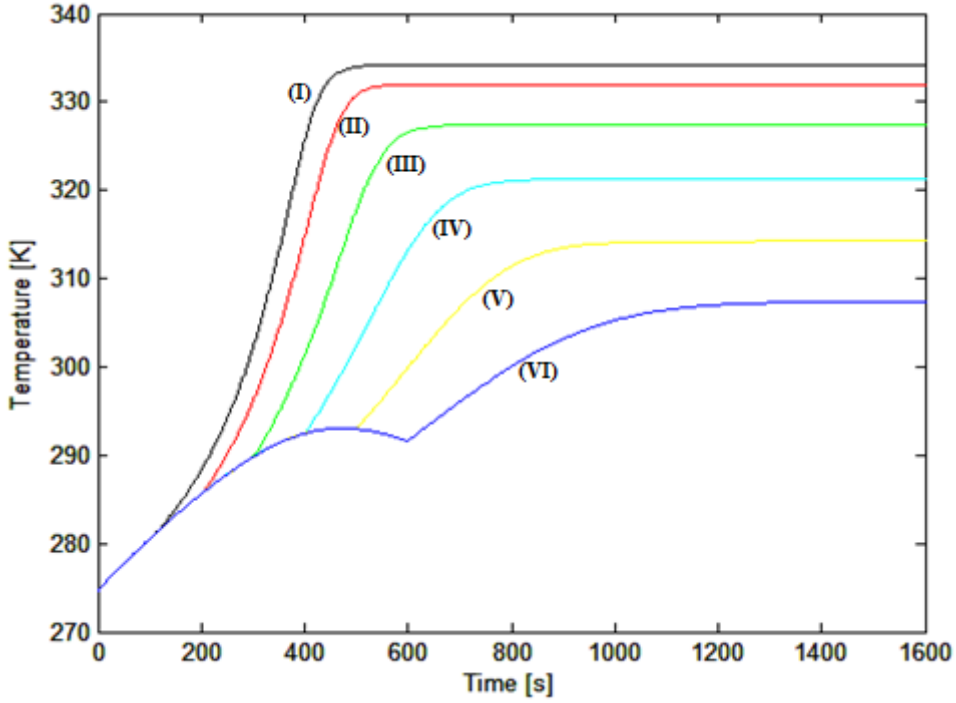

Figure 5.1. Temperature (expressed in K) profiles obtained with respect to the time (expressed in seconds) considering a shift from isoperibolic (jacket temperature equal to 5.3°C) to adiabatic behavior and considering 0.8 mol of acetic anhydride and 7 mol of methanol in order to simulate an acid catalyzed esterification. The different curves are obtained considering different time instants for the change in the behavior, i.e. 100 s for the (I) curve, 200 s for the (II) one, 300 s for the (III) one, 400 s for the (IV) one, 500 s for the (V) one and 600 s for the (VI) one.

Besides of that, the model allowed to study the effect of a change in the global heat transfer coefficient, showing that an increment in both the sulfuric acid concentration and the jacket temperature is able to enlarge the unstable zone of the system.

Concerning the considered system, it has been shown that basically every runaway criteria applied in this thesis is able to detect the boundary between stable and unstable behavior and that the construction of a model of the system is the major problem in the correct application of many of these methods, often leading to huge errors (especially close to the boundary between the stable and the unstable zones). Besides of that, the need of a model implies a knowledge of the process and a calculation speed that is usually not available in real industrial systems. Therefore, runaway criteria that does not require models (such as the Hub and Jones and the Strozzi and Zaldívar criteria) are the most suitable for the application in real industrial systems subject to a possible runaway.

In order to furtherly validate the results that are exposed in this work, the simulations of the deviations from the desired behavior of the system could be compared with experimental tests developed *ad hoc* to simulate several failures or, for example, changes in the global heat transfer coefficient of the system. Furthermore, the developed model of the system could be improved by taking into account the pressure measurements and by trying to apply it to a homogeneous gaseous phase reaction.

Annex

The names of the *MATLAB*® files that have been used to obtain the results exposed in this thesis work are listed in the following section. The scripts are collected in the compact disk attached to this paper, together with the *.txt* files containing the temperatures and the correspondent time instants retrieved through the isoperibolic experimental tests.

- `Model_kin_Arrhenius.m`: usage of the isoperibolic experimental data to retrieve the values of the parameters of the kinetic expression of the reaction, thus building a model of the system;
- `HubJones_Exp_Conc.m`: application of the Hub and Jones criterion to the isoperibolic experimental data obtained considering tests at different sulfuric acid concentration;
- `HubJones_Exp_jacket.m`: application of the Hub and Jones criterion to the isoperibolic experimental data obtained considering tests at jacket temperature;
- `HubJones_Model.m`: application of the Hub and Jones criterion to the isoperibolic model data;
- `ThomasBowes_Exp.m`: application of the Thomas and Bowes criterion to the isoperibolic experimental data;
- `ThomasBowes_Model.m`: application of the Thomas and Bowes criterion to the isoperibolic model data;
- `MorbidelliVarma_Exp_jacket.m`: application of the Morbidelli and Varma criterion to the isoperibolic experimental data, calculating the sensitivity with respect to the jacket temperature;
- `MorbidelliVarma_Exp_Acid.m`: application of the Morbidelli and Varma criterion to the isoperibolic experimental data, calculating the sensitivity with respect to the sulfuric acid concentration;
- `MorbidelliVarma_Model_jacket.m`: application of the Morbidelli and Varma criterion to the isoperibolic model data, calculating the sensitivity with respect to the jacket temperature;
- `MorbidelliVarma_Model_Acid.m`: application of the Morbidelli and Varma criterion to the isoperibolic model data, calculating the sensitivity with respect to the sulfuric acid concentration;

- `SZ_Exp.m`: application of the Strozzi and Zaldívar criterion to the isoperibolic experimental data;
- `SZ_Model.m`: application of the Strozzi and Zaldívar criterion to the isoperibolic model data;
- `Model.m`: generation of the *.txt* files containing the temperatures and the correspondent time instants related to the adiabatic simulations;
- `HubJones_Model_Adiab.m`: application of the Hub and Jones criterion to the adiabatic model data;
- `ThomasBowes_Model_Adiab.m`: application of the Thomas and Bowes criterion to the adiabatic model data;
- `HubJones_Model_Isoperibolic_100s.m`: application of the Hub and Jones criterion to the curves obtained considering a shift from isoperibolic to adiabatic behavior occurring at 100 seconds from the beginning of the simulation;
- `HubJones_Model_Isoperibolic_200s.m`: application of the Hub and Jones criterion to the curves obtained considering a shift from isoperibolic to adiabatic behavior occurring at 200 seconds from the beginning of the simulation;
- `HubJones_Model_Isoperibolic_300s.m`: application of the Hub and Jones criterion to the curves obtained considering a shift from isoperibolic to adiabatic behavior occurring at 300 seconds from the beginning of the simulation;
- `HubJones_Model_Isoperibolic_400s.m`: application of the Hub and Jones criterion to the curves obtained considering a shift from isoperibolic to adiabatic behavior occurring at 400 seconds from the beginning of the simulation;
- `HubJones_Model_Isoperibolic_500s.m`: application of the Hub and Jones criterion to the curves obtained considering a shift from isoperibolic to adiabatic behavior occurring at 500 seconds from the beginning of the simulation;
- `HubJones_Model_Isoperibolic_600s.m`: application of the Hub and Jones criterion to the curves obtained considering a shift from isoperibolic to adiabatic behavior occurring at 600 seconds from the beginning of the simulation;
- `MorbidelliVarma_Model_UA_30_variablejacket.m`: application of the Morbidelli and Varma criterion to the isoperibolic model data, calculating the sensitivity with respect to the product between the global heat transfer coefficient and the exchange surface (considering a constant sulfuric acid concentration and three different jacket temperatures);
- `MorbidelliVarma_Model_UA_5jacket_variableacid.m`: application of the Morbidelli and Varma criterion to the isoperibolic model data, calculating the sensitivity with respect to

the product between the global heat transfer coefficient and the exchange surface (considering a constant jacket temperature and three different sulfuric acid concentration).

Nomenclature and Symbols

c	=	reactant concentration (mol)
t	=	time (s)
$k\,(T)$	=	reaction rate constant ((mol/m^3)$^{1-n}$/s)
n	=	reaction order
V	=	volume of the reagents (m^3)
c_P	=	specific heat capacity of the reaction mixture (J/K/kg)
T	=	temperature (K)
ΔH_R	=	heat of reaction (J/mol)
S	=	external surface area (m^2)
U	=	overall heat transfer coefficient (J/m^2/s/K)
T_a	=	average ambient/jacket temperature (K)
$c^{initial}$	=	initial reactant concentration (mol)
$T^{initial}$	=	initial temperature (K)
X	=	conversion (-)
$E_{activation}$	=	activation energy (J/mol)
R	=	ideal gas constant (J/K/mol)
B	=	dimensionless heat of reaction (-)
X_m	=	conversion value that corresponds to the temperature maximum (-)
Q	=	parameter used in the van Welsenaere and Froment criterion (-)
s	=	local sensitivity
x	=	generic variable describing the behavior of a system
f	=	function describing the time behavior of x
$x^{initial}$	=	initial value og the generic variable x
s_{norm}	=	normalized sensitivity (-)
s^{obj}	=	objective function sensitivity

s_{norm}^{obj}	=	normalized objective function sensitivity (-)
I	=	objective function
$\dot{Q}_{acc}$	=	accumulated heat flow (W)
$\dot{Q}_{chem}$	=	heat flow generated by the reaction (W)
$\dot{Q}_{exc}$	=	heat flow exchanged by the jacket (W)
$\dot{Q}_{loss}$	=	heat flow dissipated in the environment (W)
$P_{stirrer}$	=	power developed in the mixing process (W)
$\dot{Q}_c$	=	compensation heat flow (W)
C_P	=	heat capacity of the reaction mixture (J/K)
r	=	reaction velocity (mol/s/m^3)
M_d	=	stirrer torque (J)
N	=	agitator speed (s^{-1})
ΔT_{ad}	=	adiabatic temperature rise (K)
m	=	initial moles of the reagent (mol)
M	=	mass of the reacting system (kg)
m_s	=	mass of the sample (kg)
m_h	=	mass of the sample holder (kg)
c_{Ps}	=	specific heat capacity of the sample (J/K/kg)
c_{Ph}	=	specific heat capacity of the sample holder (J/K/kg)
$n_{Ac.\ Anh.}^{i}$	=	initial number of moles of acetic anhydride (mol)
$n_{Ac.\ Anh.}(t')$	=	number of moles of acetic anhydride at the time instant t' (mol)
$m_{Ac.\ Anh.}$	=	mass of acetic anhydride into the calorimeter (kg)
T_{max}	=	locus of the temperature maxima (K)
$[H_2SO_4]$	=	sulfuric acid concentration (mol/m^3)
dV	=	infinitesimal volume variation in the phase space

Greek letters

ρ	=	density of the reaction mixture (kg/m^3)
τ	=	dimensionless time (-)

θ	=	dimensionless temperature (-)
γ	=	Arrhenius number (-)
Ψ	=	Semenov number (-)
θ_a	=	dimensionless ambient/jacket temperature (-)
θ^*	=	dimensionless temperature maximum (-)
θ_+	=	rate of temperature increase due to the heat released by the reaction (-)
θ_-	=	rate of temperature decrease due to the heat removed by cooling (-)
Ψ_c	=	critical Semenov number for thermal runaway (-)
Ψ_c'	=	critical Semenov number for intrinsically stable operation (-)
θ_c	=	critical dimensionless temperature (-)
Ψ_c^{VF}	=	modified critical Semenov number (-)
Φ_i	=	generic parameter of a system
$\mathbf{\Phi}$	=	vector containing all the parameters of the system
ϕ	=	phi-factor (-)

Acronyms

EWDS	=	Early Warning Detection System
DSC	=	Differential Scanning Calorimetry
DTA	=	Differential Thermal Analysis
TSU	=	Thermal Screening Unit

Bibliographic References

1. Maschio G. Explosions. *Analisi del rischio nell'industria di processo*. Class notes A.Y. 2014-2015, University of Padova.
2. Saada R., D. Patel, B. Saha (2015). Causes and consequences of thermal runaway incidents-Will they ever be avoided?. *Process Safety and Environmental Protection*, **97**, 109-115.
3. Nolan P.F. and J.A. Barton (1987). Some lessons from thermal-runaway incidents. *Journal of Hazardous Materials*, **14**, 233-239.
4. Varma A., M. Morbidelli, H. Wu (1999). *Parametric Sensitivity in Chemical Systems*. Cambridge University Press, Cambridge (UK).
5. Semenov N. N. (1959). *Some problems of chemical kinetics and reactivity (vol. 2).* Pergamon Press, London (UK).
6. Thomas P. H. and P.C. Bowes (1961). Some aspects of the self-heating and ignition of solid and cellulosic materials. *British Journal of Applied Physics*, **12**, 222.
7. Hlavacek V., M. Marek, T.M. John (1969). Modeling of chemical reactors-XII. *Coll. Czech. Chem. Commun.*, **34**, 3868.
8. Morbidelli M. and A. Varma (1982). Parametric sensitivity and runaway in tubular reactors. *A.I.Ch.E. Journal*, **28**, 705.
9. Adler J. and J.W. Enig (1964). The critical conditions in thermal explosion theory with reactant consumption. *Combustion and Flames*, **8**, 97.
10. van Welsenaere R. J. and G.F. Froment (1970). Parametric sensitivity and runaway in fixed bed catalytic reactors. *Chemical Engineering Science*, **25**, 1503.
11. Hub L. and J. D. Jones (1986). Early on-line detection of exothermic reactions. *Plant/Operation Progress*, **5**, 221-224.
12. Morbidelli M. and A. Varma (1985). On parametric sensitivity and runaway criteria of pseudo-homogeneous tubular reactor. *Chemical Engineering Science*, **40**, 2165.
13. Morbidelli M. and A. Varma (1988). A generalized criterion for parametric sensitivity: application to thermal explosion theory. *Chemical Engineering Science*, **43**, 91.
14. Strozzi F., J. M. Zaldívar, A. E. Kronberg, K. R. Westerterp (1999). On-line runaway detection in batch reactors using chaos theory techniques. *A.I.Ch.E. Journal*, **45**, 2429-2443.

15. Bosch J., D.C. Kerr, T. J. Snee, F. Strozzi, J. M. Zaldívar (2004). Runaway detection in a pilot plant facility. *Industrial and Chemical Engineering Research*, **43**, 7019-7024.
16. Zaldívar J. M., J. Cano, M. A. Alòs, J. Sempere, R. Nomen, D. G. Lister, G. Maschio, T. Obertopp, E. D. Gilles, J. Bosch, F. Strozzi (2003). A general criterion to define runaway limits in chemical reactors. *Journal of Loss Prevention in the Process Industries,* **16**, 187-200.
17. Casson V., D. G. Lister, M. F. Milazzo, G. Maschio (2011). Comparison of criteria for prediction of runaway reactions in the sulphuric acid catalyzed esterification of acetic anhydride and methanol. *Journal of Loss Prevention in the Process Industries*, **25**, 209-217.
18. Bosch J., F. Strozzi, D. G. Lister, G. Maschio, J. M. Zaldívar (2004). Sensitivity analysis in polymerization reactions using the divergence criterion. *Process Safety and Environmental Protection,* **82**, 18-25.
19. Landau R. N. (1996). Expanding the role of reaction calorimetry. *Thermochimica Acta*, **289**, issue 2, 101-126.
20. Wiss J. (1995). Reaction calorimetry at low temperatures. *Thermochimica Acta*, **255**, 9-16.
21. Ronnback R., T. Salmi, A. Vuori, H. Haario, J. Lehtonen, A. Sundqvist, E. Tirronen (1997). Development of a kinetic model for the esterification of acetic acid with methanol in the presence of a homogeneous acid catalyst. *Chemical Engineering Science*, **52**, 3369-3381.
22. Liu Y., E. Lotero, J. G. Goodwin Jr. (2006). A comparison of the esterification of acetic acid with methanol using heterogeneous versus homogeneous acid catalysis. *Journal of Catalysis*, **242**, 278-286.

Websites

`https://www.emars.jrc.ec.europa.eu/` (last access: 04/06/2016)

`http://www.bst-tsb.gc.ca/` (last access: 04/06/2016)